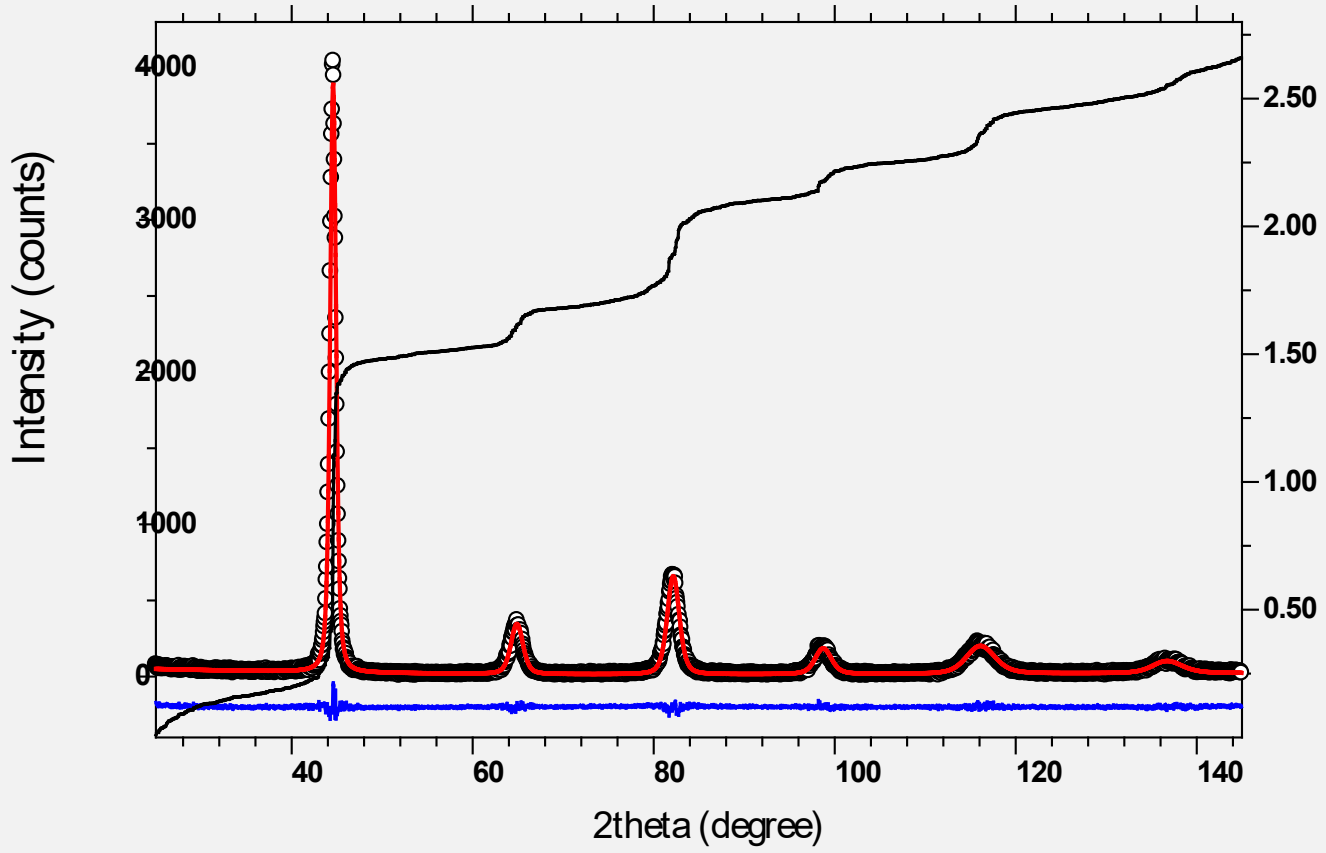

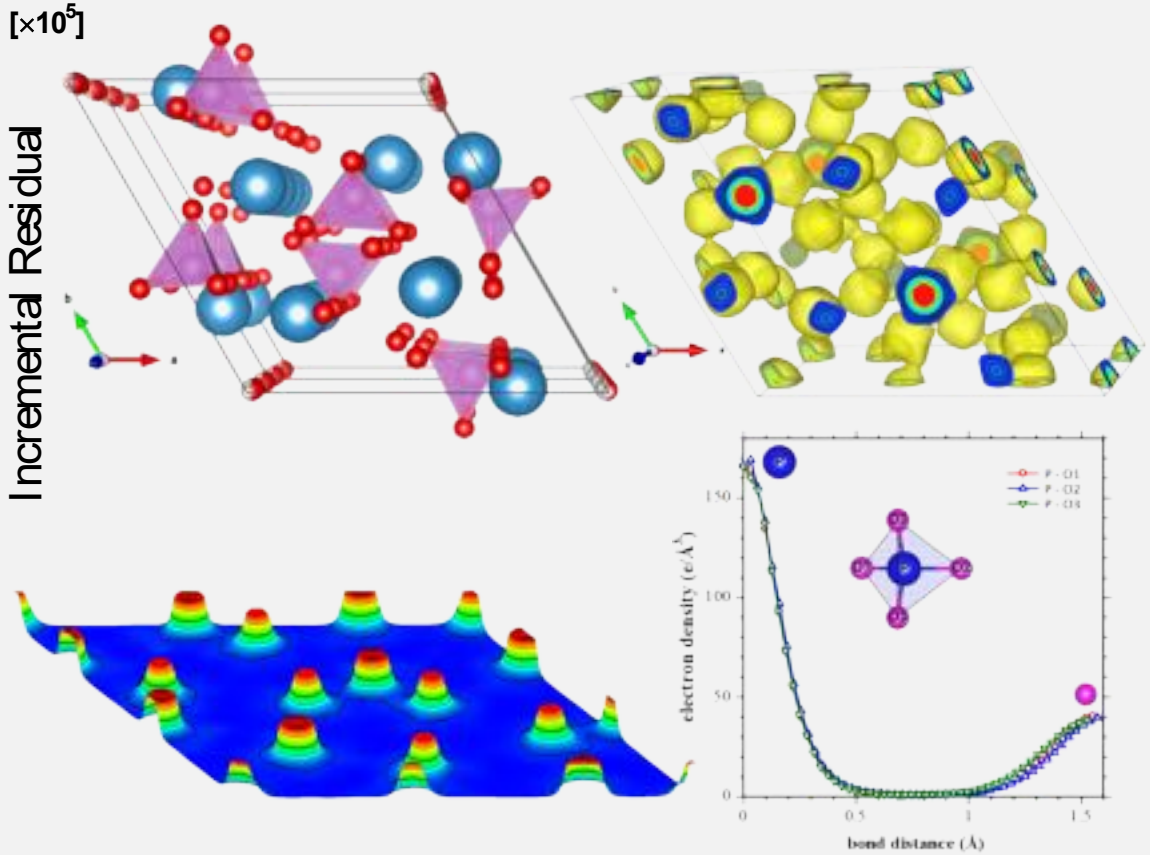

Visualizing/Assessing ion-conduction pathway using Powder Diffraction

Dr. Maykel T. E. Manawan //

Elements & Phases

- **Phase**:

  A physically distinctive form of matter, such as a solid, liquid, gas or plasma. A phase of matter is characterized by having relatively uniform

chemical and physical properties.

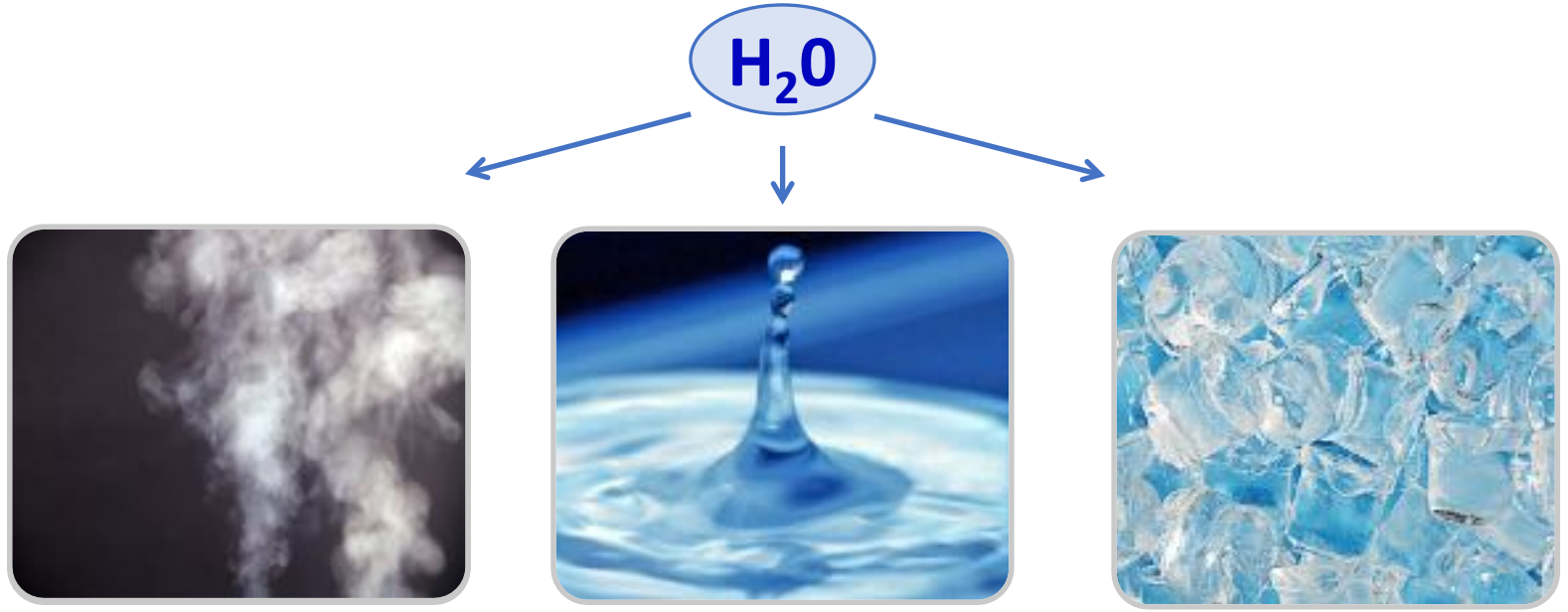

gaseous liquid solid

Elements & Phases

- **Phase**:

  A physically distinctive form of matter, such as a solid, liquid, gas or plasma. A phase of matter is characterized by having relatively uniform

chemical and physical properties.

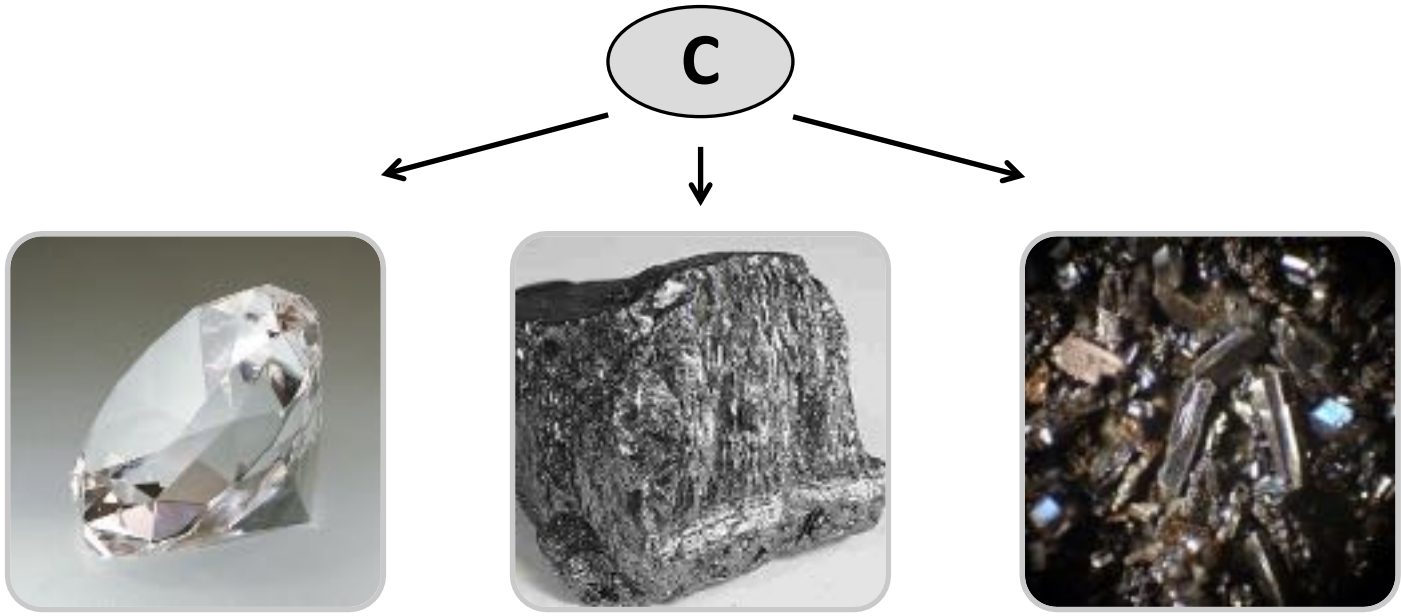

solid solid solid

Elements & Phases

- **Phase**:

  A physically distinctive form of matter, such as a solid, liquid, gas or plasma. A phase of matter is characterized by having relatively uniform

chemical and physical properties.

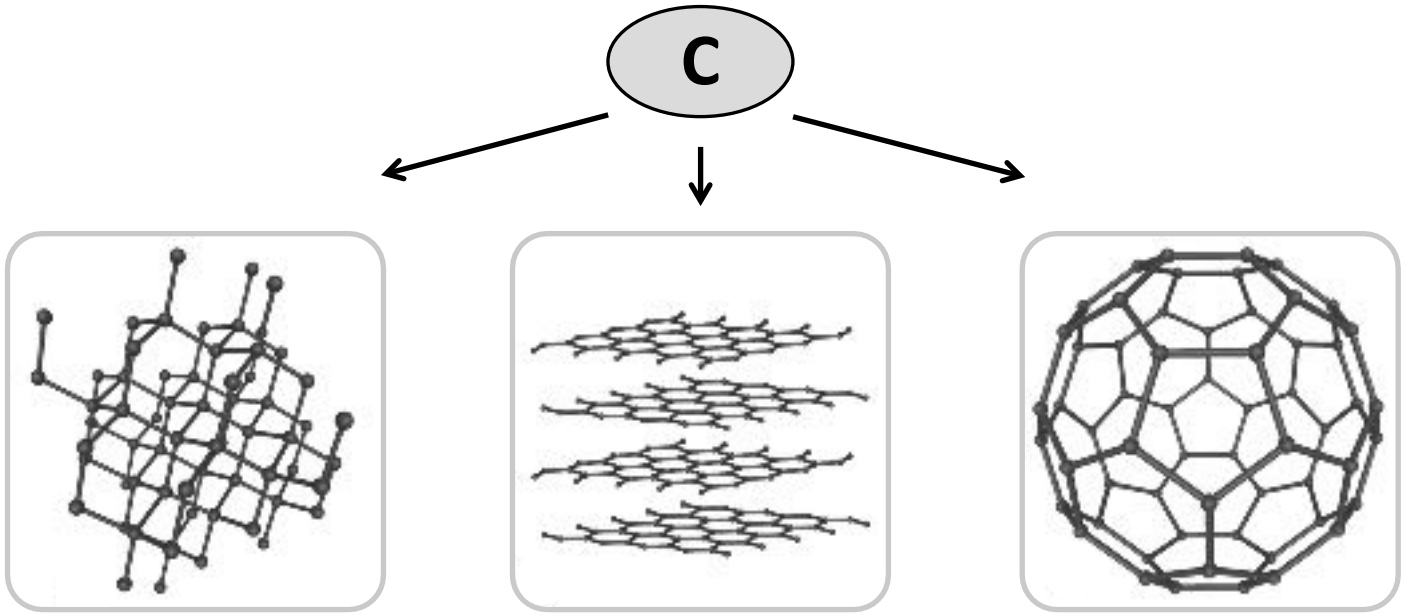

solid solid solid

Diffent Phases – Different XRD Pattern

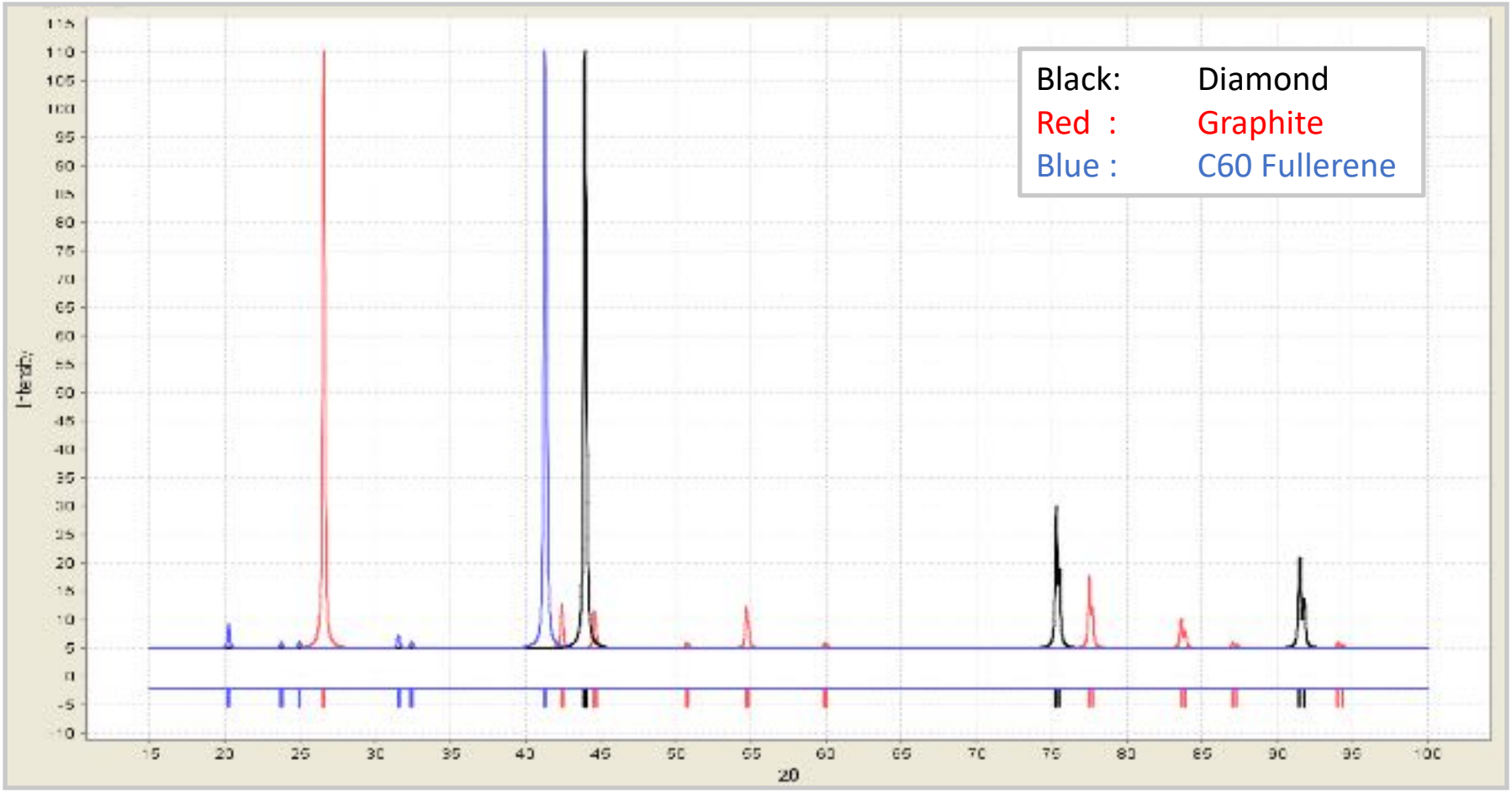

Ideal calculated diffraction patterns from the 3 phases mentioned above

Phase Identification - SiO2

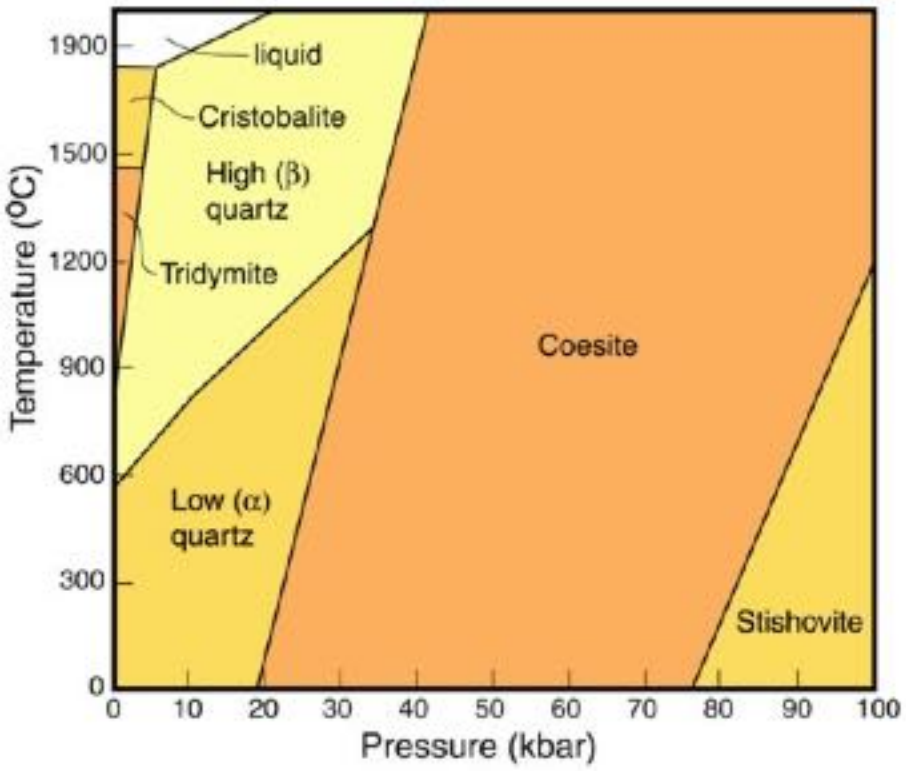

Phase diagram of SiO_2

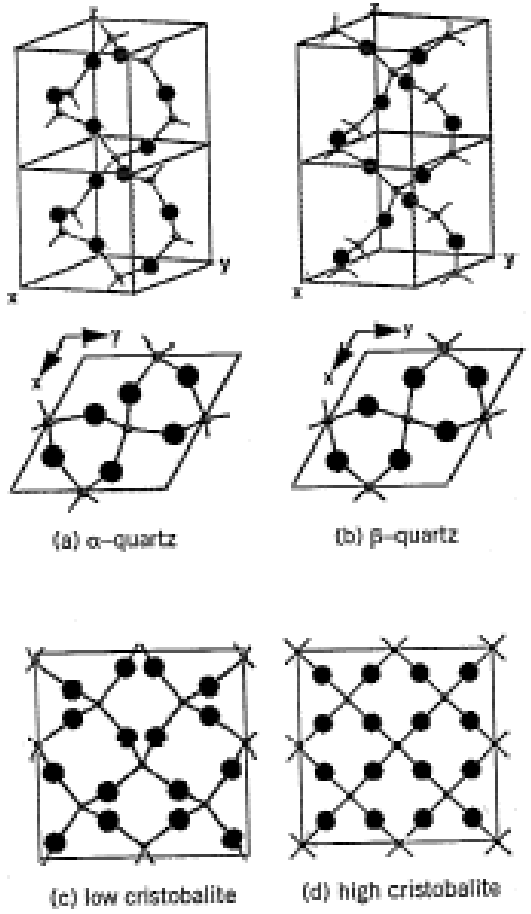

Crystal Structures

(Jenkins & Snyder 1996)

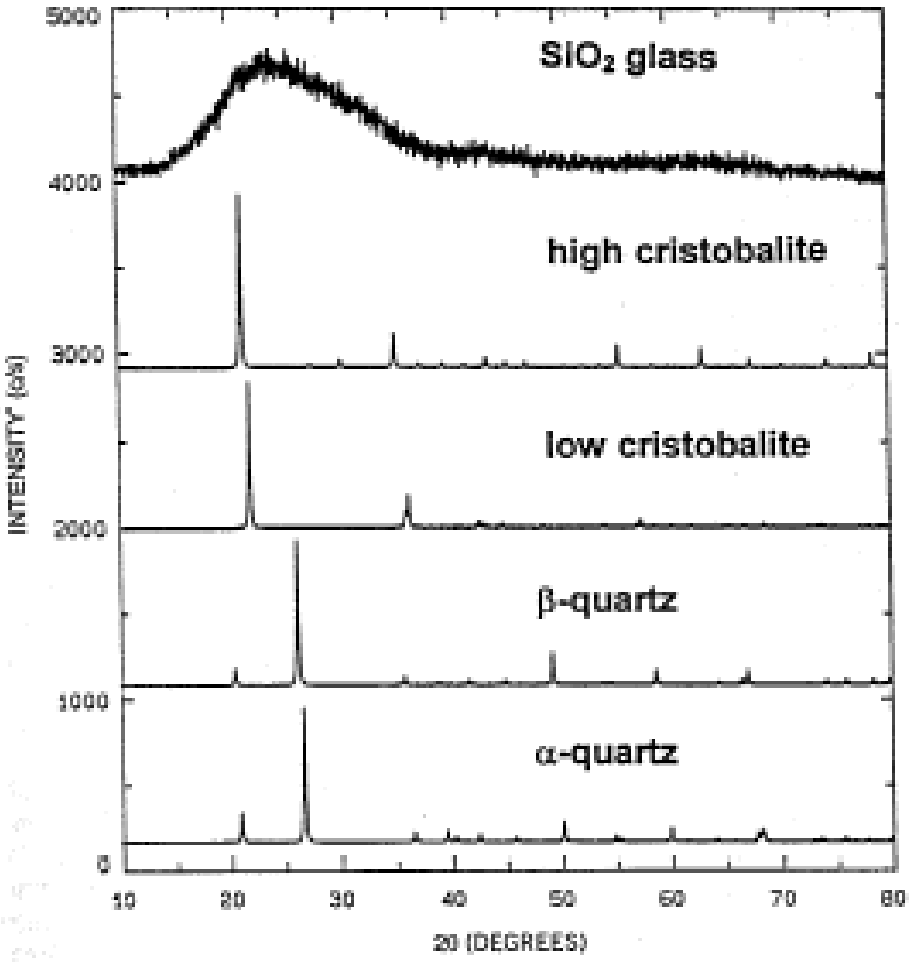

Powder Diffraction

(Jenkins & Snyder 1996)

How does PXRD work?

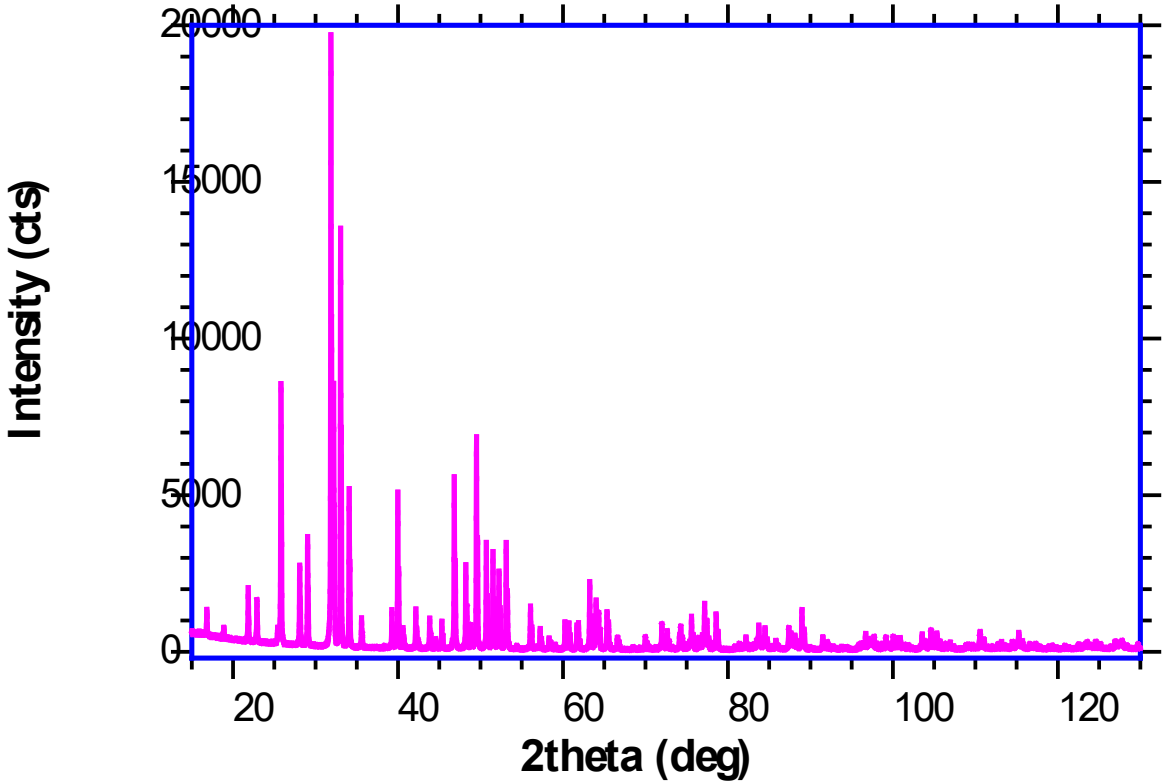

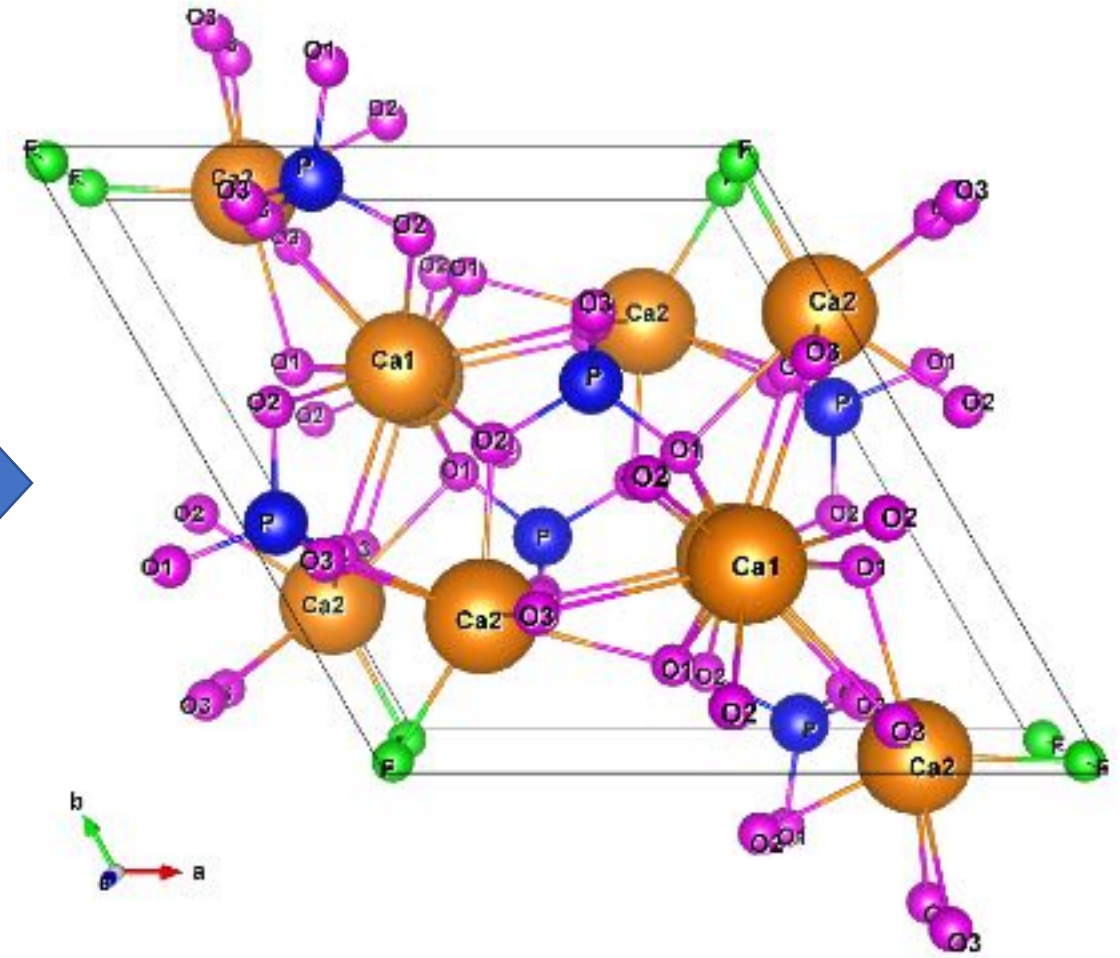

Powder Diffraction Pattern

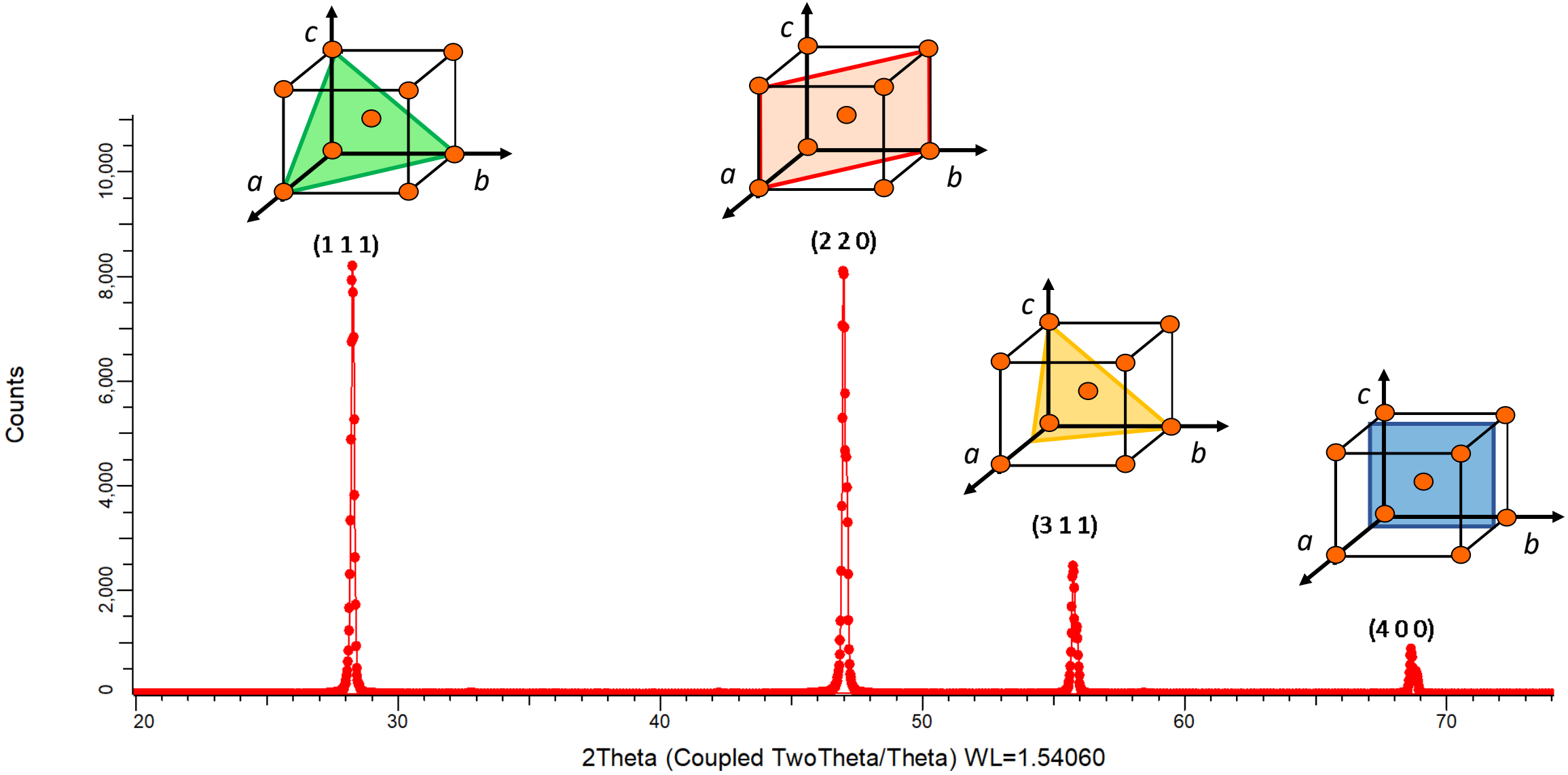

Diffraction by Planes of Atom

- Path difference Δ = 2x => phase shift
- Constructive interference if Δ = nλ
- Criterion for constructive interference:

$$\Delta = 2d_{hkl}\sin(\theta) = n\lambda$$

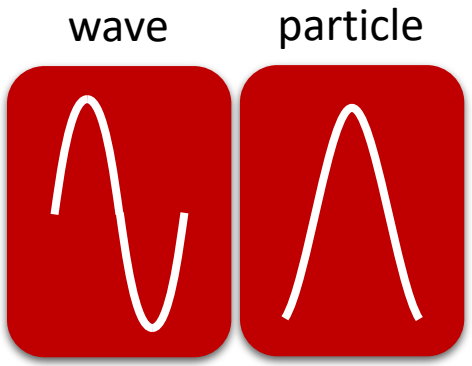

$$\sin(\theta) = \frac{x}{d_{hkl}}$$

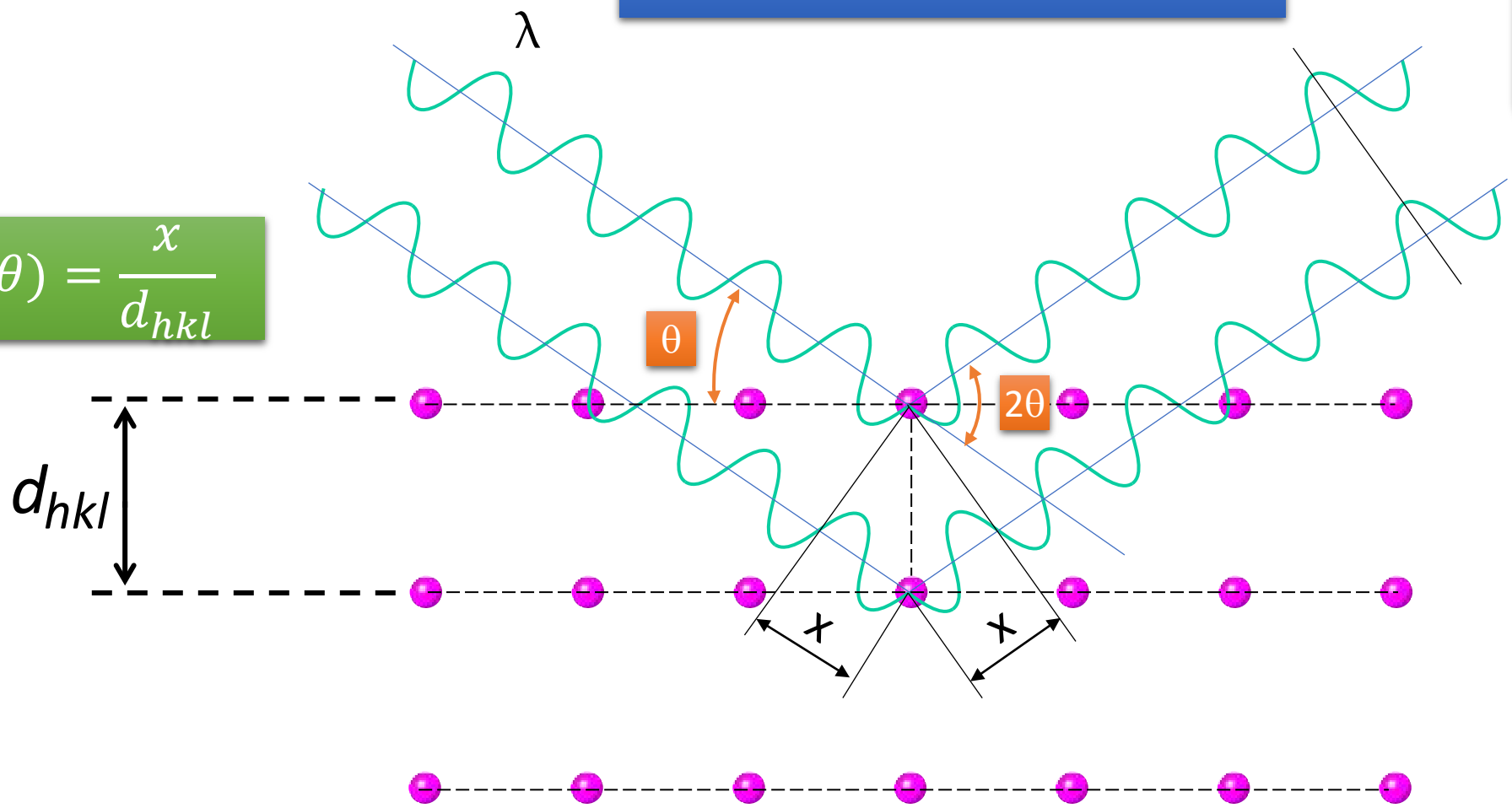

Diffraction by Planes of Atom

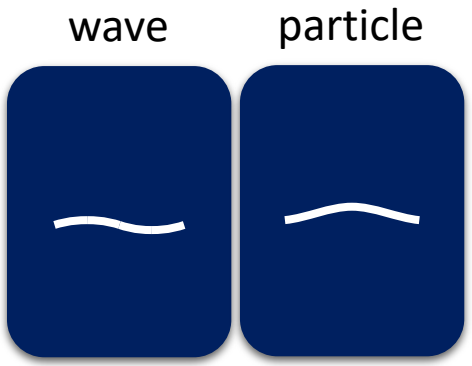

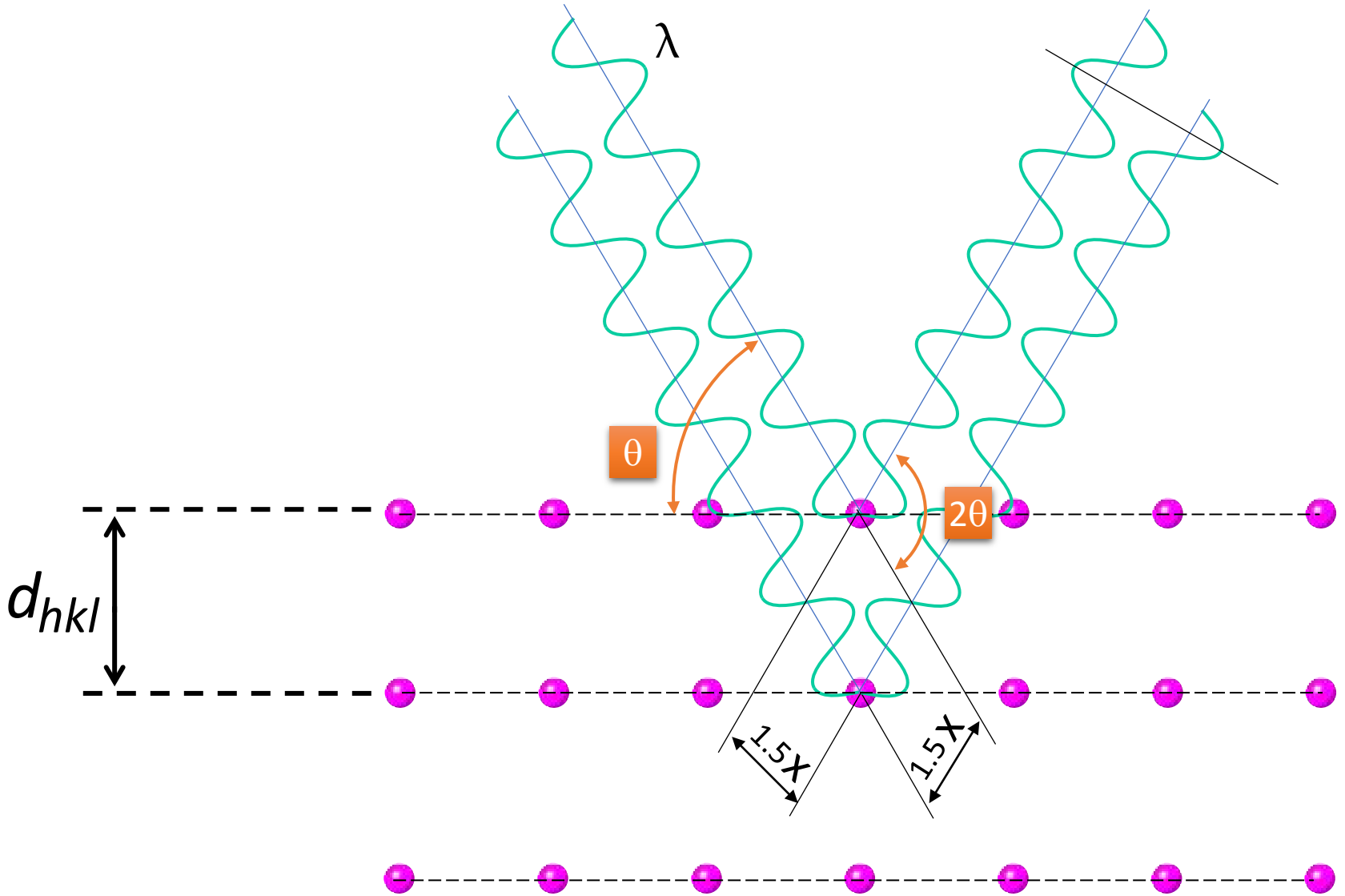

Diffraction Intensities – Structure factor

$$F_{hkl} = \sum_{1}^{N} f_n \, e^{2\pi i(hx_n + ky_n + lz_n)}$$

$$F_{hkl} = \sum_{1}^{N} f_n \left[\cos 2\pi(hx_n + ky_n + lz_n) + i \sin 2\pi(hx_n + ky_n + lz_n)\right]$$

$$F^2 = [f_1 \cos 2\pi(hx_1 + ky_1 + lz_1) + f_2 \cos 2\pi(hx_2 + ky_2 + lz_2) + \cdots]^2 + [f_1 \sin 2\pi(hx_1 + ky_1 + lz_1) + f_2 \sin 2\pi(hx_2 + ky_2 + lz_2) + \cdots]^2$$

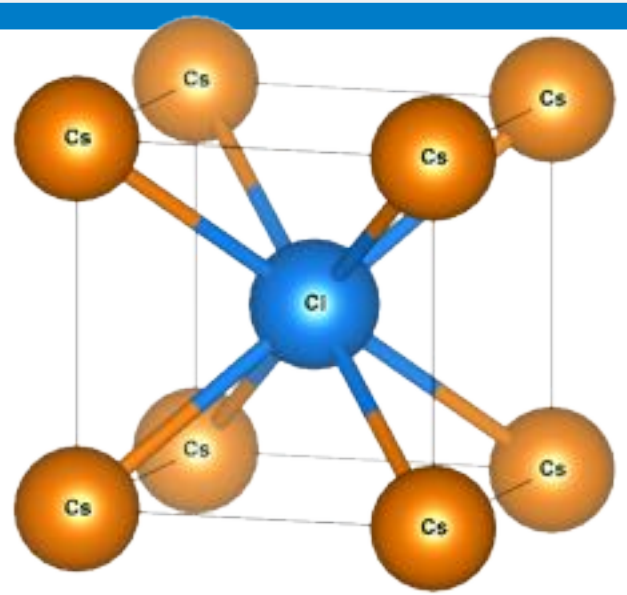

- The structure factor quantifies the amplitude of X-rays scattered by a crystal
- F_{hkl} sums the result of scattering from all of the atoms in the unit cell to form a diffraction peak from the (*hkl*) planes of atoms
- The amplitude of scattered light is determined by:
  - where the atoms are on the (*hkl*) planes
    - ➢ this is expressed by the fractional coordinates x_j y_j z_j
  - what atoms are on the atomic planes
    - ➢ the scattering factor f_j quantifies the relative efficiency of scattering at any angle by the group of electrons in each atom

Diffraction Intensities - Atomic scattering factor

$$|f|^2 = \left(f_0 \exp\left[-\frac{B \sin^2 \theta}{\lambda^2} \right] + (\Delta f')^2 \right)^2 + (\Delta f'')^2$$

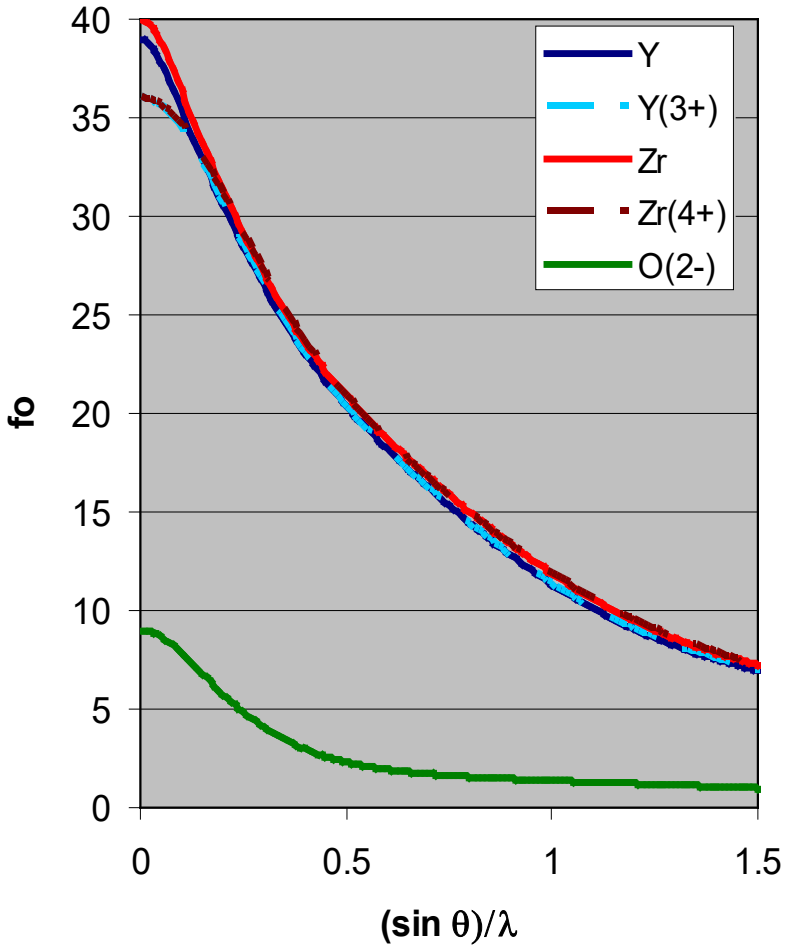

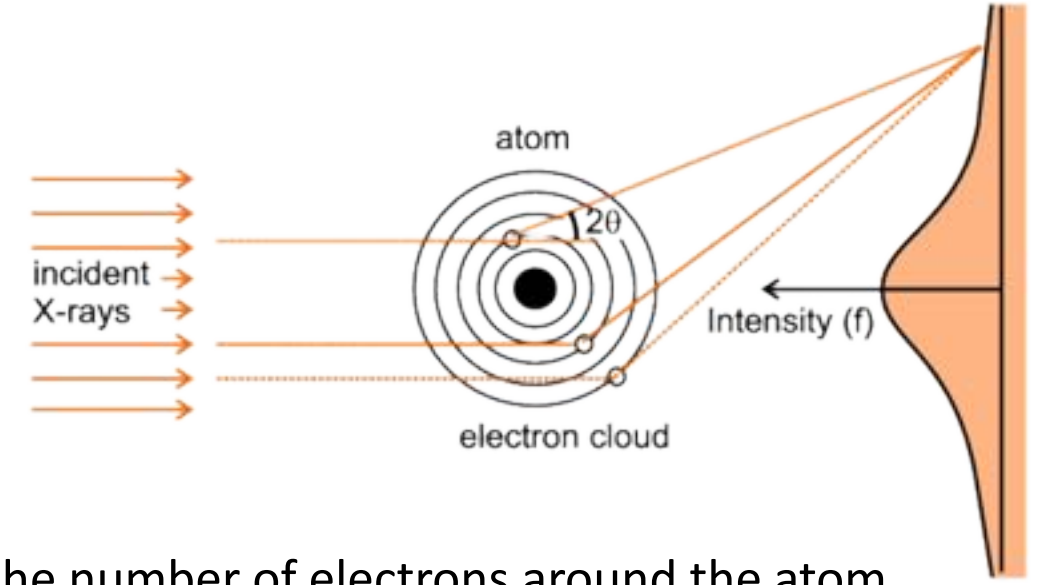

- f_0 at 0° is equal to the number of electrons around the atom
  - Y and Zr are similar, but slightly different, at 0°
  - Zr and Zr^{4+} are slightly different at 0°
  - Y^{3+} and Zr^{4+} are identical at 0°
- The variation with (sin θ)/λ depends on size of atom
  - smaller atoms drop off quicker
  - at higher angles, the difference between Y^{3+} and Zr^{4+} is more readily discerned
  - at higher angles, the difference between different oxidation states (eg Zr and Zr^{4+}) is less prominent

Diffraction Intensities – Temperature Factor

$$f = f_0 \exp\left[-\frac{B \sin^2 \theta}{\lambda^2}\right]$$

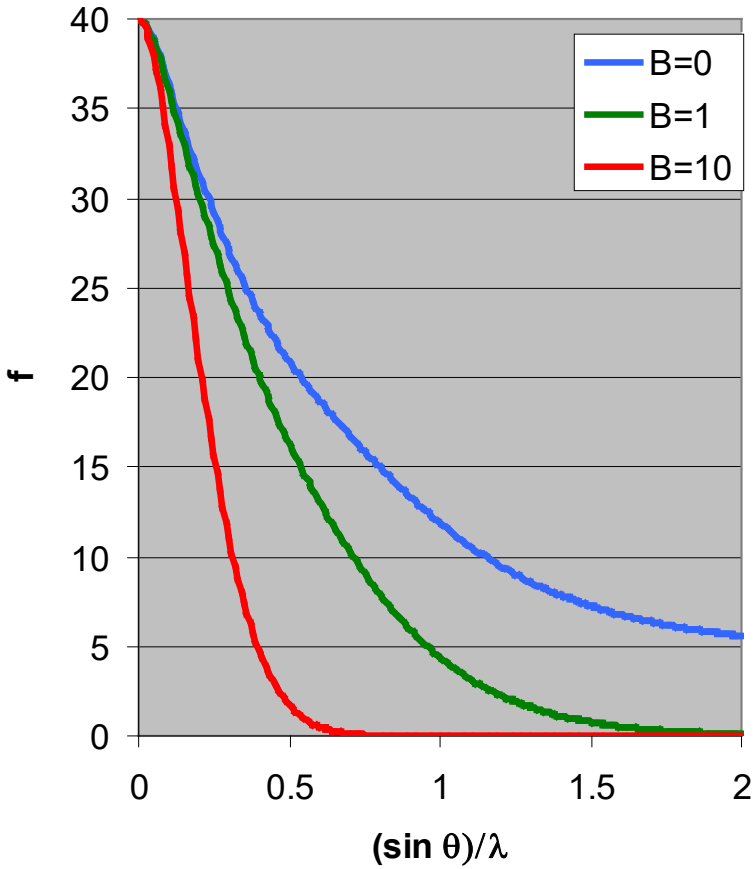

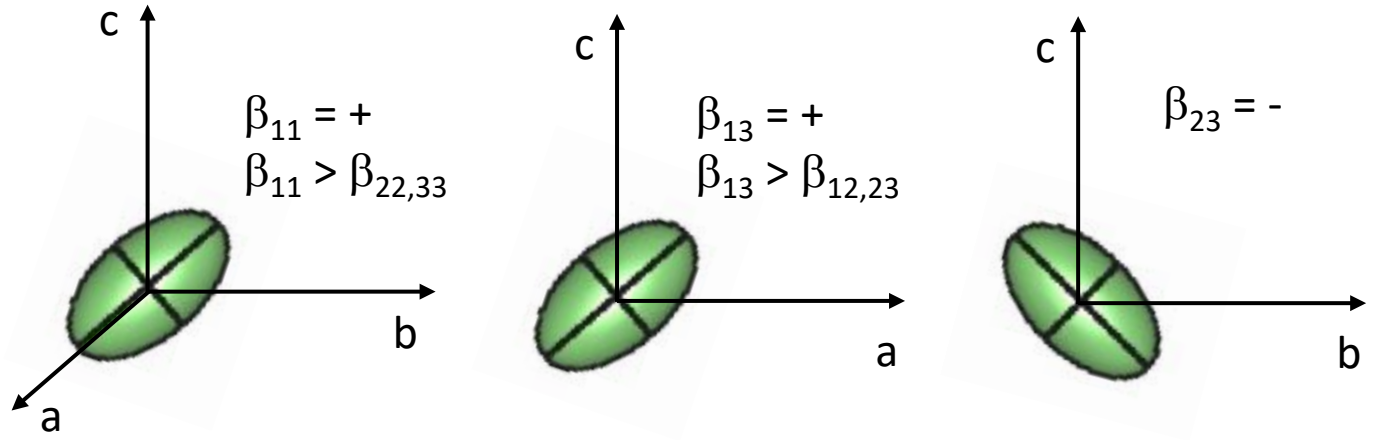

- Efficiency of scattering by an atom is reduced because the atom and its electrons are not stationary - atom is vibrating about its equilibrium lattice site
- The amount of vibration is quantified by the Debye-Waller temperature factor:
  - $B=8\pi^2U^2$, U^2 is the mean-square amplitude of the vibration
  - this is for isotropic vibration: sometimes B is broken down into six Bij anisotropic terms if the amplitude of vibration is not the same in all directions.
  - aka temperature factor, displacement factor, thermal displacement parameter

Exp. Structure Factor Calculations

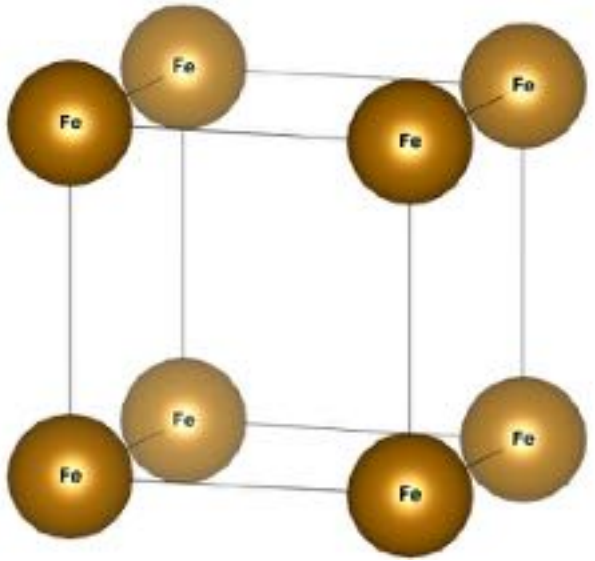

The simplest case of a unit cell containing only one atom at the origin, i.e., having fractional coordinates 0 0 0. Its structure factor is

$$F = fe^{2\pi i(0)};$$
$$F^2 = f^2$$

F^2 is thus independent of *h*, *k*, and *l* and is the same for all reflections.

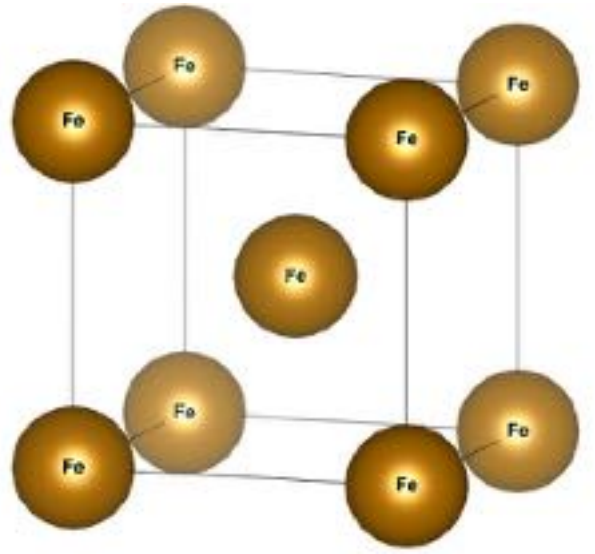

Consider the base-centered cell with two atoms of the same kind per unit cell located at 0 0 0 and ½ ½ ½.

$$F = fe^{2\pi i(0)} + fe^{2\pi i\left(\frac{h}{2}+\frac{k}{2}+\frac{l}{2}\right)}$$

$$= f\left[1 + e^{2\pi i(h+k+l)}\right]$$

$$F = 2f \quad \text{when } (h+k+l) \text{ is even; } F^2 = 4f^2$$

$$F = 0 \quad \text{when } (h+k+l) \text{ is odd; } F^2 = 0$$

Exp. Structure Factor Simulation

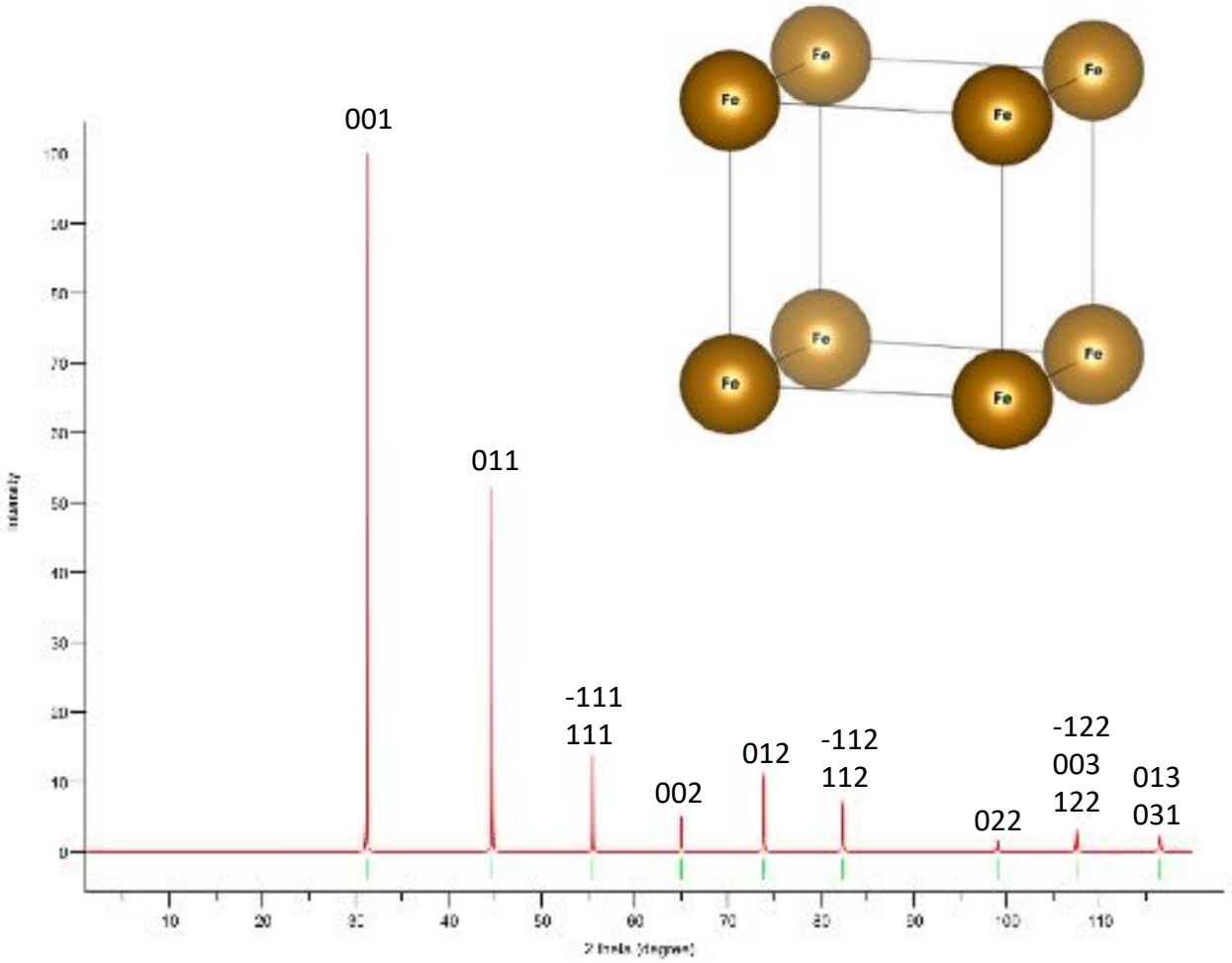

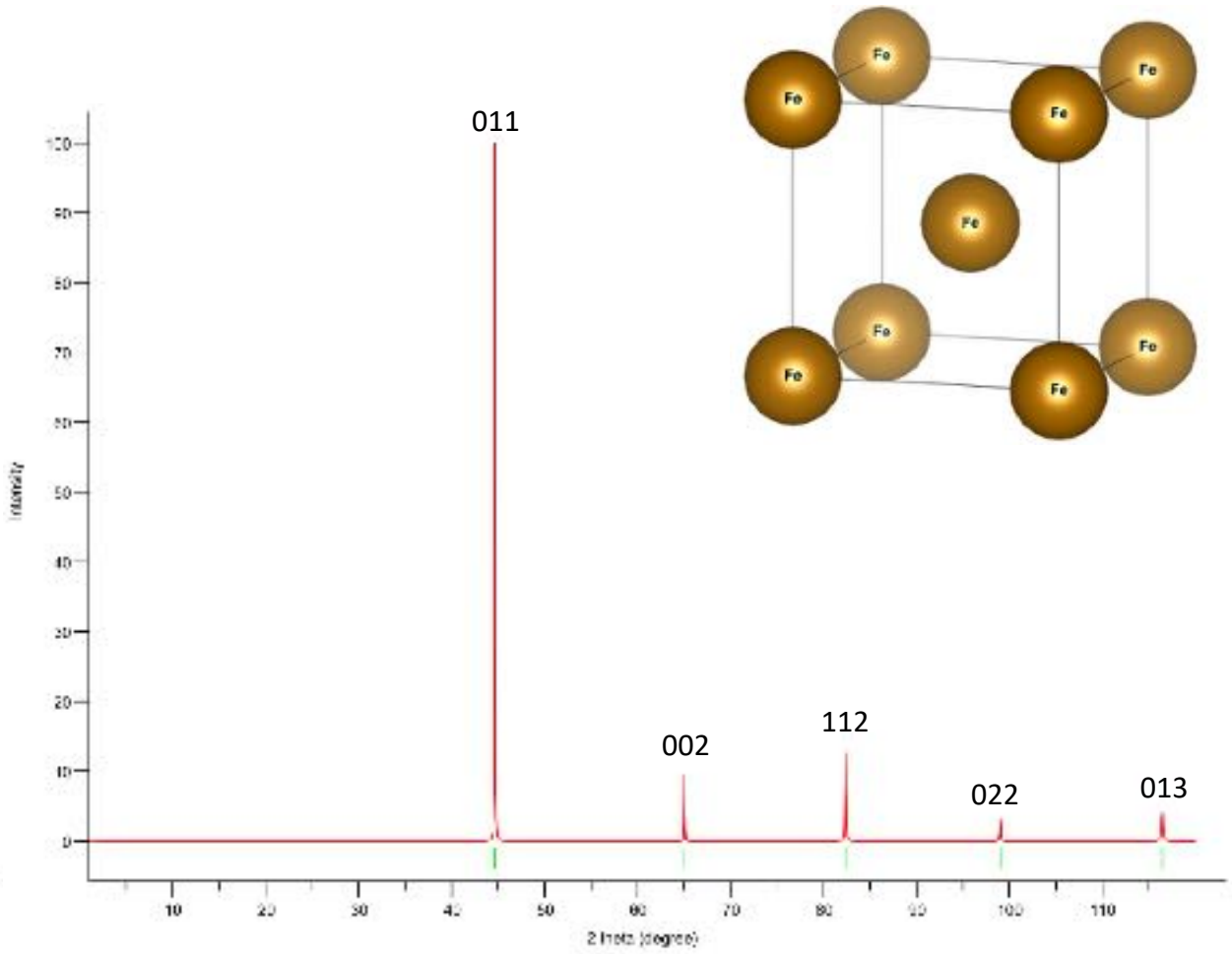

No.	h	k	l	d (Å)	F(real)	F(imag)	|F|	2θ	I	M
1	1	1	0	2.02600	33.6292	6.20768	34.1973	44.6928	100.0000	12
2	2	0	0	1.43260	26.7047	6.05816	27.3832	65.0532	13.7590	6
3	2	1	1	1.16971	22.1339	5.91224	22.9099	82.3764	24.8582	24
4	2	2	0	1.01300	18.875	5.76983	19.7372	99.0007	8.0713	12
5	3	1	0	0.90606	16.4507	5.63086	17.3877	116.459	14.4626	24

Crystals and Symmetry

Imagine…

- having to describe an infinite crystal with an **infinite number of atoms**
- or even a **finite crystal**, with some **10^{20} atoms**

Sounds horrible?... Well, there's **symmetry** to help you out! Instead of an infinite number of atoms, you only need to describe the contents of **one-unit cell**, the structural repeating motif…

- and life could be even easier, if there are **symmetry** elements present inside the **unit cell**!
- you only need to describe the **asymmetric unit** if this is the case

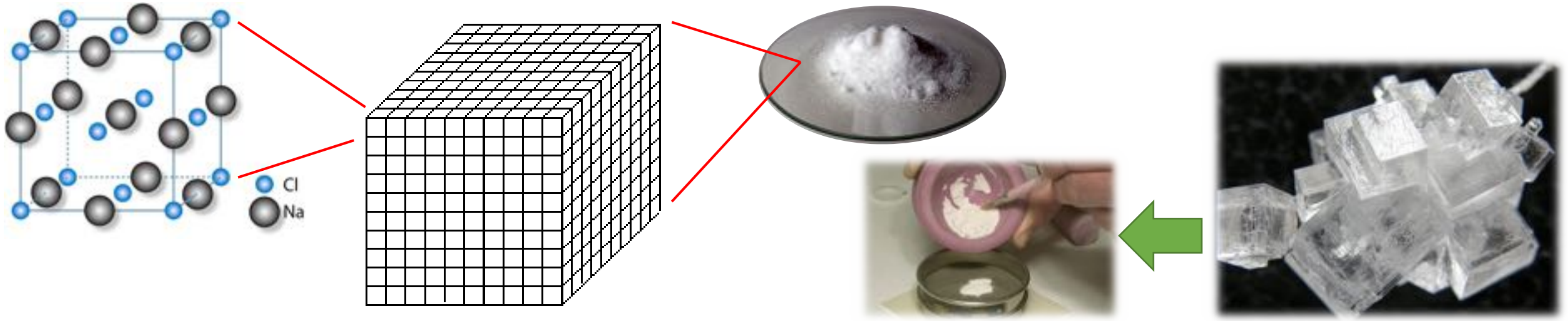

Single Crystal vs Powder Diffraction

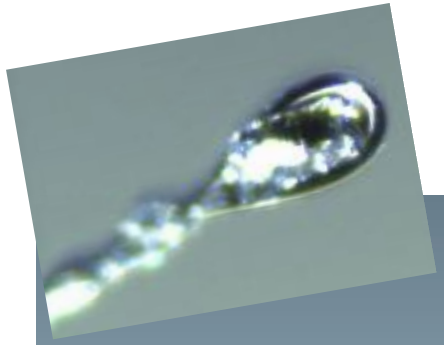

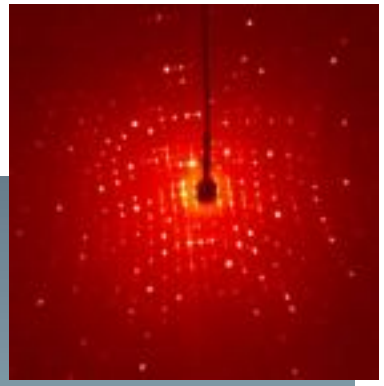

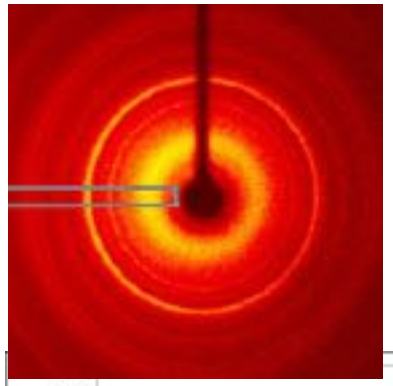

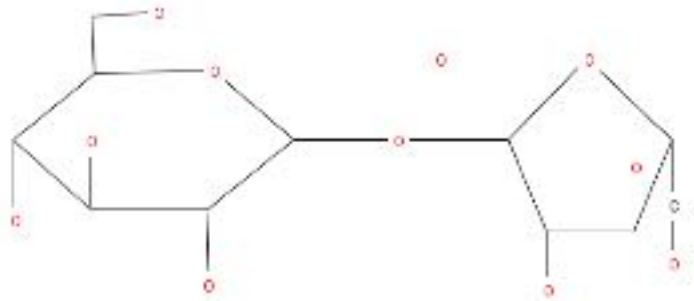

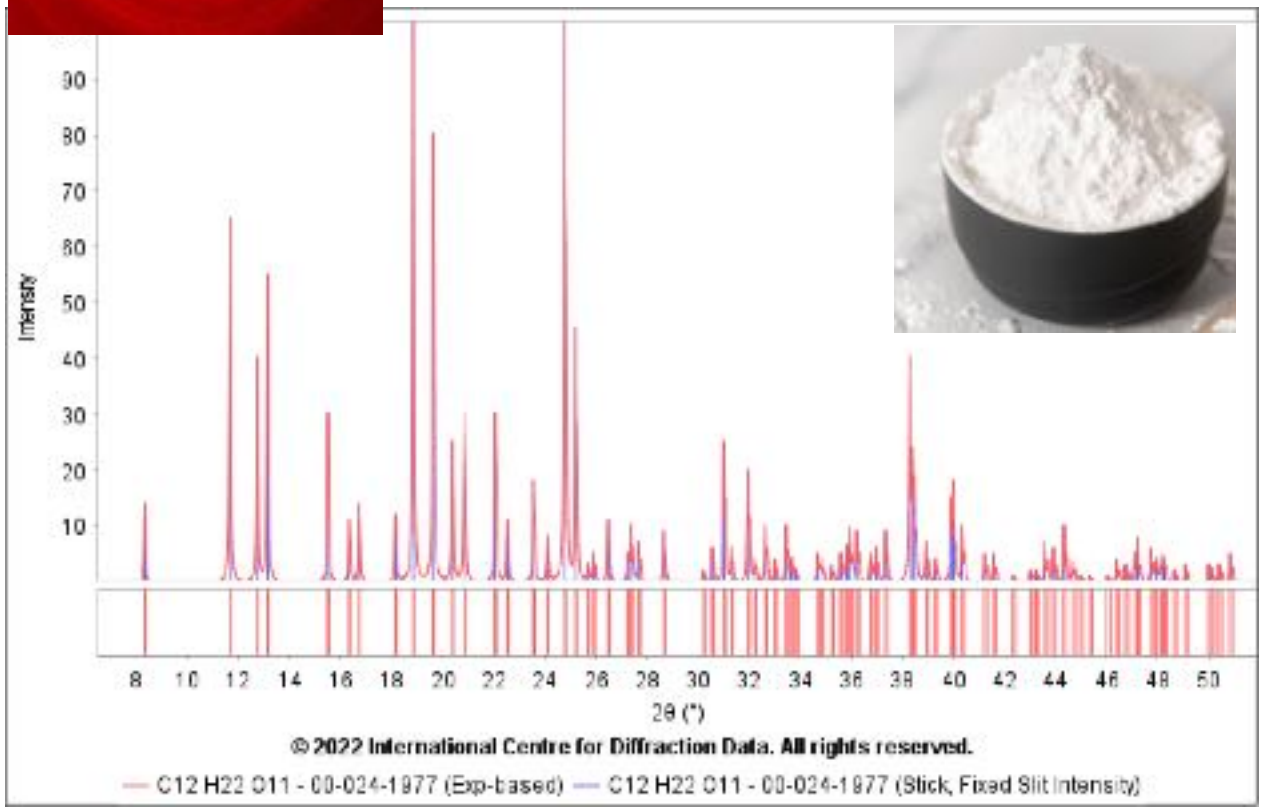

XRD Machine

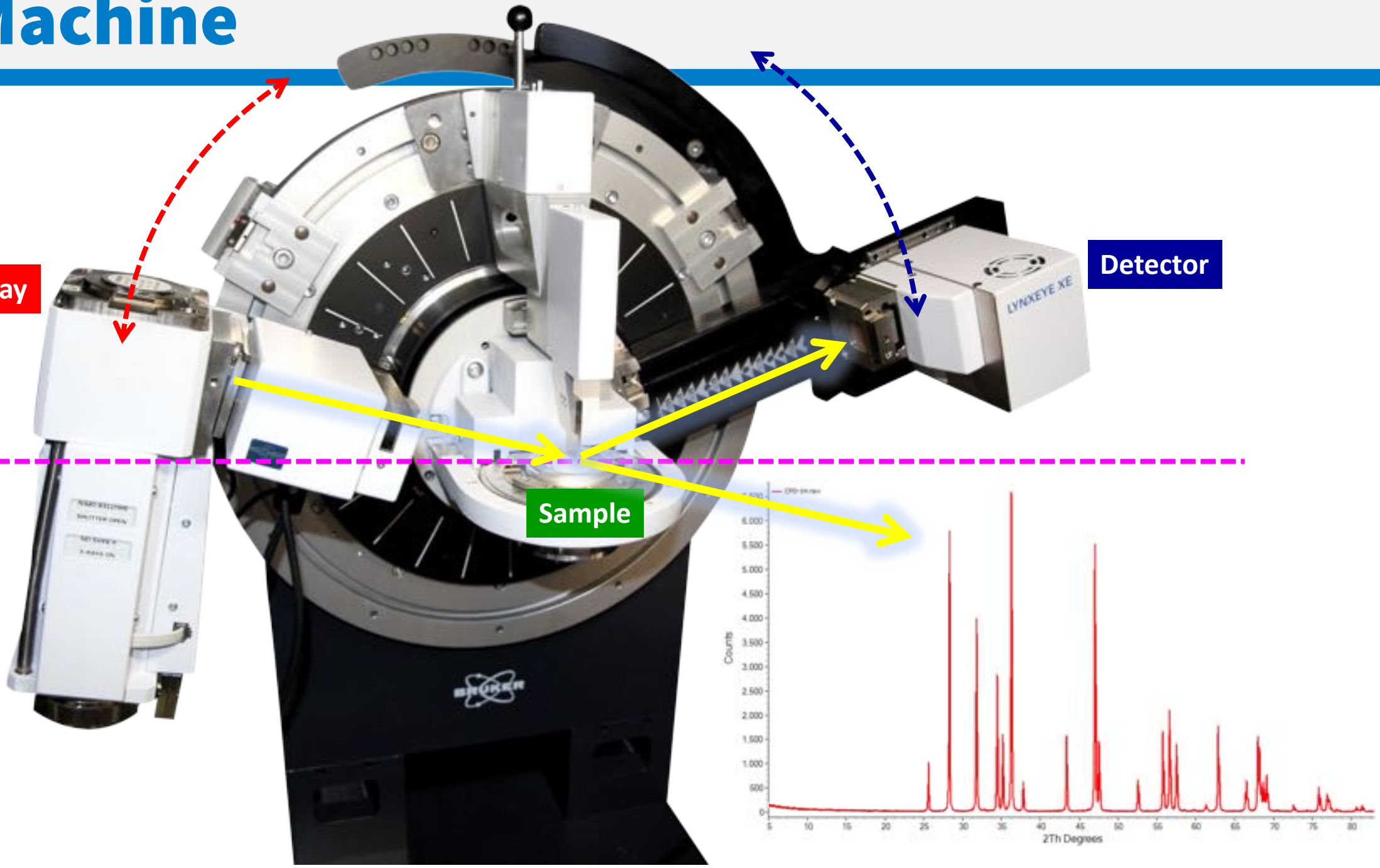

PXRD fingerprints

- A particular phase (particular atoms arranged in a particular crystal structure) gives a particular set of diffractions peaks

Peak intensities

- Atoms on each site
- Quantitative analysis
- Texture/Preferred Orientation

Crystal structure

Peak positions

- Space group
- Lattice parameters

Profile width and shape

- Instrument contributions
- Microstructure of sample (Size, strain, stacking faults, ...)

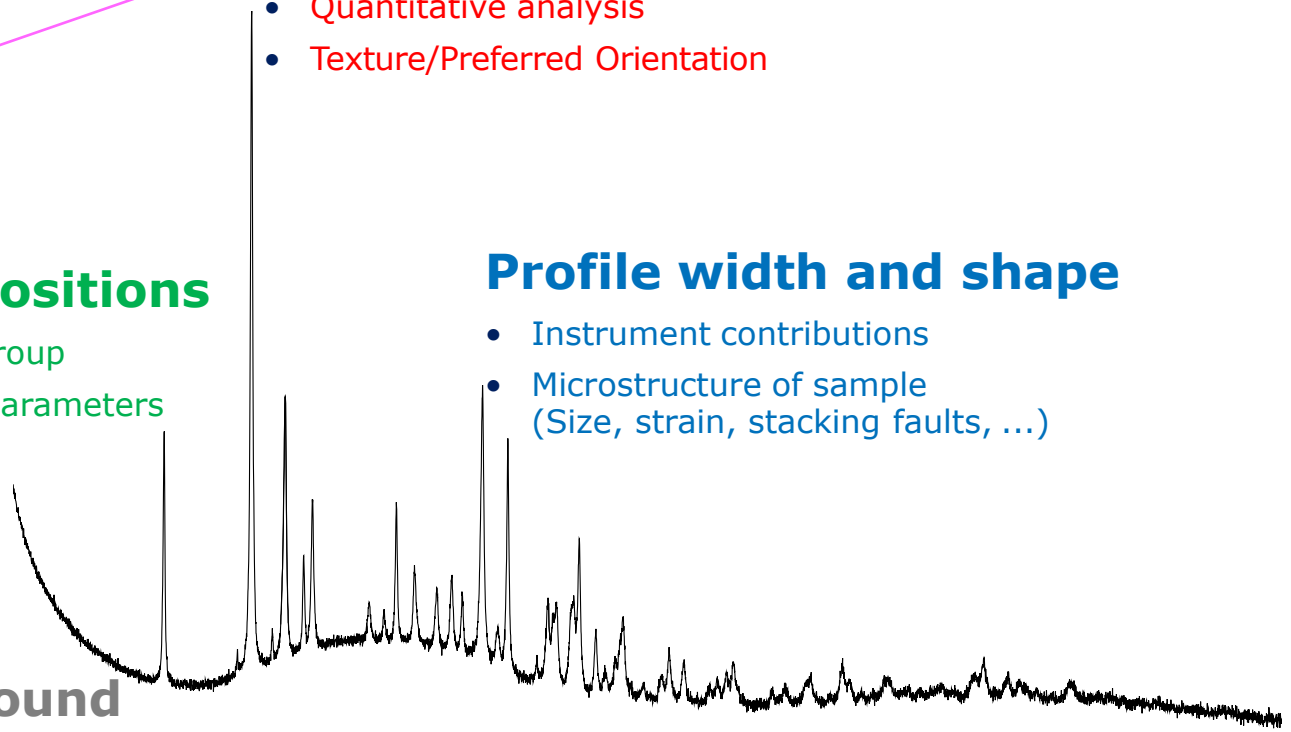

Background

- Scattering from sample environment (air, sample holder, ...)
- Local order / disorder
- Amorphous phase amounts, "degree of crystallinity"

Quality of PXRD

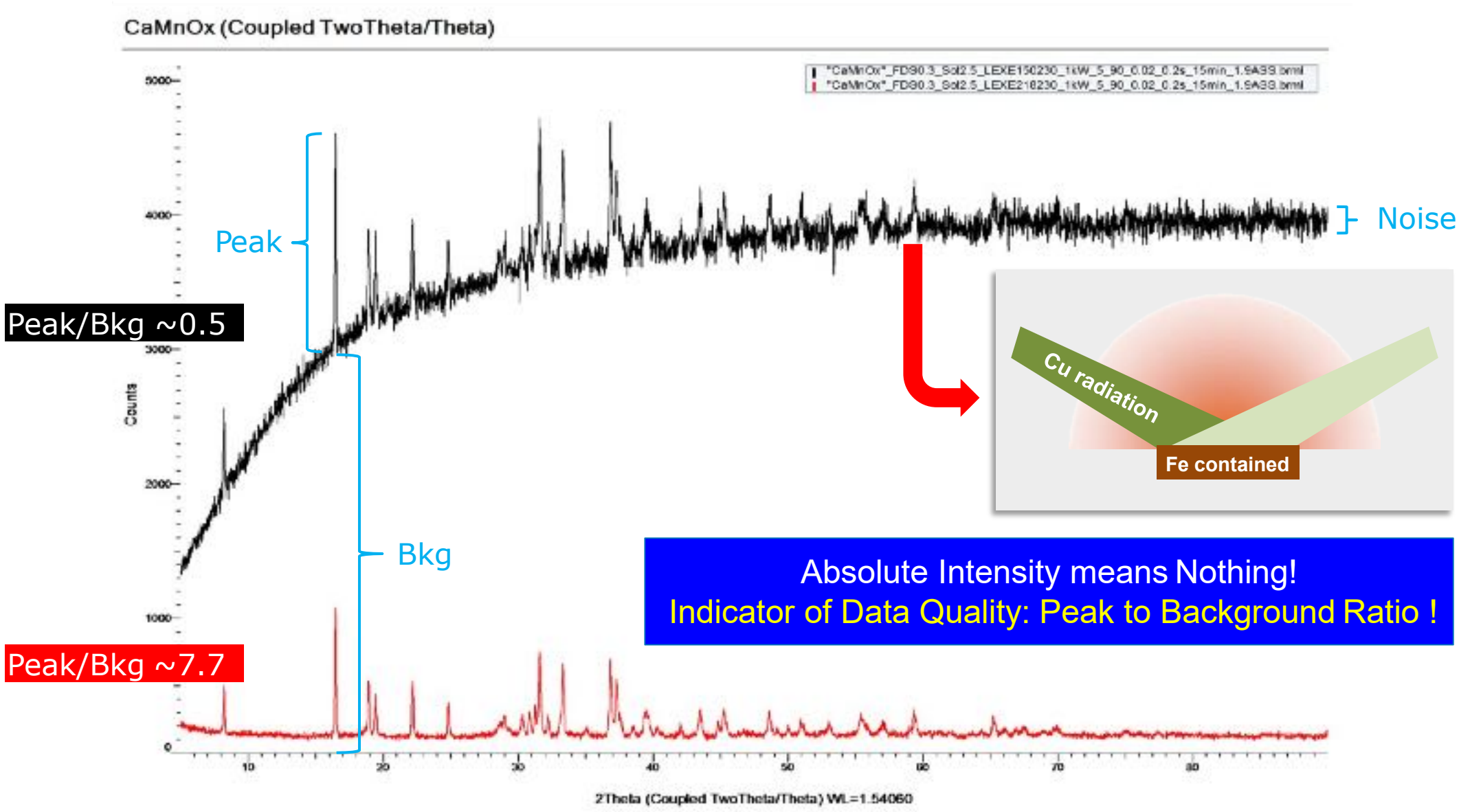

Phase Analysis Flow Chart

XRD (Emission, Radius, Optics, Detector)

RAW data (.brml, .raw, .xy)

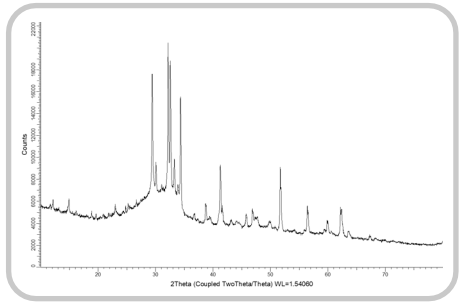

EVA

Qualitative Analysis (Search and Match)

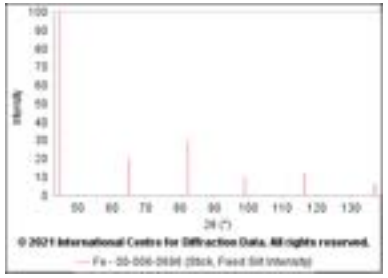

Stick pattern

ICDD-PDF4 (Database)

TOPAS

Quantitative Analysis (Rietveld analysis)

*.CIF, *.STR

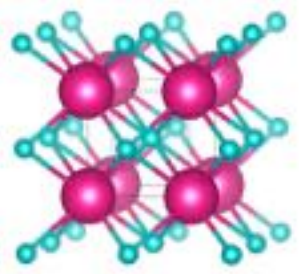

VESTA

Refinement report
- Diffractogram
- R-factors
- Structure
- QPA
- Crystallite Size
- Preferred Orientation
- etc.

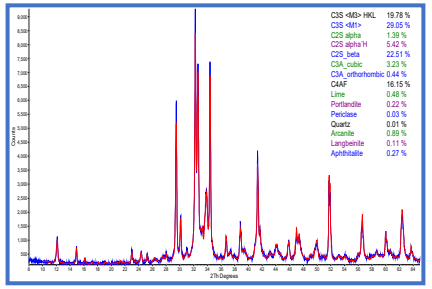

Refined Structure files
- *.CIF
- *.STR

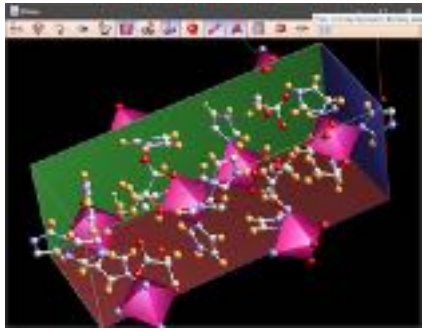

ICDD PDF-4+ 2021 Database (444.133)

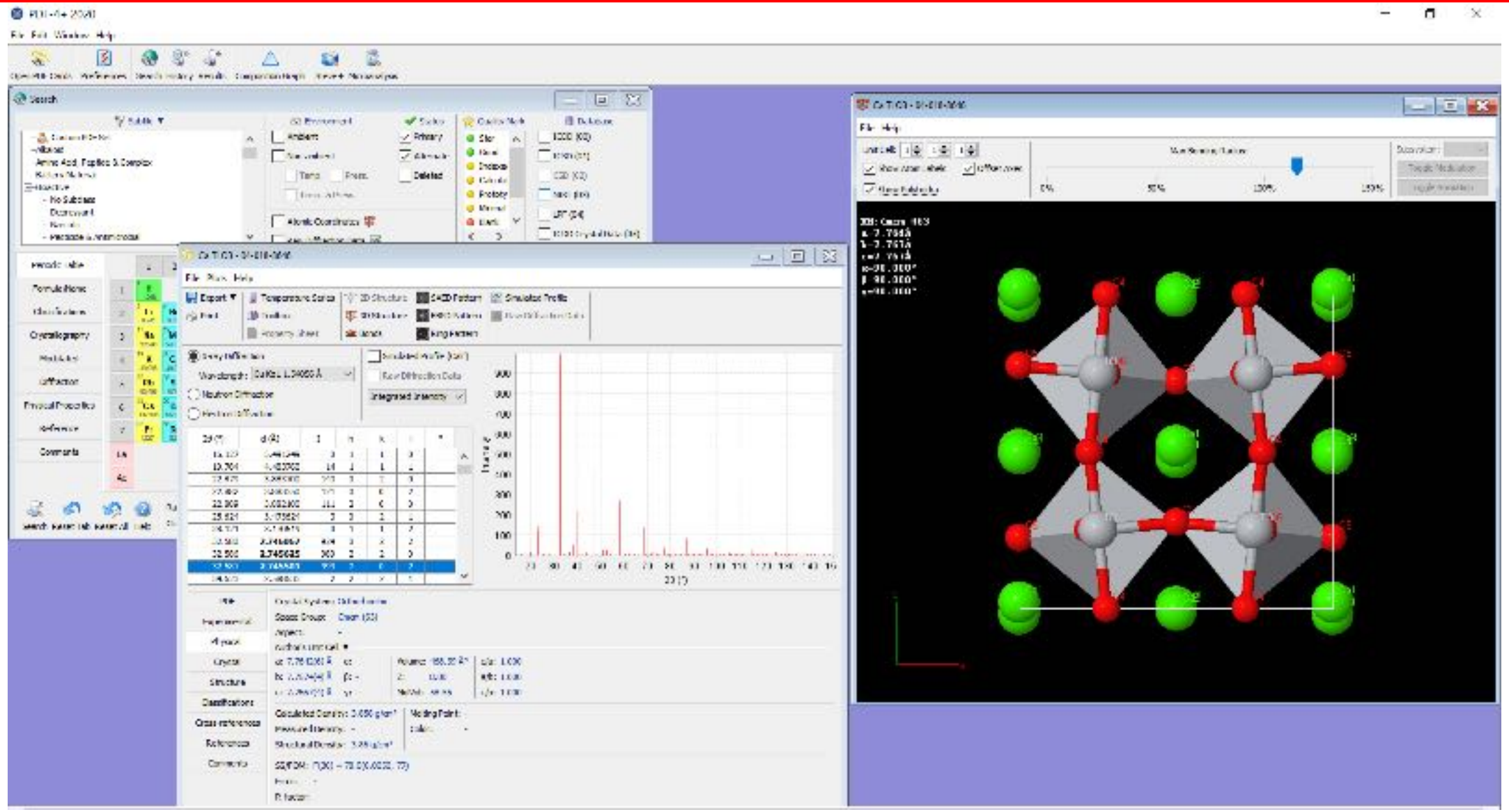

Nucleation & Grain Boundary

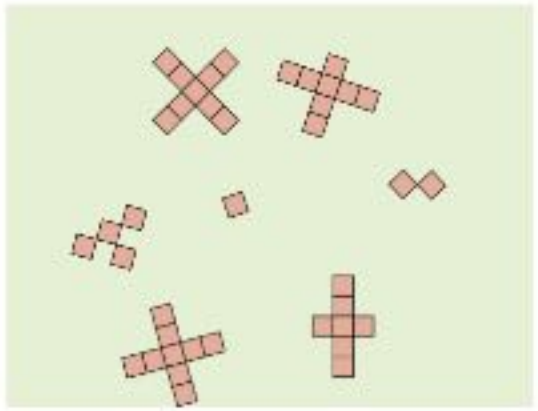

(a)

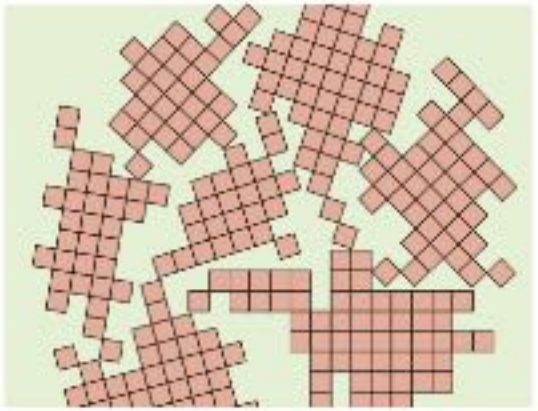

(b)

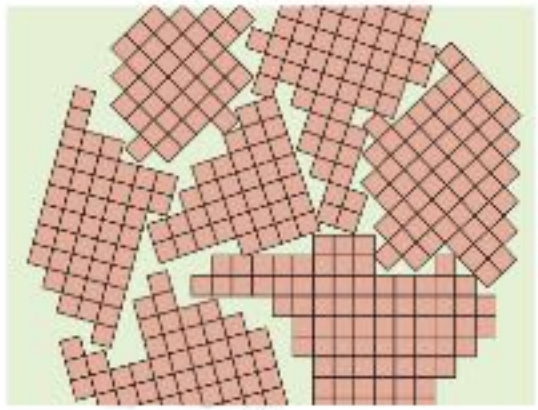

(c)

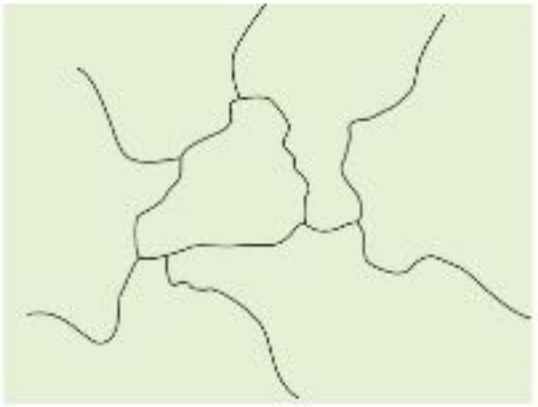

(d)

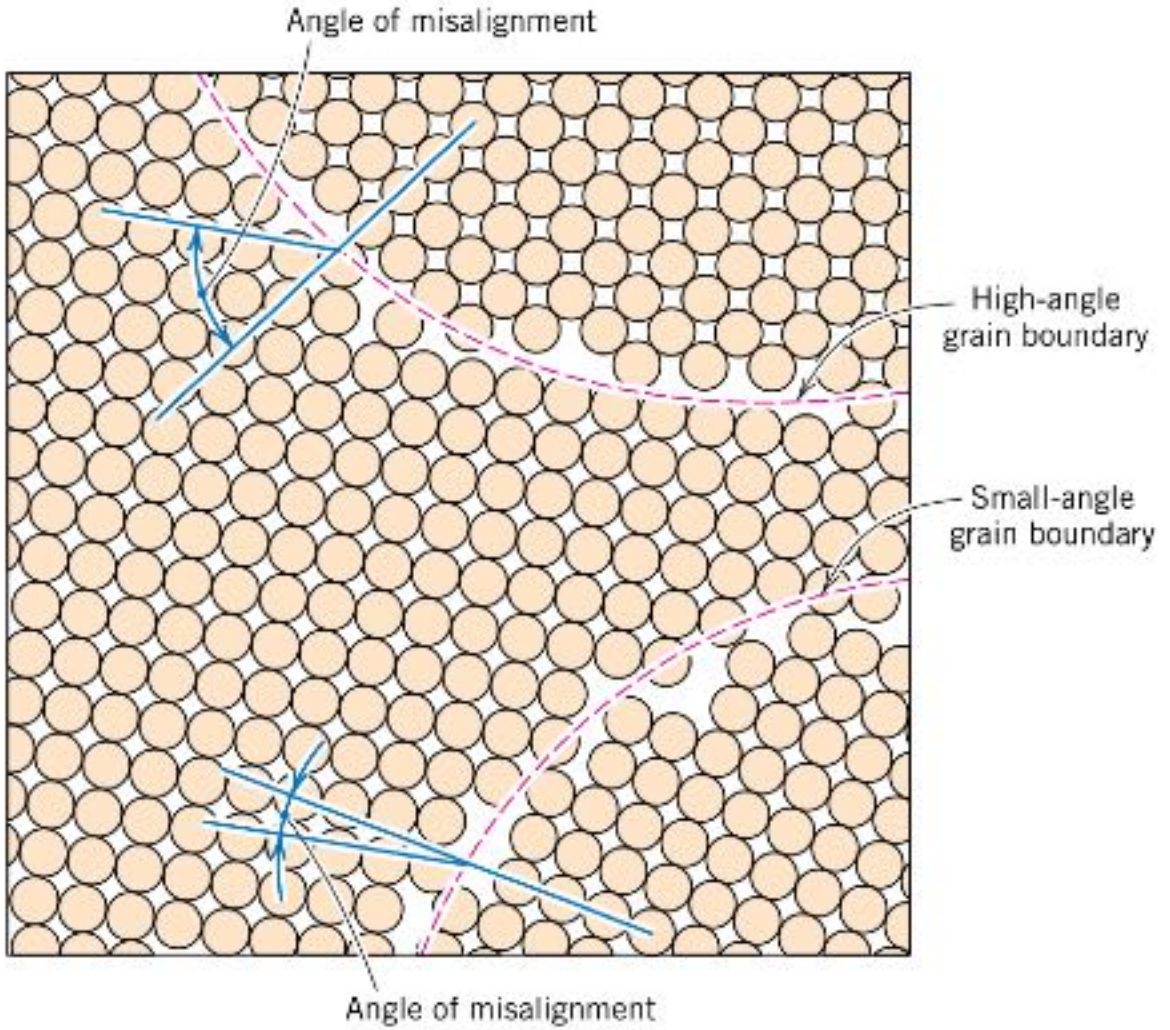

Sampel Broadening – Crystallite Size

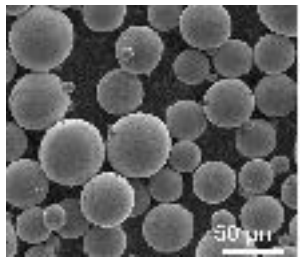

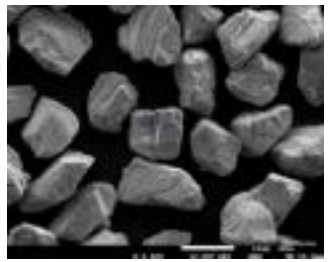

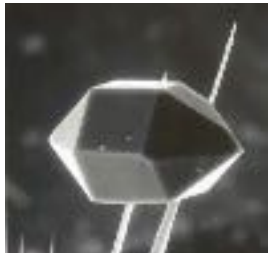

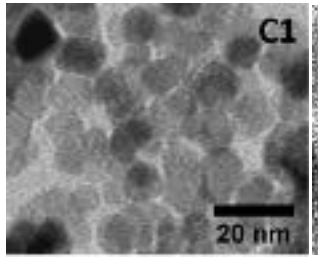

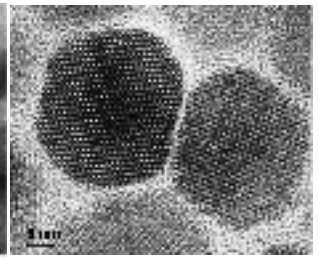

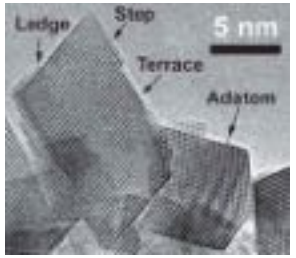

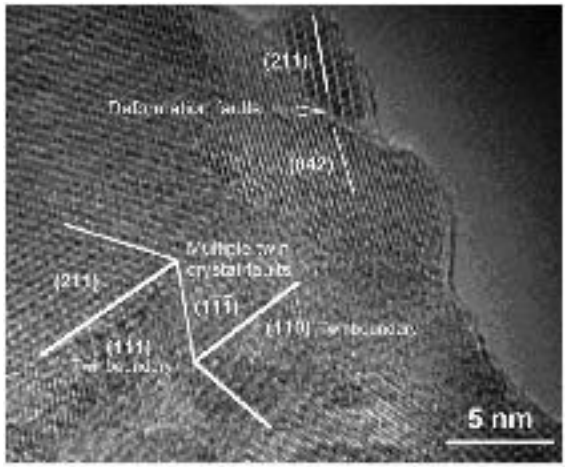

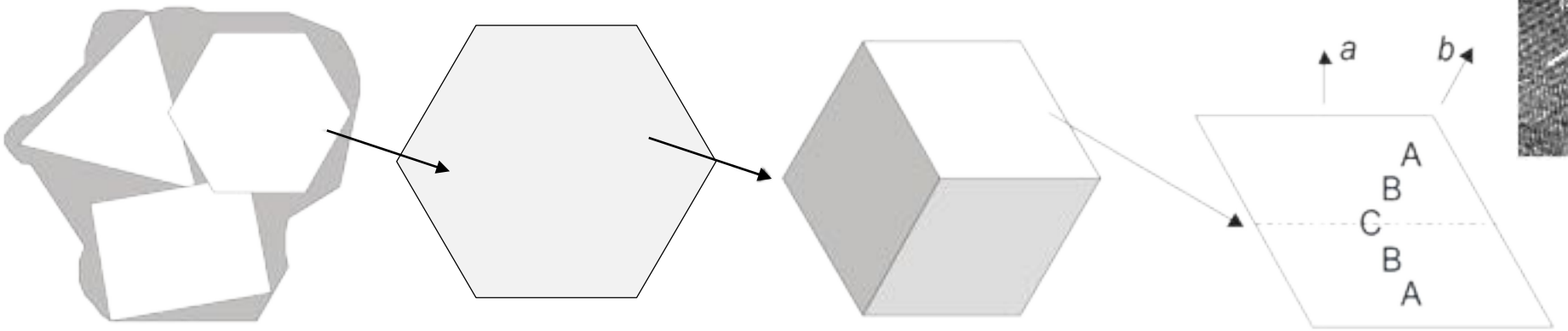

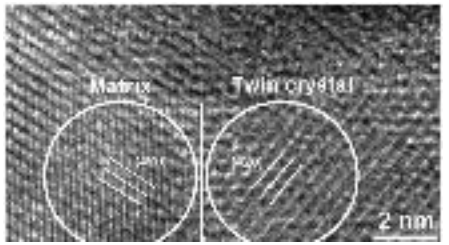

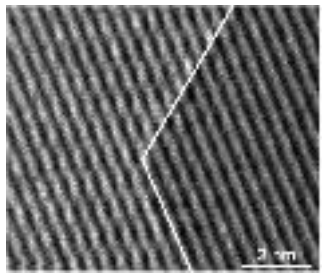

Particle

- Consists of several, separated crystals

Crystal

- Infinite, 3D periodic lattice
- Surface → 2D defect

Crystallite

- Small crystals
- Possibly held together through defective boundaries

Indirectly determined by PXRD

Domains

- Coherently diffracting volumes without 2D defects

Underlying source of size broadening

Topas 6 - Technical Reference (2017)

Lattice – Surroundings (Surface Energy)

- Lattice = infinite arrangement of points in space (3D) / in the plane (2D) / on a line (1D),
  in which all points have the same surrounding

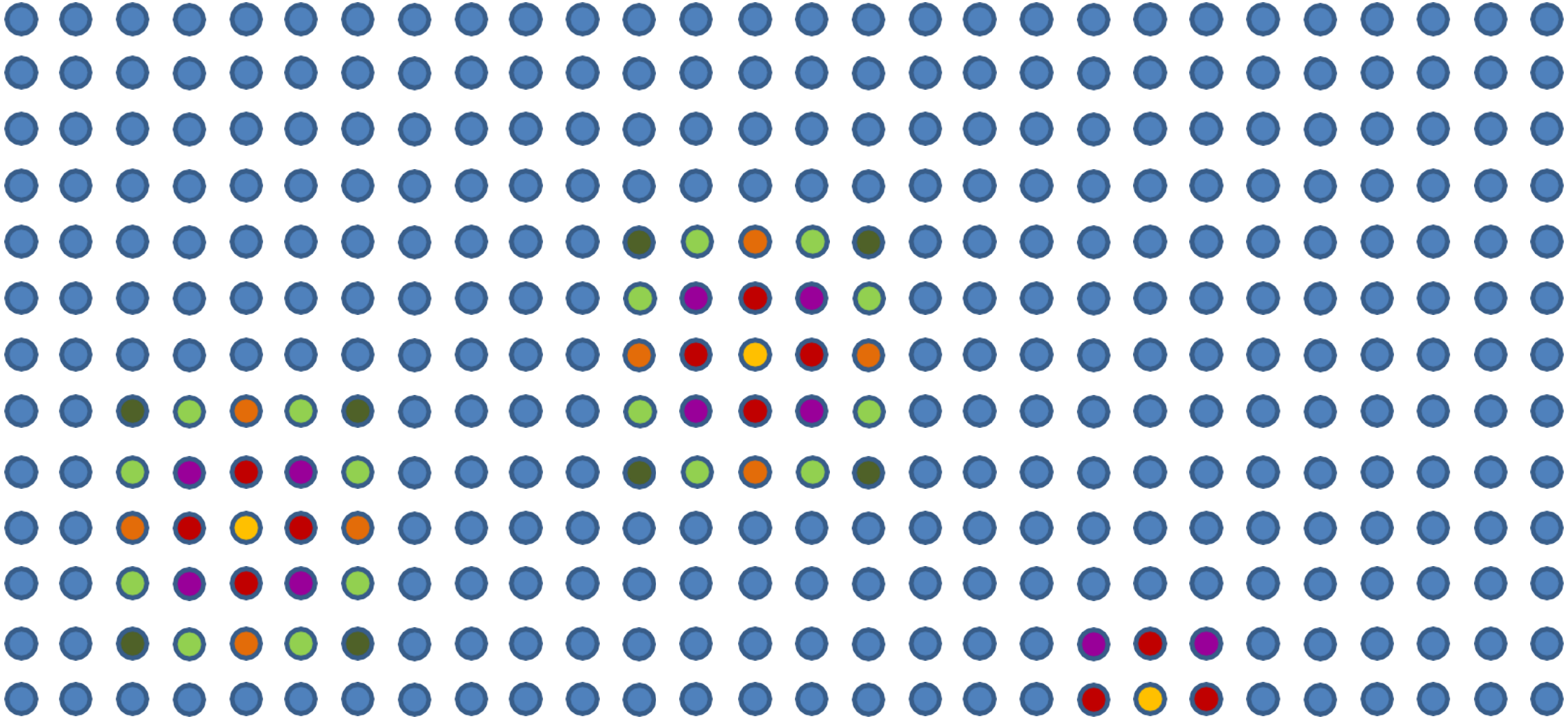

Texture Analysis

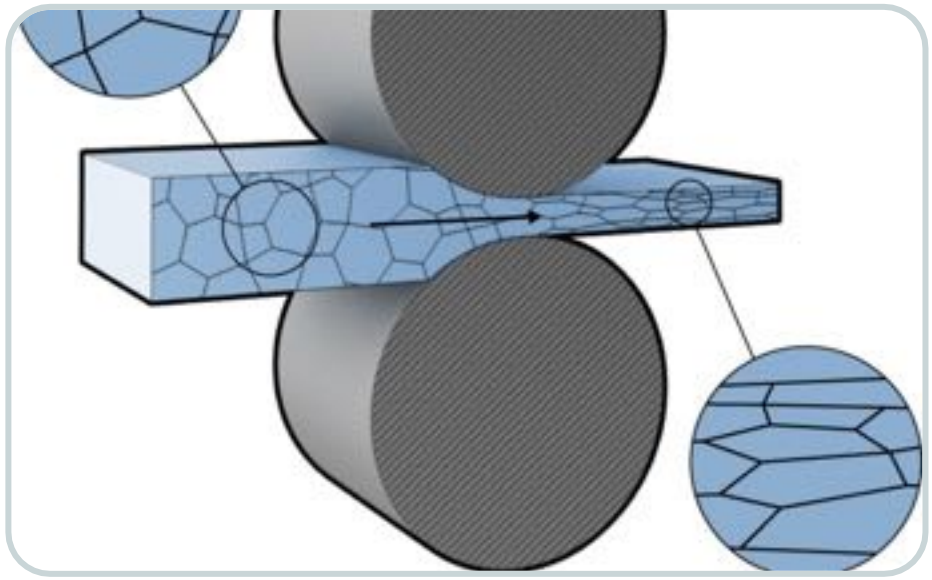

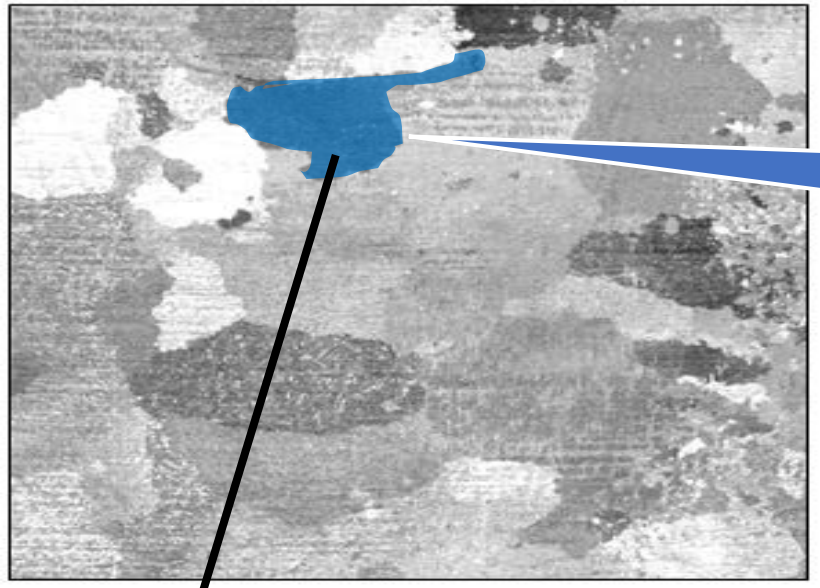

Crystal orientation in cold rolled steel

Crystal orientation dictates:

- Strength
- Elasticity
- Hardness
- Thermal expansion
- Conductivity
- Optical properties
- Magnetic properties
- etc

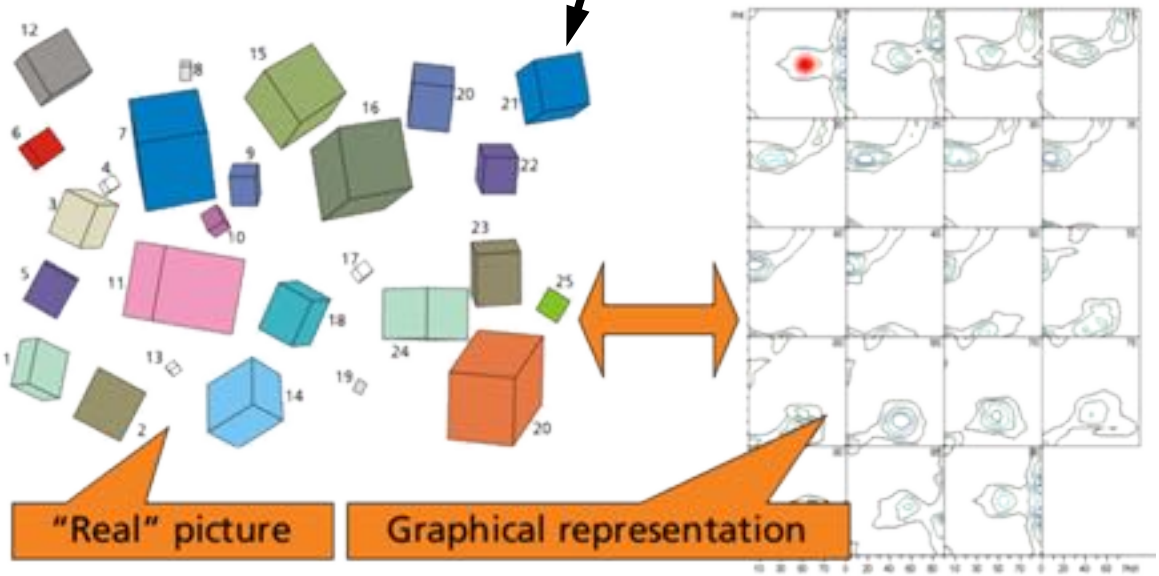

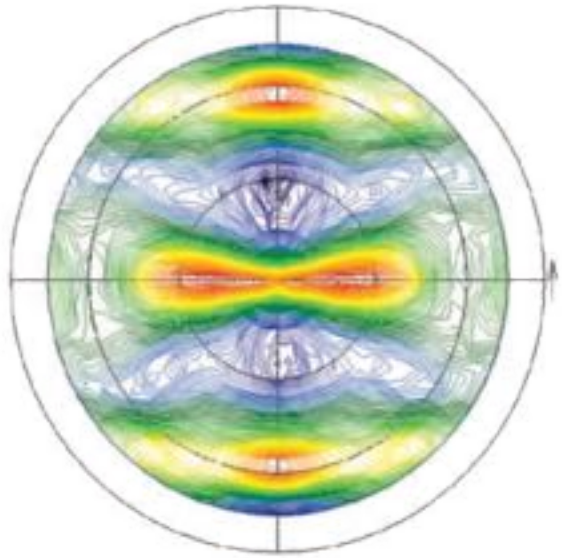

Residual Stress Analysis

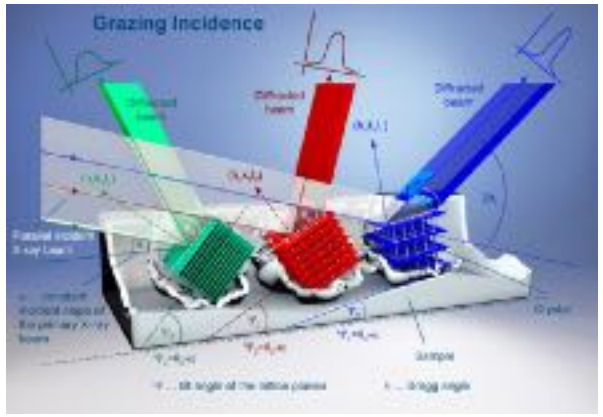

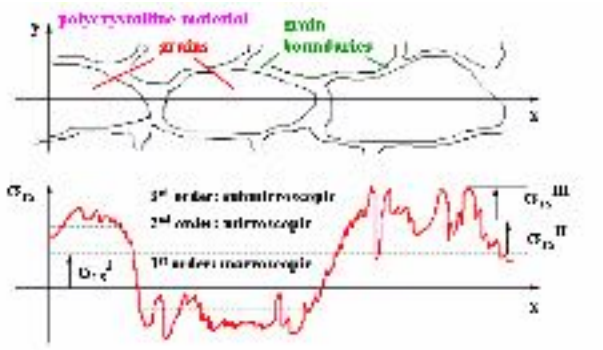

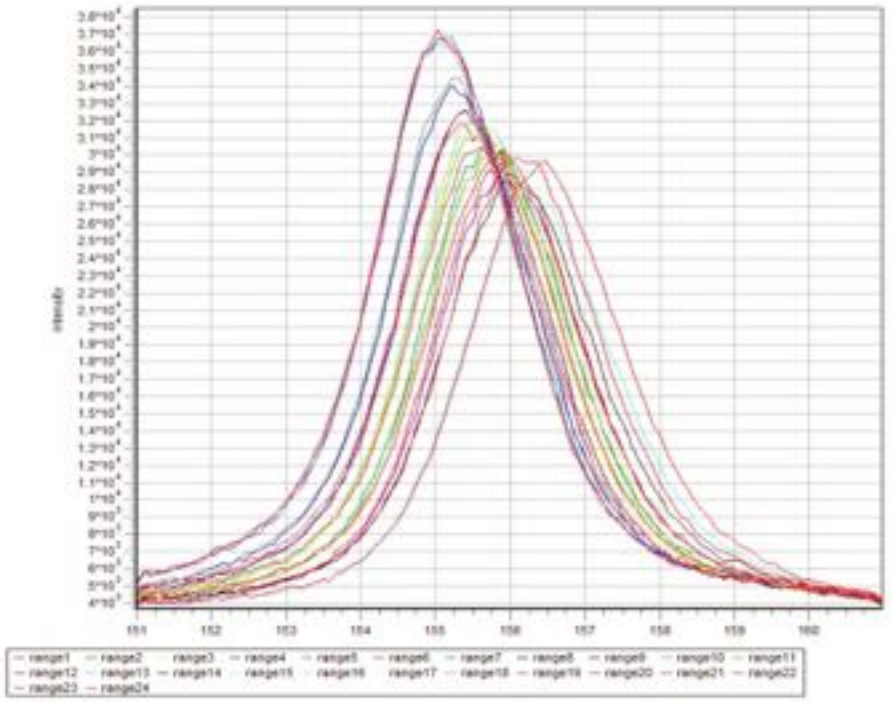

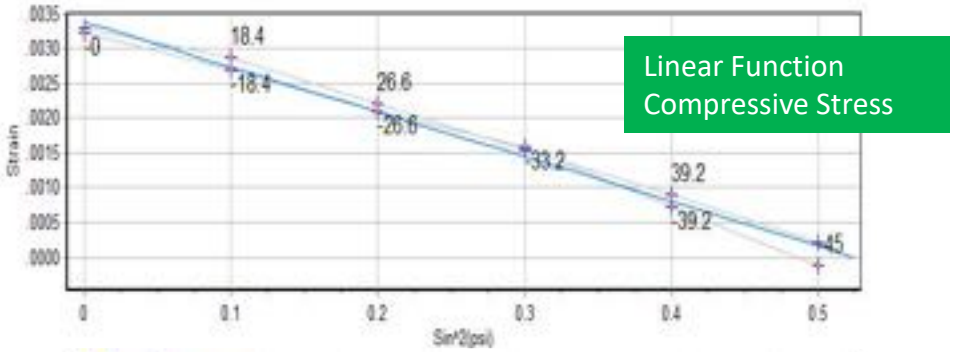

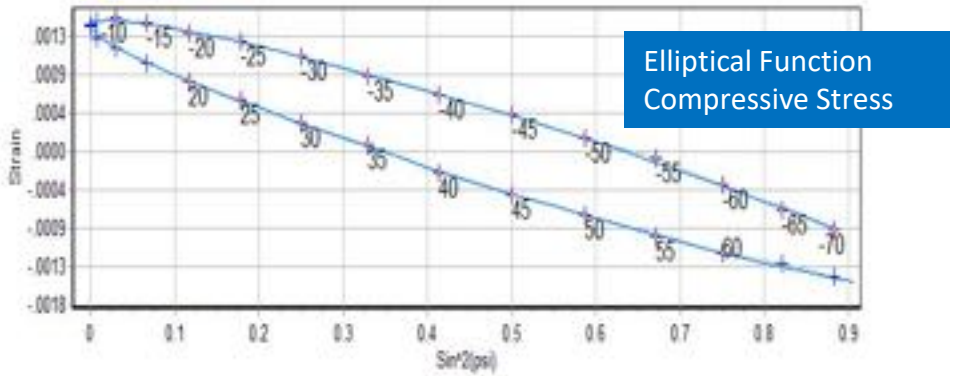

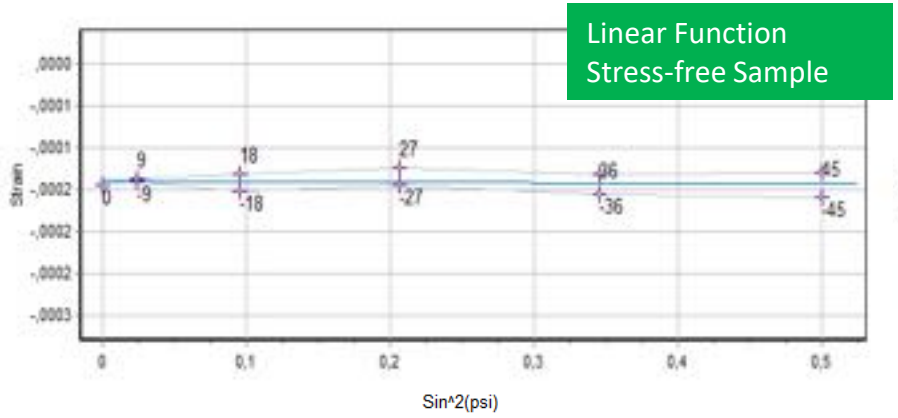

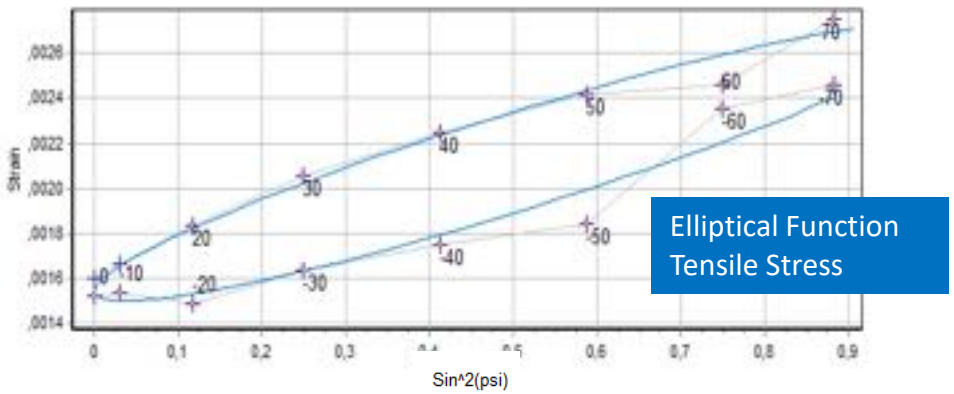

Micro-Diffraction

Human hair

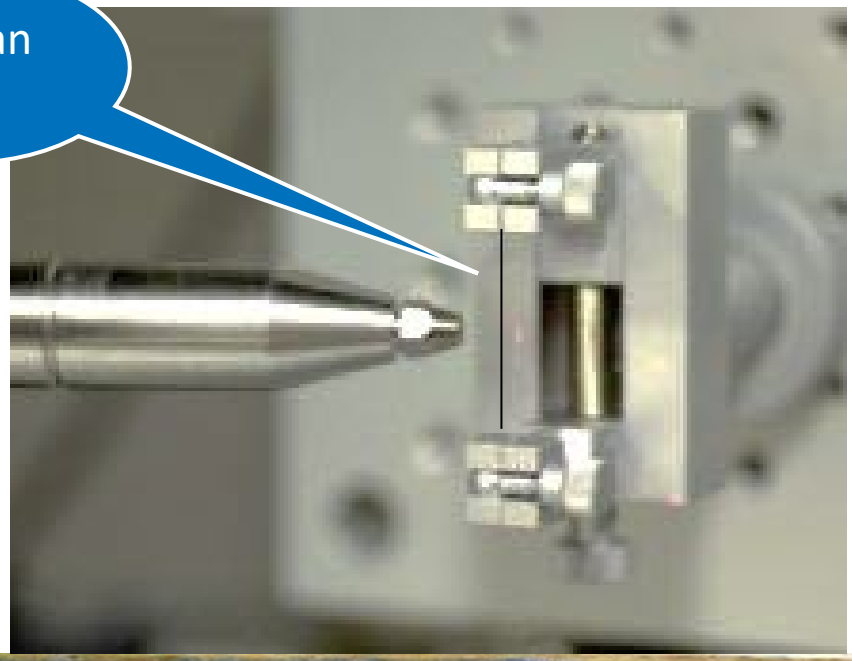

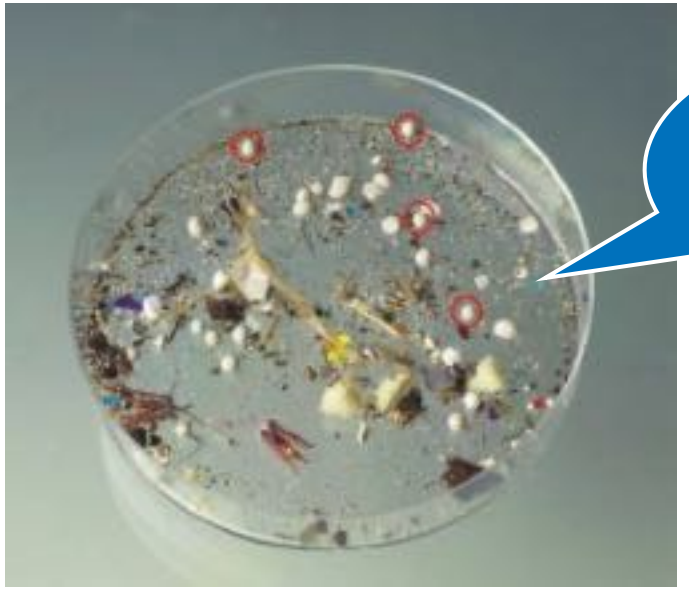

Crime scene samples

Color pigment

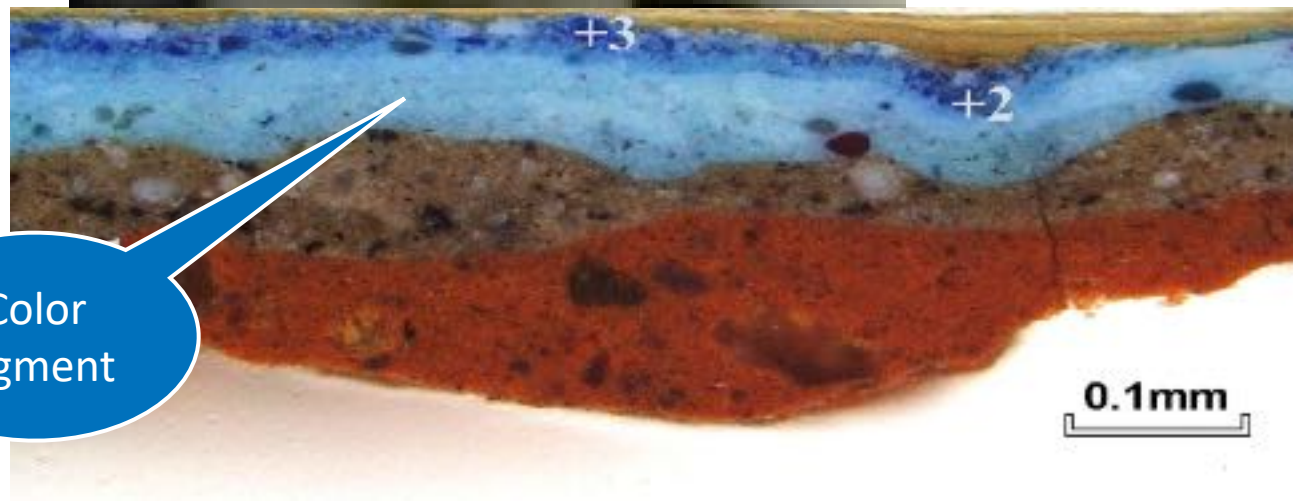

Rock Crystal

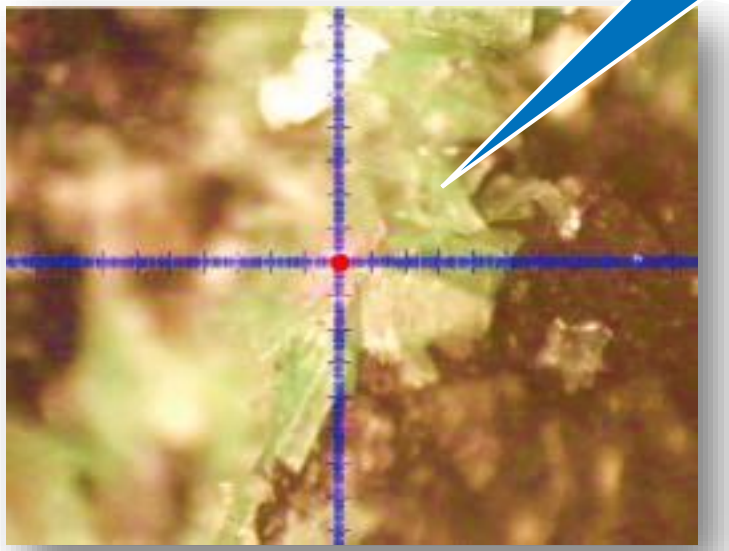

Thin Film - XRR

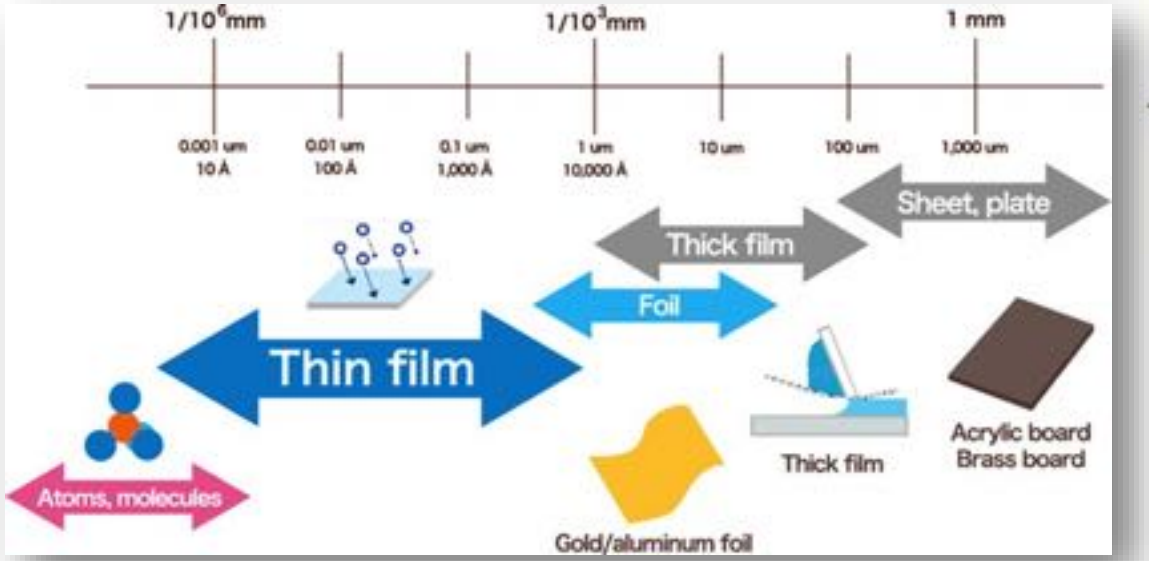

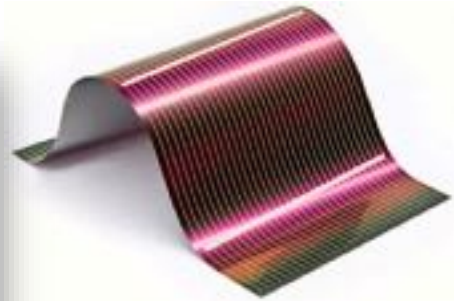

Reflectivity information:

- ✓ Density
- ✓ Thicknesses
- ✓ Roughness
- ✓ Interface quality

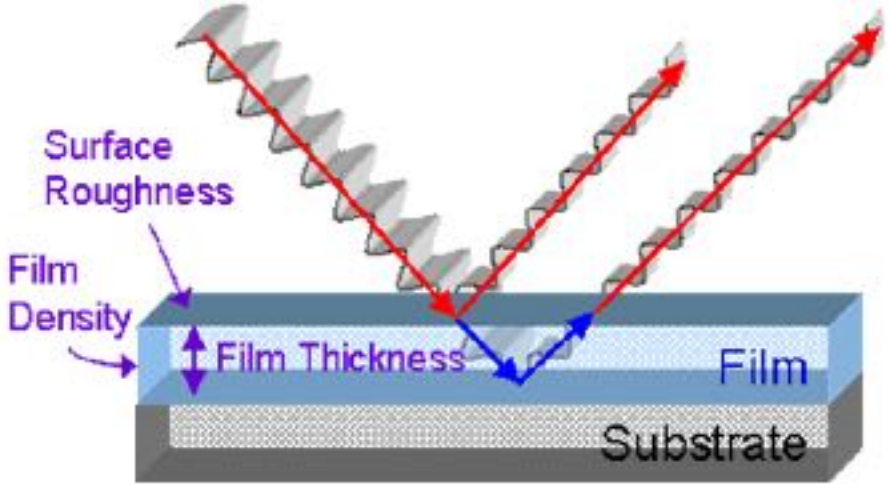

- ❖ X-rays interact with the whole film
- ❖ Thickness 0.1 - 1,000 nm
- ❖ Structural scale > nm measurement
- ❖ $\omega < 7°$ or $(2\theta < 14°)$

Thin Film - Depth Profile Analysis

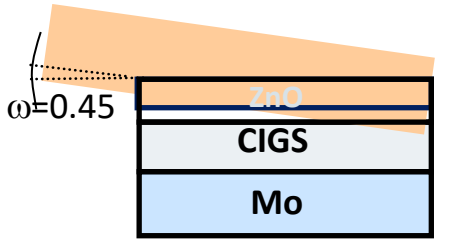

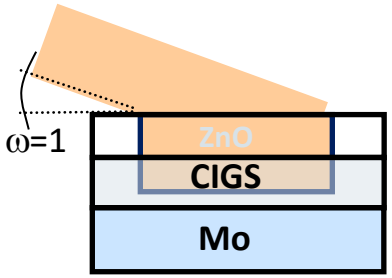

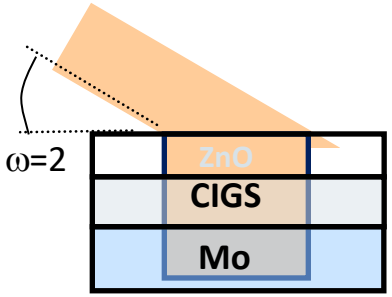

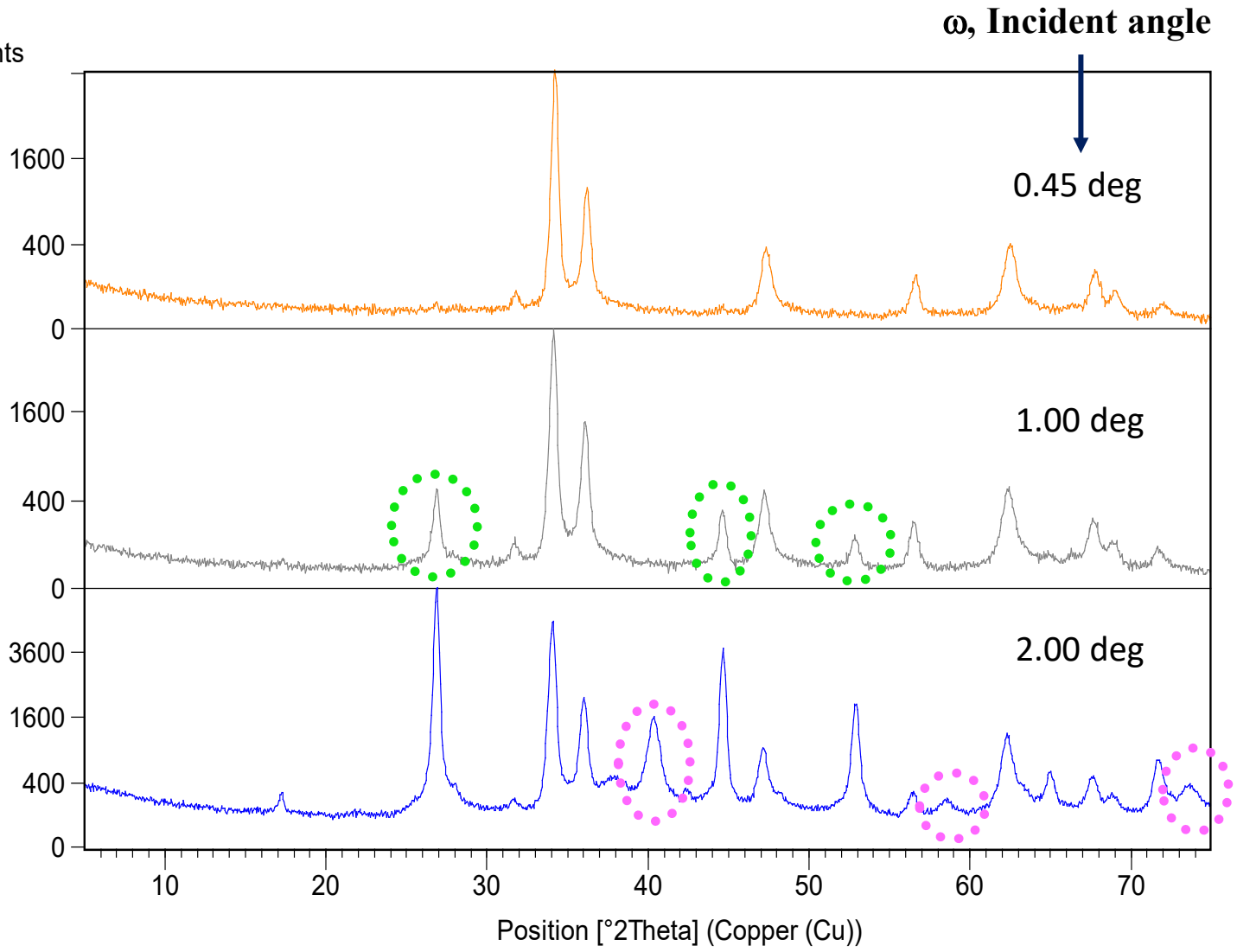

Thin Film - Reciprocal Space Map

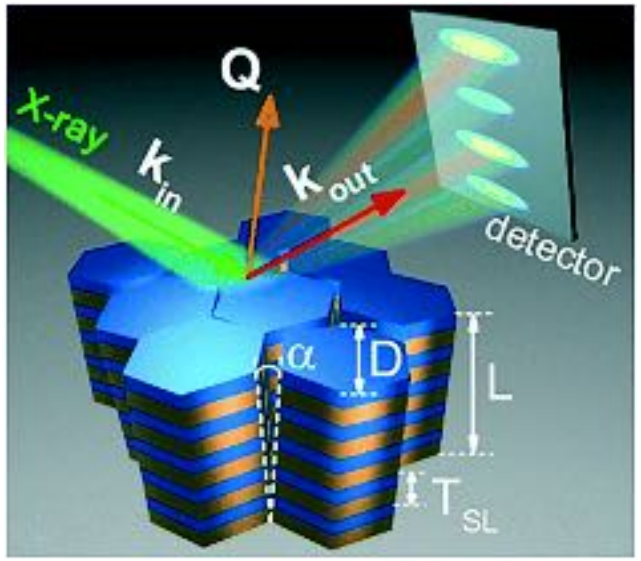

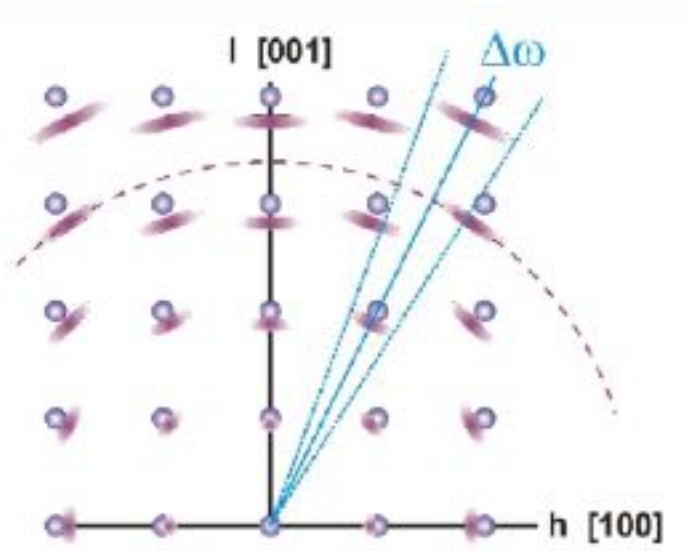

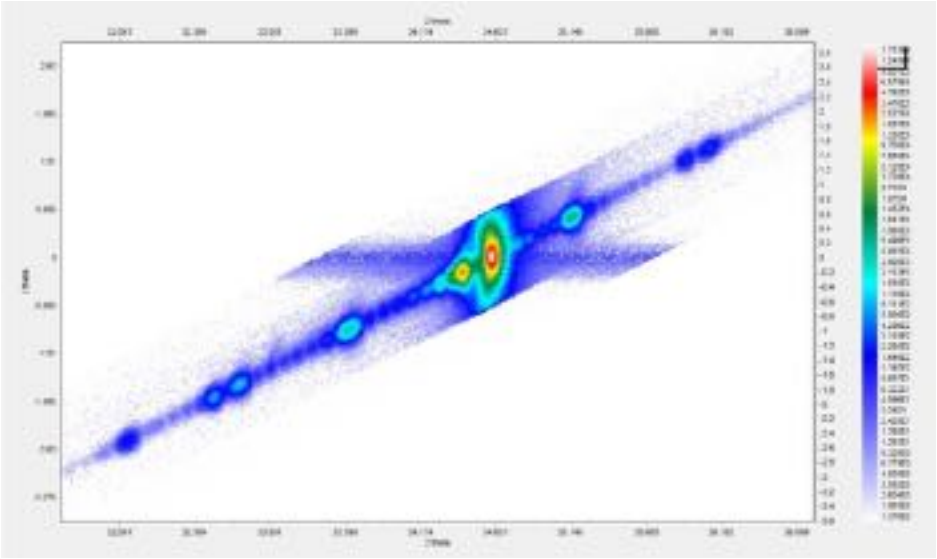

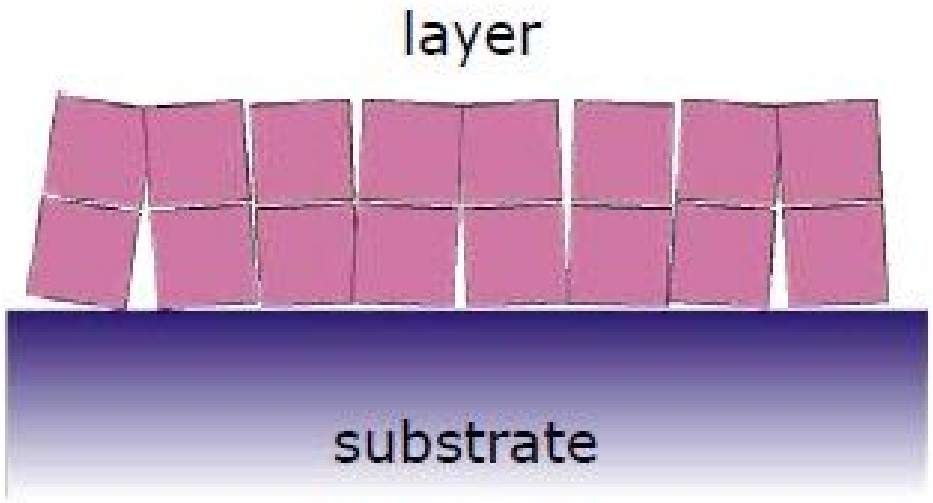

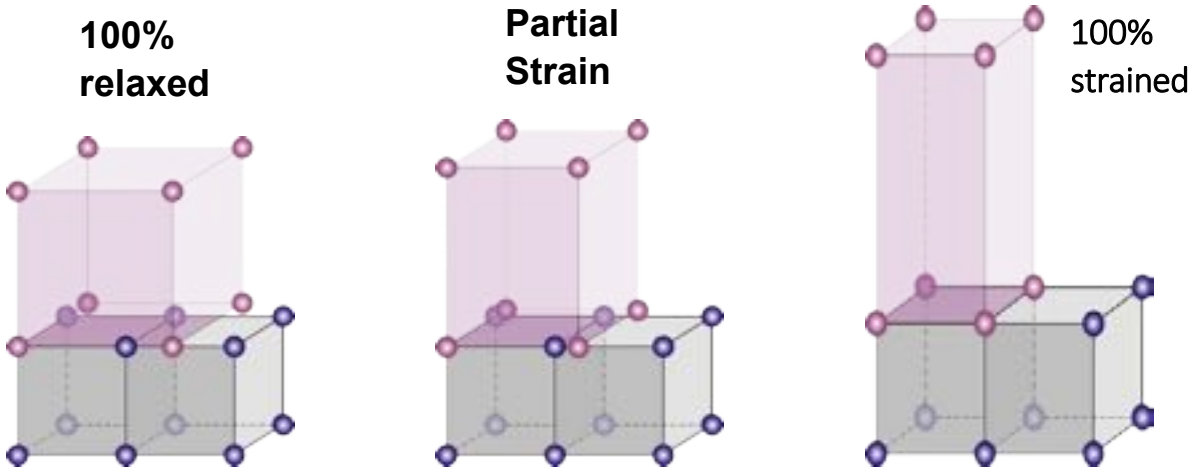

Micro-Diffraction

Human hair

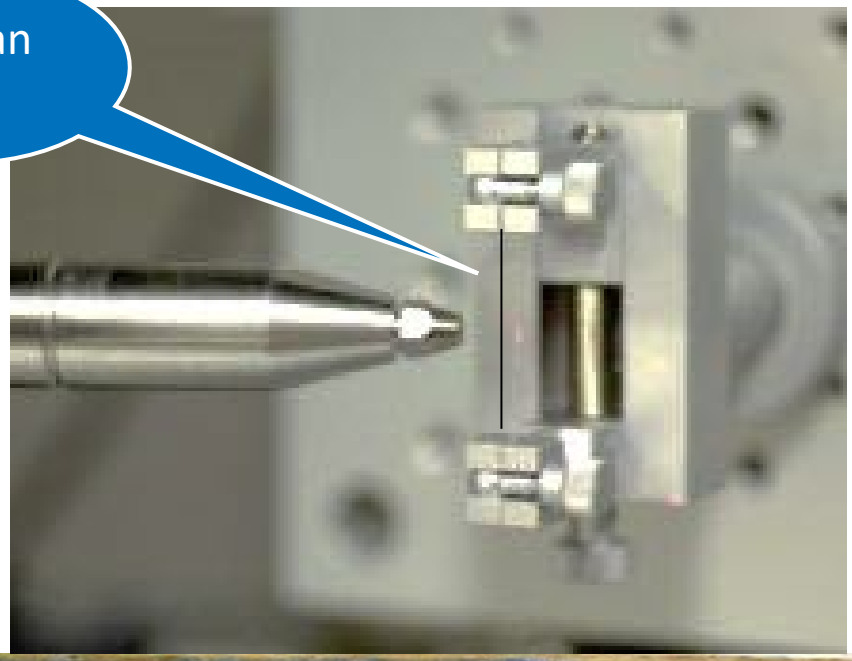

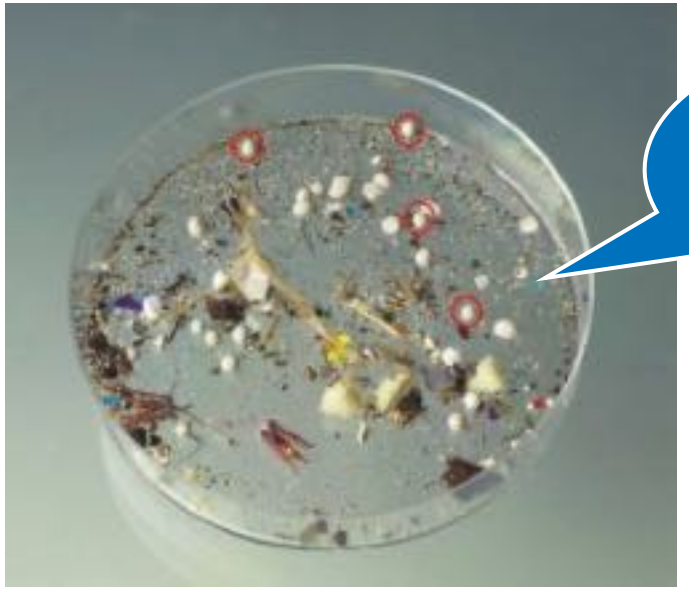

Crime scene samples

Color pigment

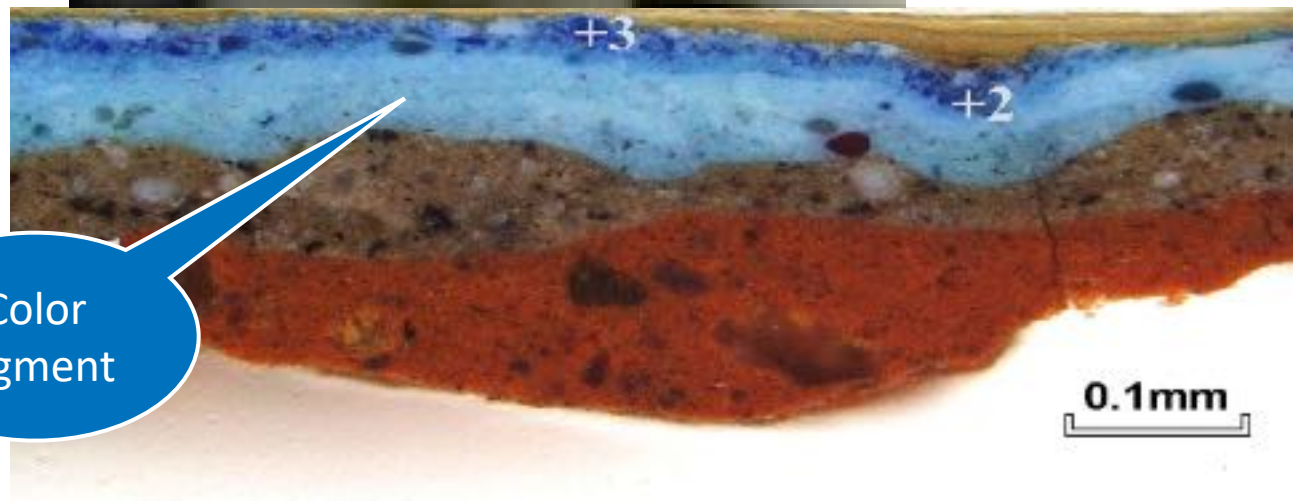

Rock Crystal

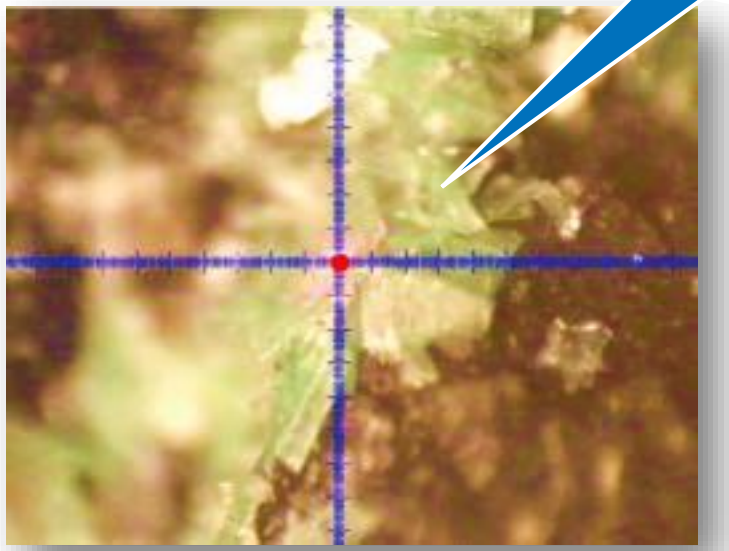

Short Range Order

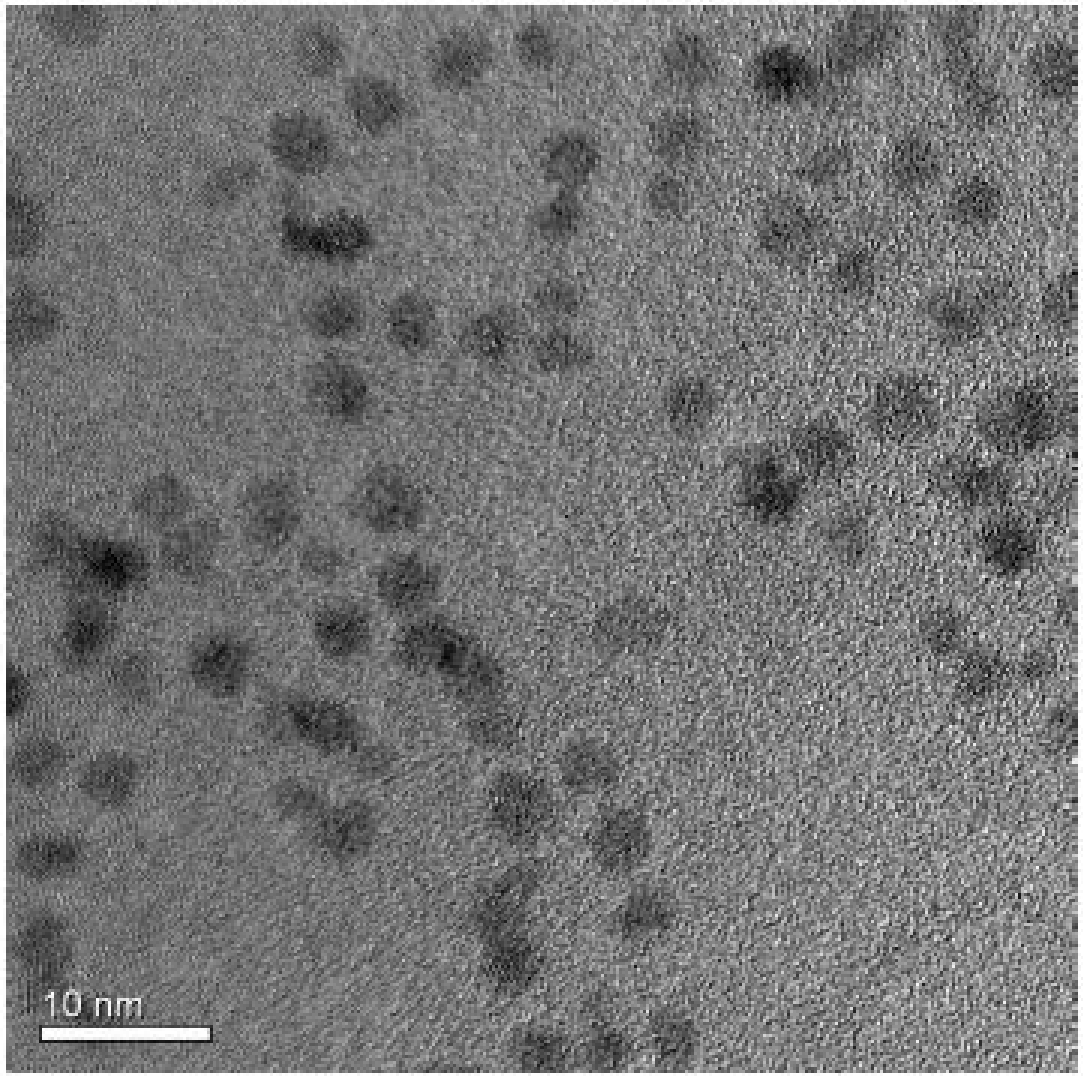

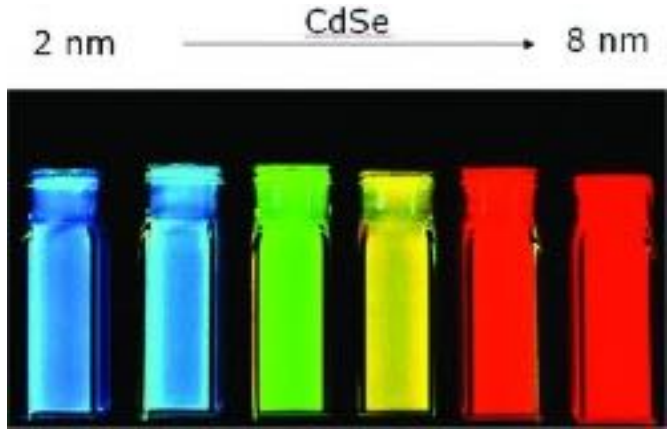

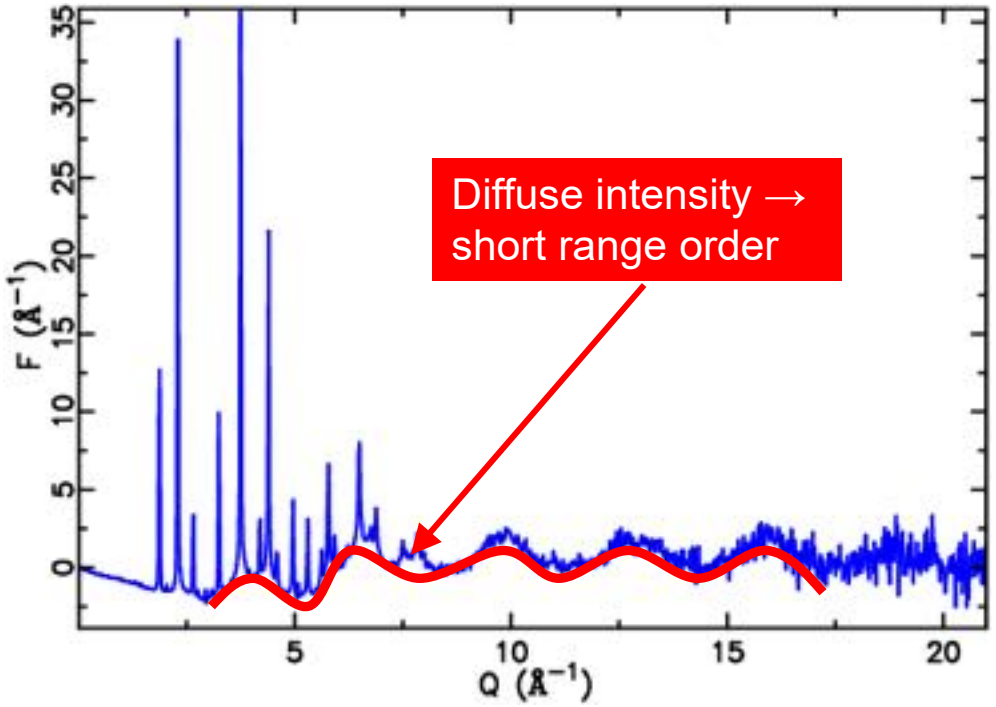

Polimer Crystalline States

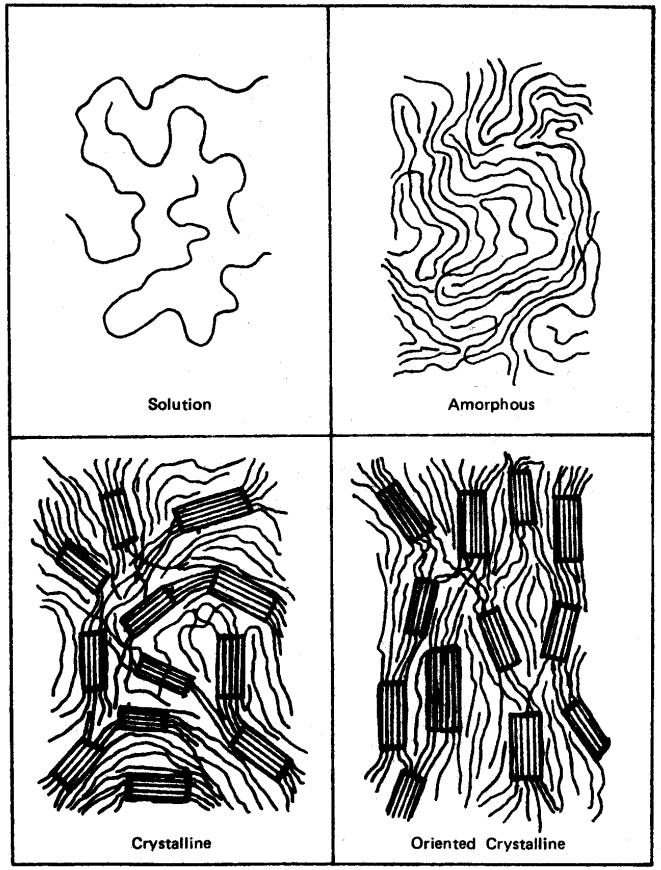

From “Selected Papers Of Turner Alfrey”, Marcel Dekker Inc, 1986

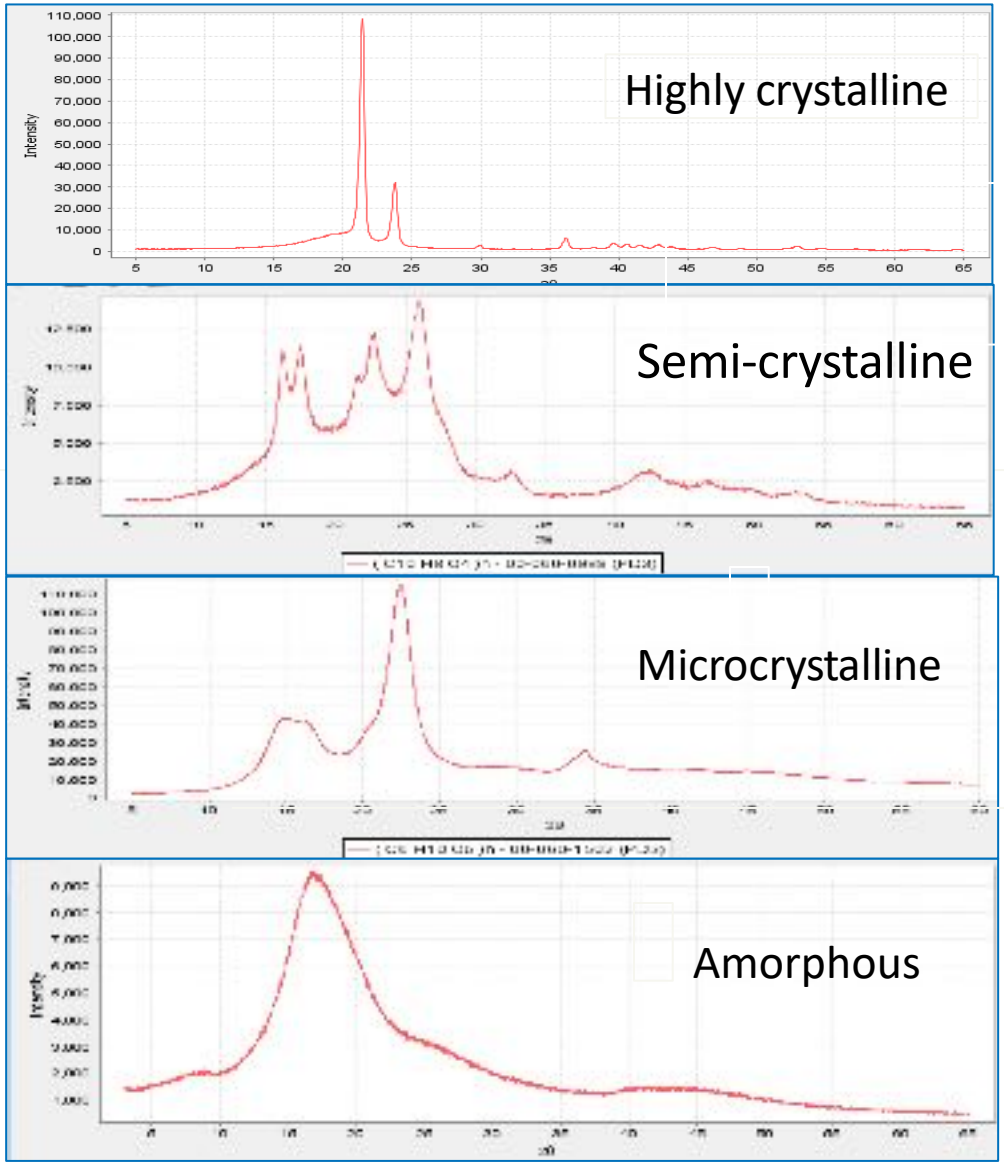

Whole Powder Pattern Modeling

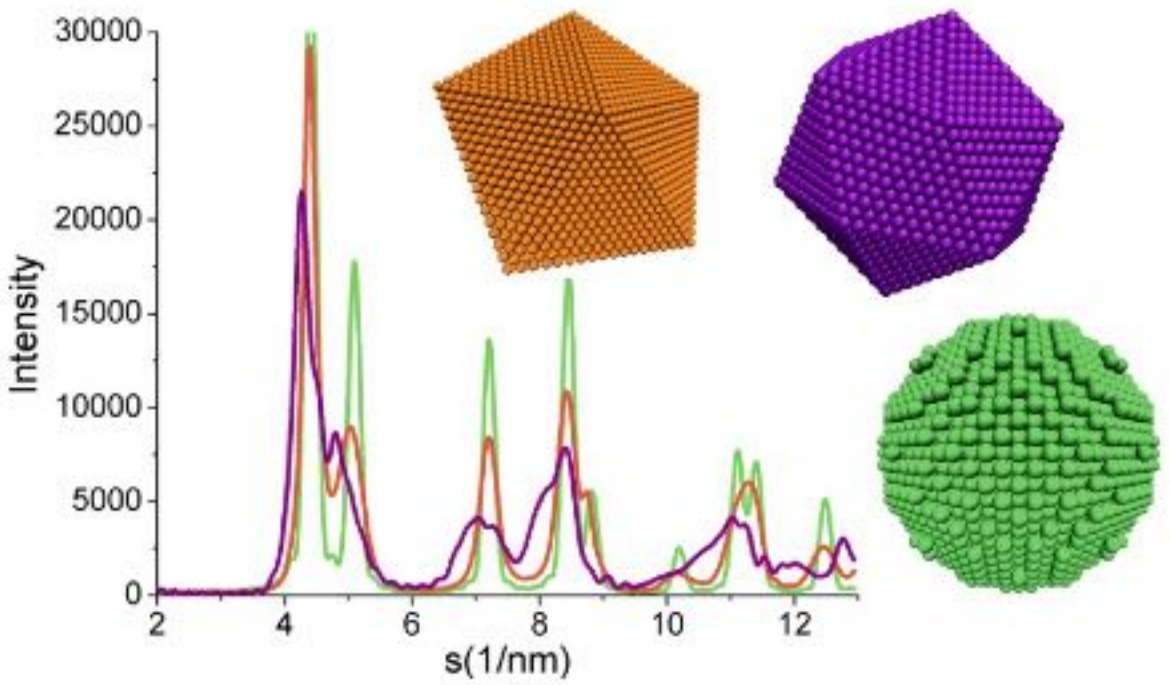

Domain size

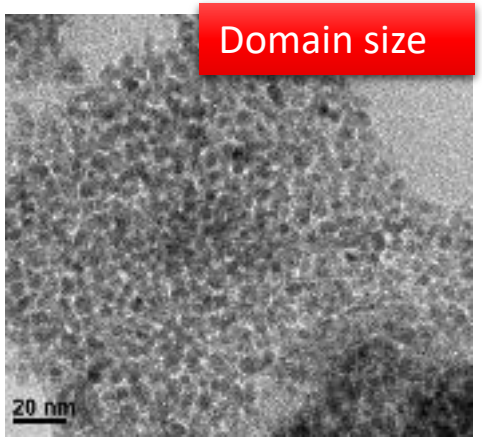

Dislocation

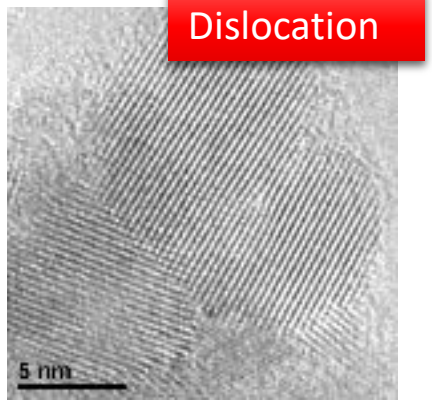

Faulting

Grain Surface Relaxation

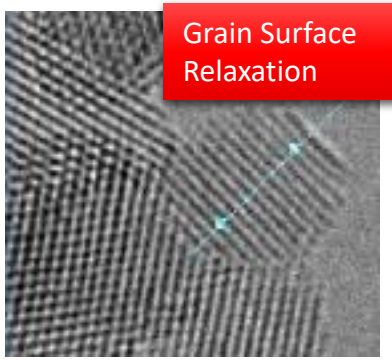

Anti Phase Boundary

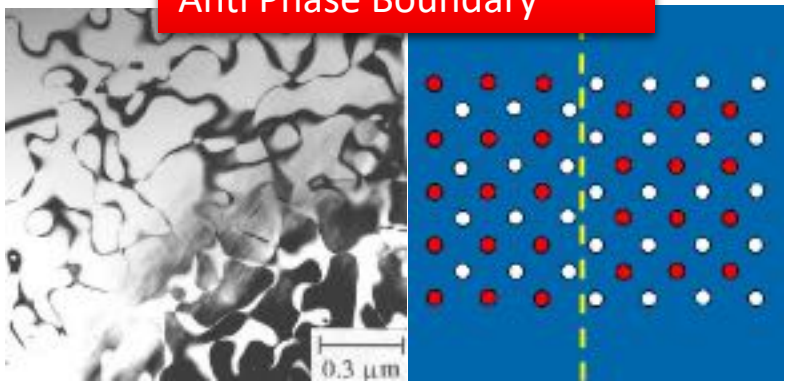

$$T_{pV}^{IP} \cdot A_{\{hkl\}}^{S} \cdot A_{\{hkl\}}^{D} \cdot (A_{hkl}^{F} + iB_{hkl}^{F}) \cdot A_{\{hkl\}}^{APB} \cdot (A_{hkl}^{GSR} + iB_{hkl}^{GSR}) \cdot (A_{hkl}^{CF} + iB_{hkl}^{CF}) \cdot \ldots$$

Instrumental Profile | Faulting | APB | Stoichiometry fluctuations

Domain size | Dislocations | Grain surface relaxation

Additional line broadening sources can be included through the corresponding FTs

Refer to Prof. Matteo Leoni, Matteo.Leoni@unitn.it

The Structure Fourier Transform

X-Ray

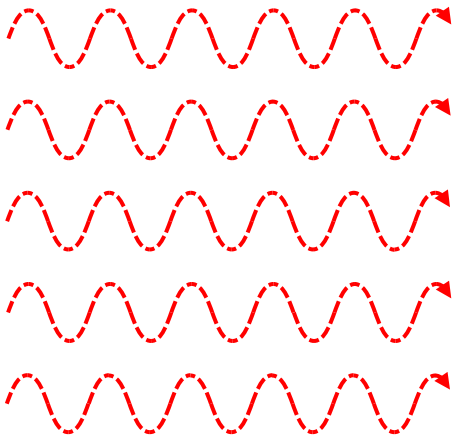

Crystal Space

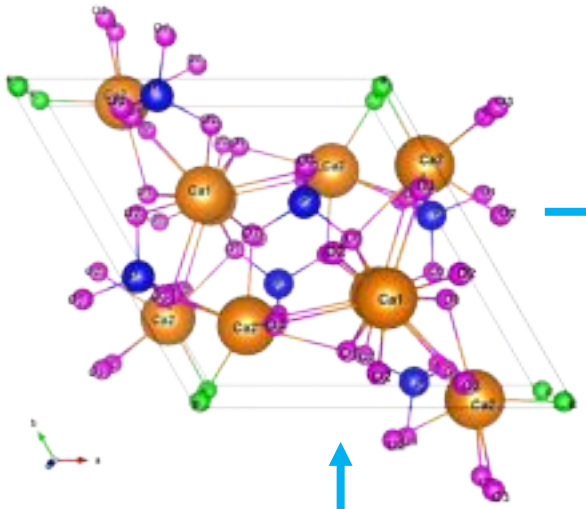

Reciprocal Space

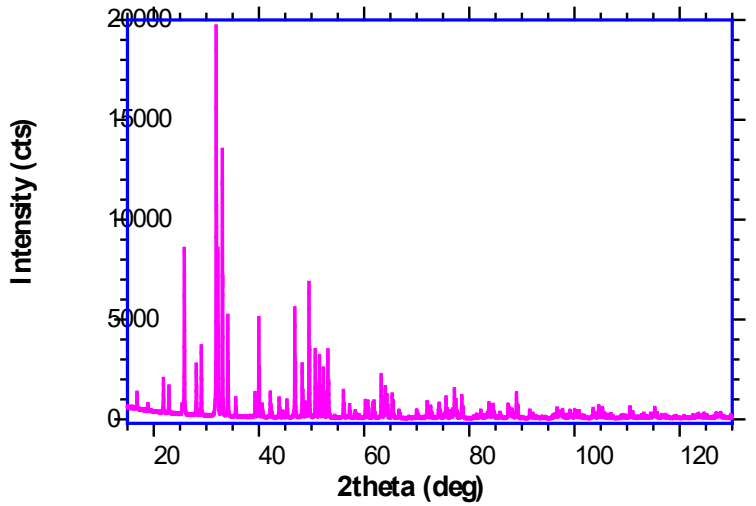

$I \sim F^2$

$$F_{hkl} = \sum_{1}^{N} f_n \, e^{2\pi i(hx_n + ky_n + lz_n)}$$

Fourier Synthesis

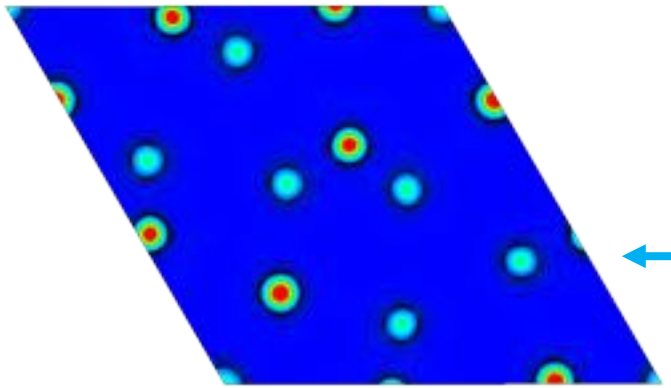

Electron/nuclear density map

Electron Density Map

Mn – O - Mn

Fobs electron density maps to visualize the difference in the position of oxygen atoms on the b-axis and the distribution of electrons due to the bonding mechanism

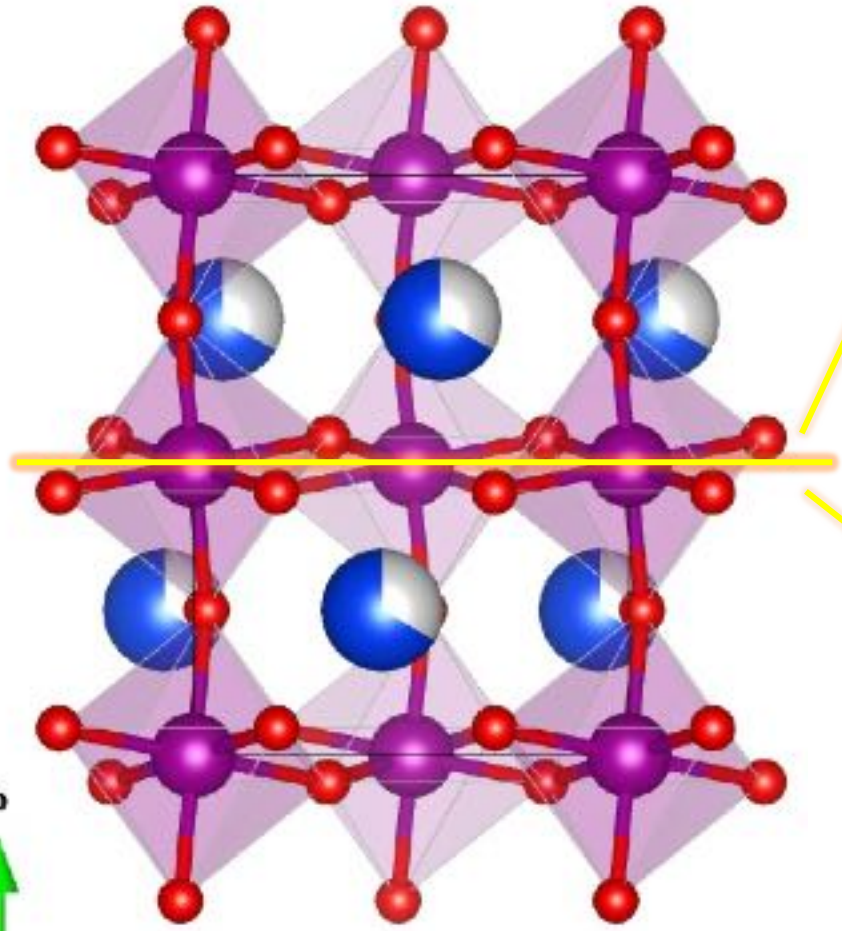

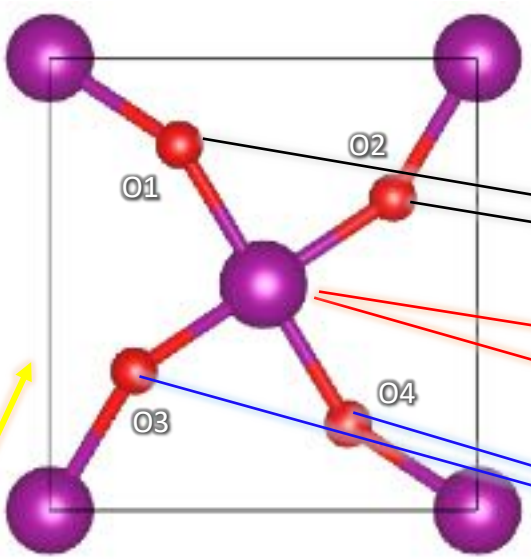

max scale (red) : 10 e/Å³

10 e/Å³

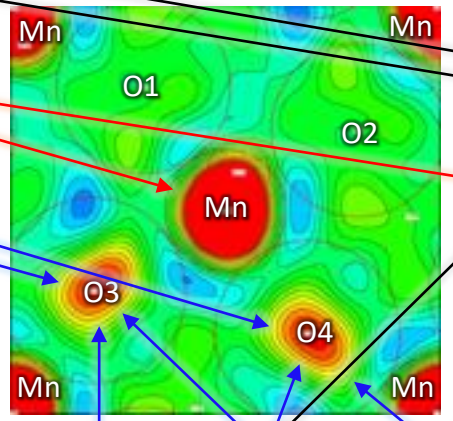

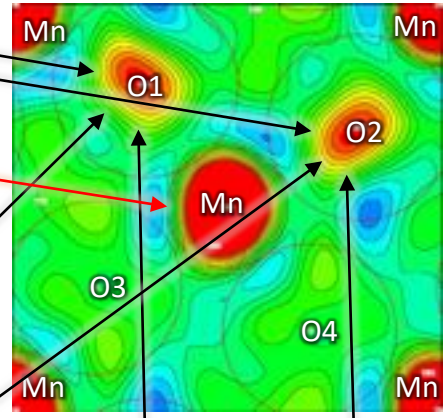

0 e/Å³

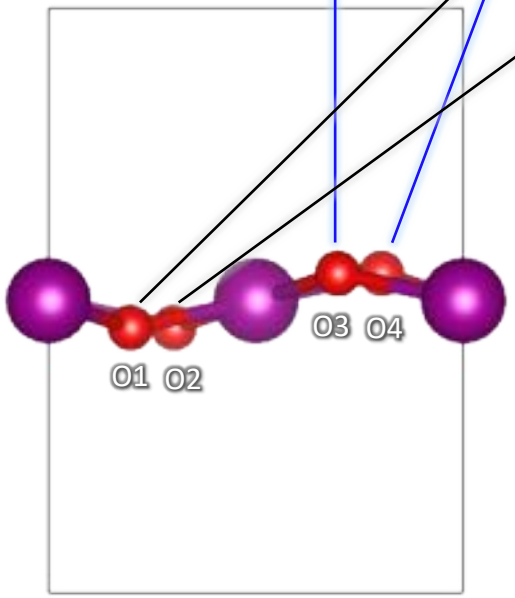

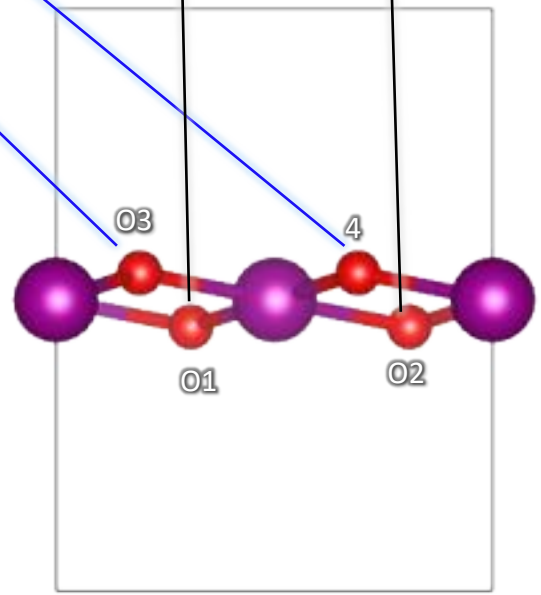

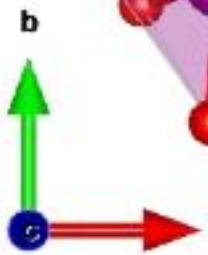

Ho Ca Mn O

Electron Density Map

(Ho0.669 Ca0.331 MnO3)

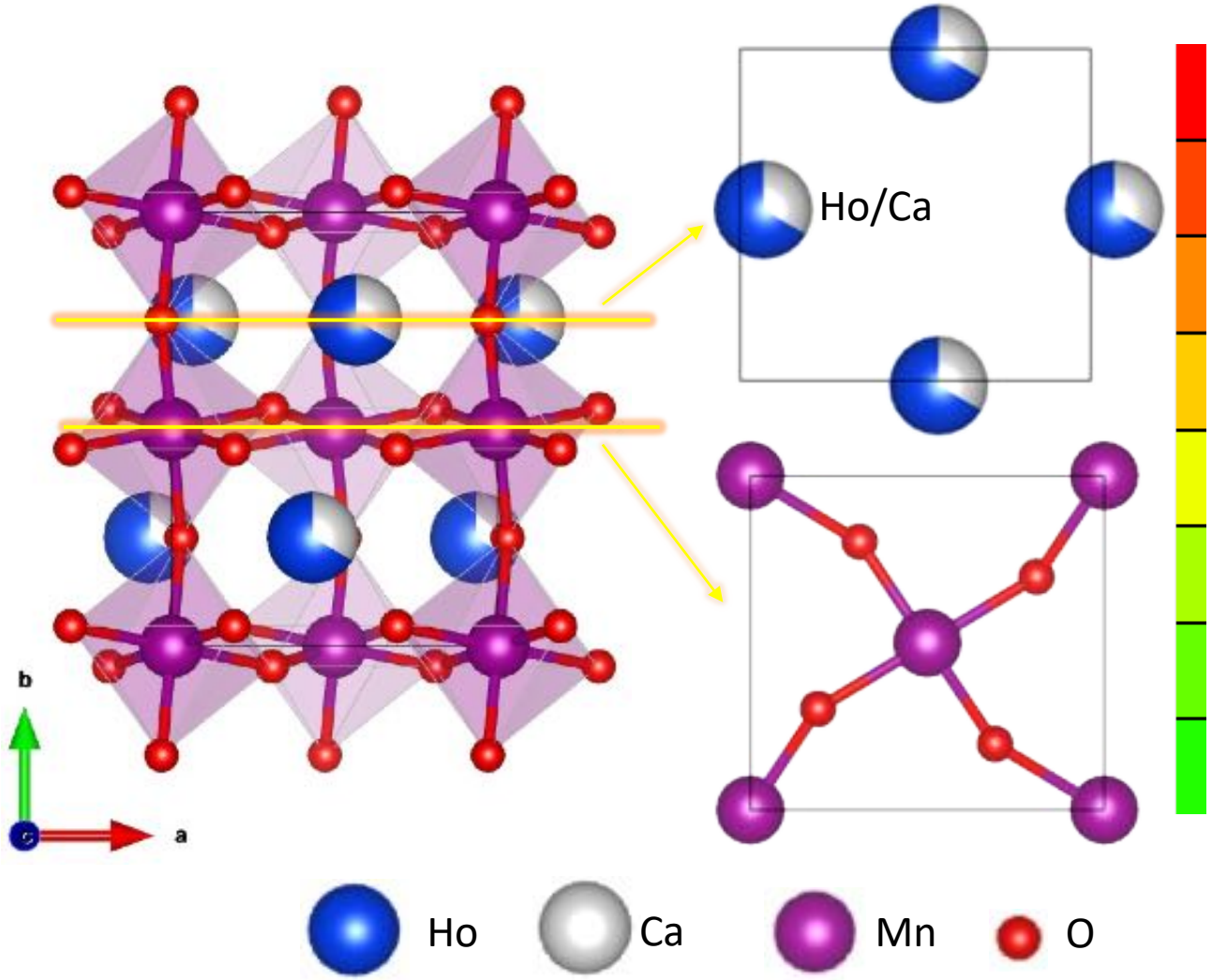

Fobs
max scale (red): 75.6 e/Å^3

Fcalc
max scale (red): 75.4 e/Å^3

(Fobs – Fcalc)
max scale (red): 2 e/Å^3

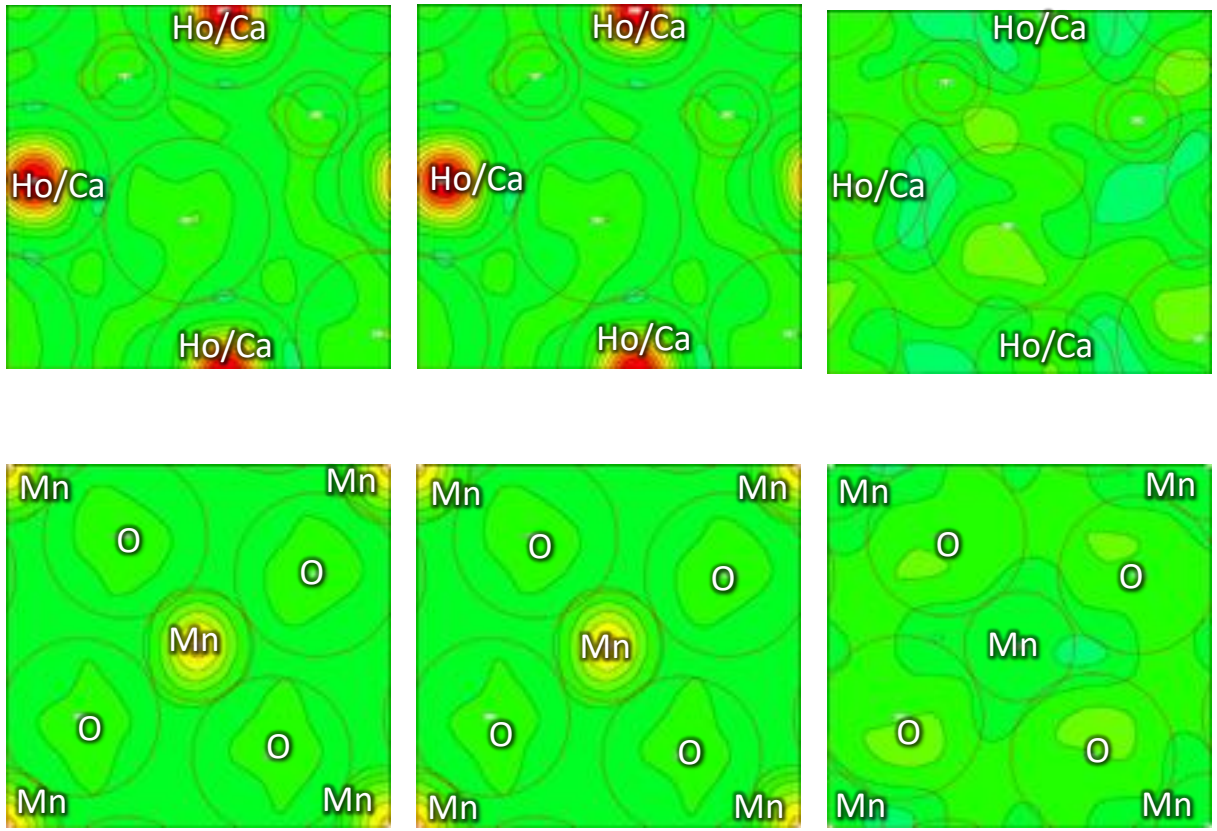

Fobs : Fourier electron density map from Observed data
Fcalc : Fourier electron density map from Calculated structure
Fobs-Fcalc : Fourier electron density difference (indicate if calculated structure are match with observed data)

Electron Density Map
(Ho0.799 Ca0.201 MnO3)

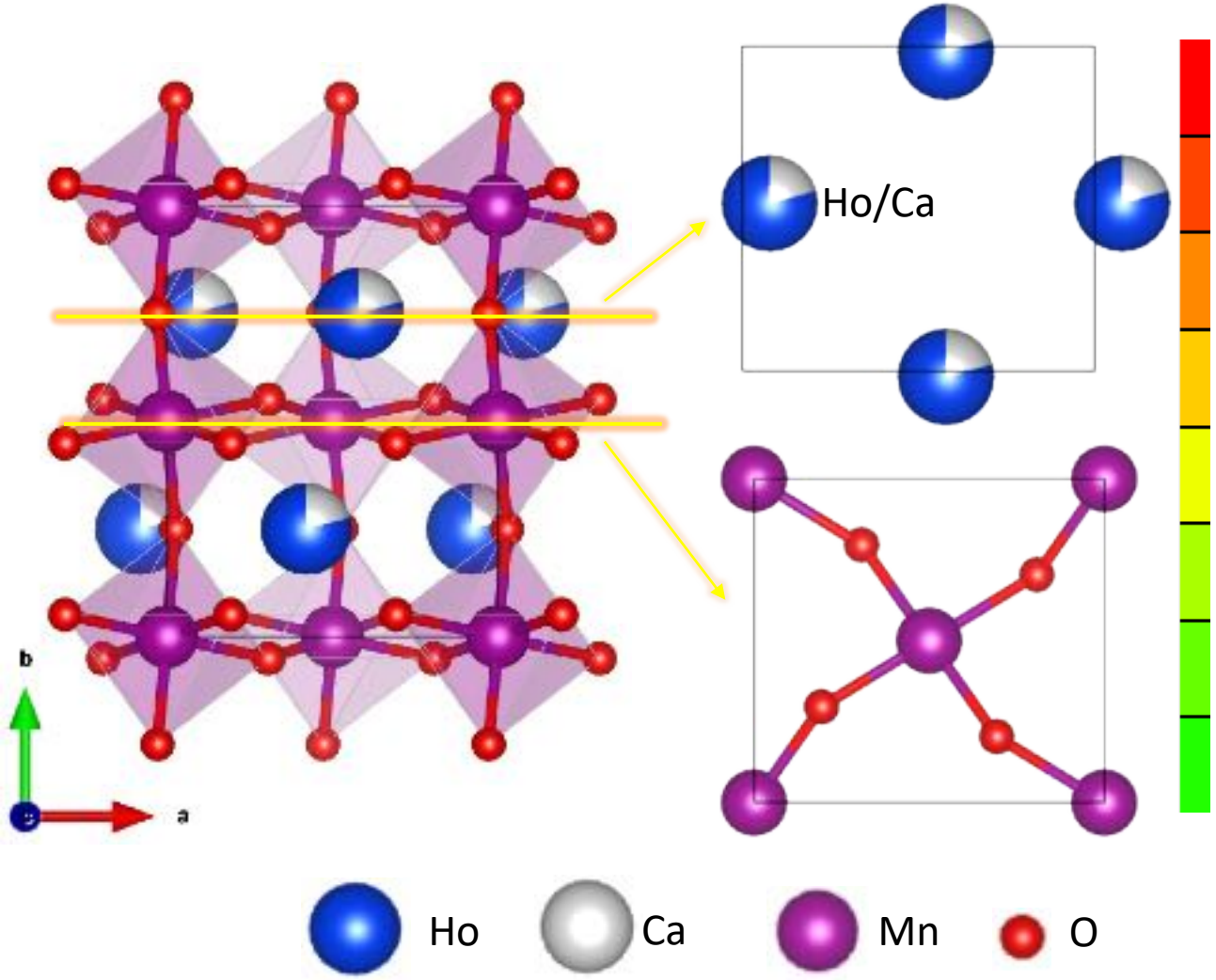

From impurity phase

Fobs	Fcalc	(Fobs – Fcalc)
max scale (red): 88.6 e/Å^3	max scale (red): 86.4 e/Å^3	max scale (red): 2 e/Å^3

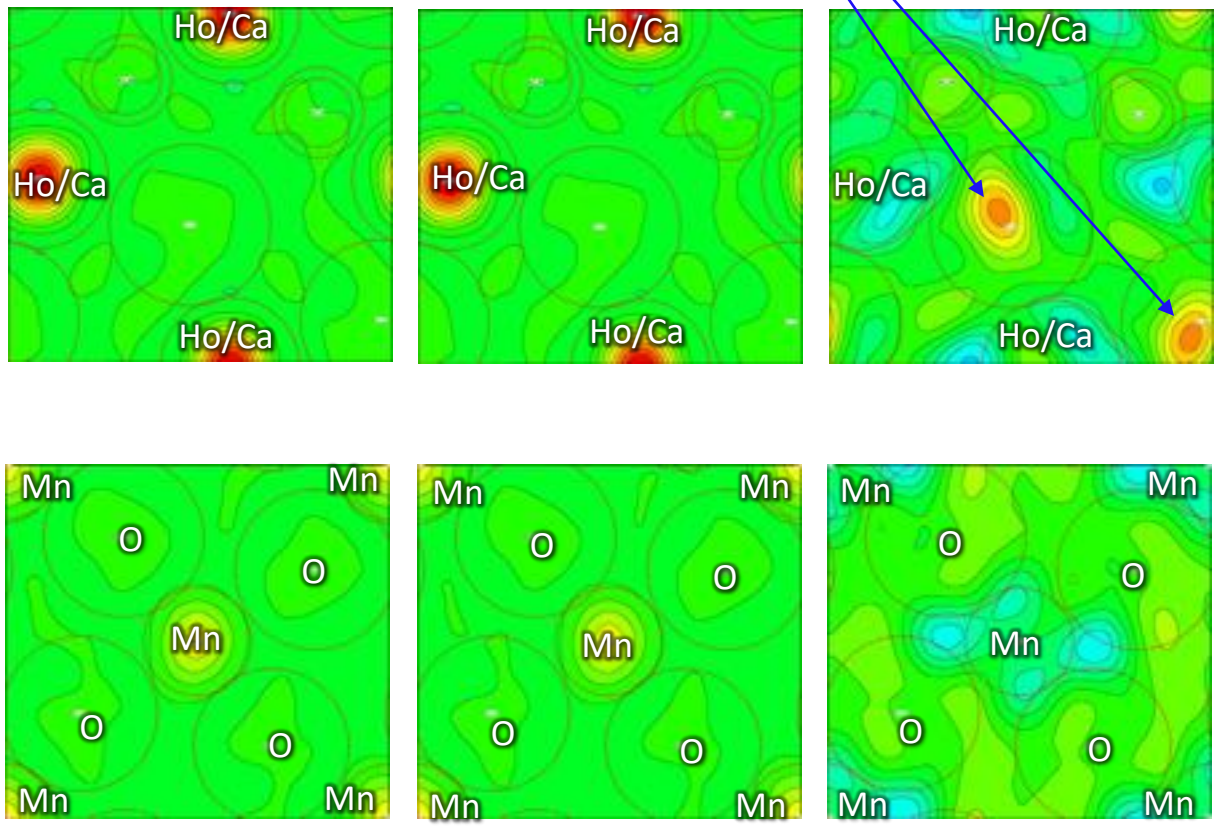

Fobs	:	Fourier electron density map from Observed data
Fcalc	:	Fourier electron density map from Calculated structure
Fobs-Fcalc	:	Fourier electron density difference (indicate if calculated structure are match with observed data)

Electron Density Map

(Ho0.812 Ca0.188 MnO3)

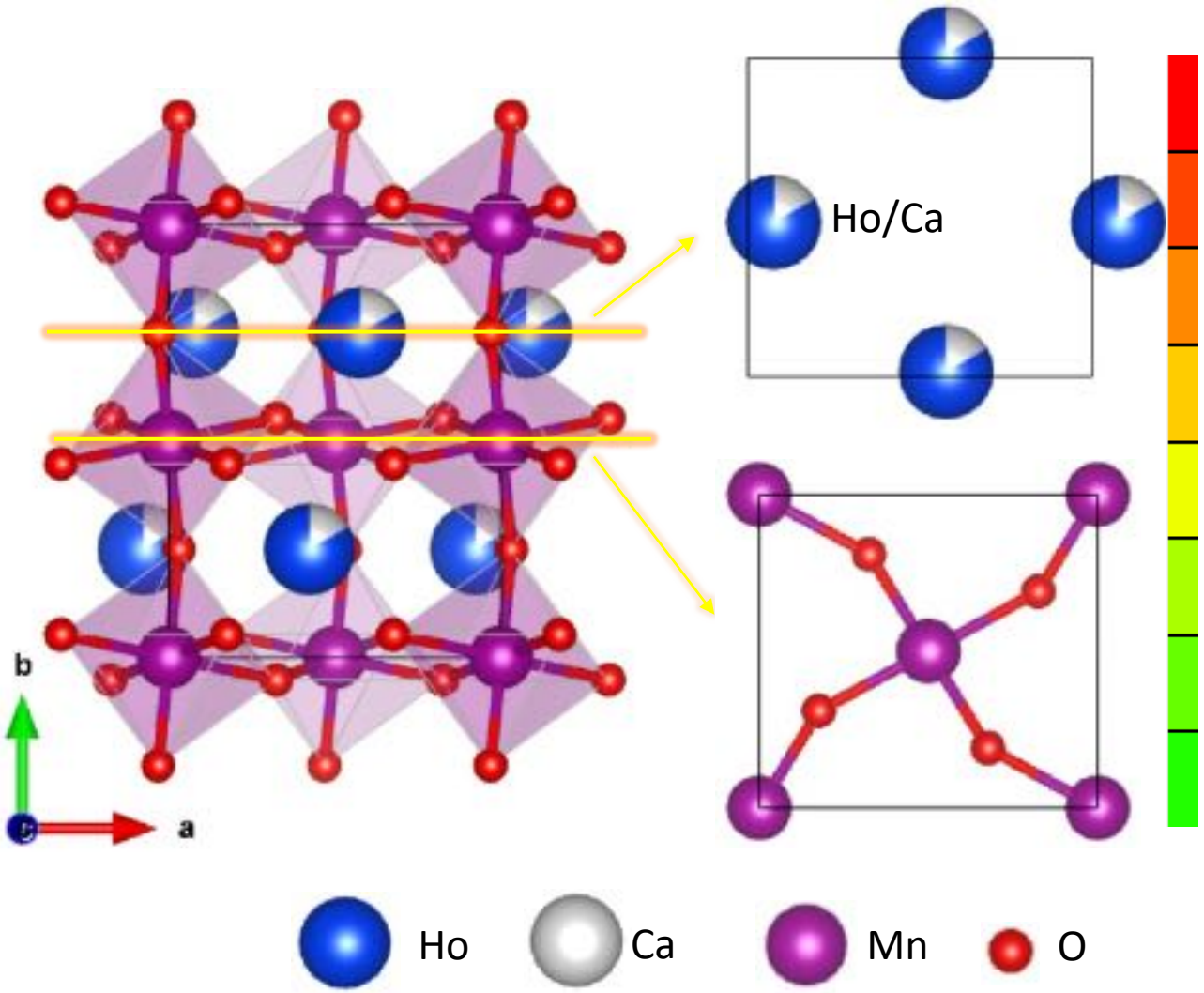

From impurity phase

Fobs	Fcalc	(Fobs – Fcalc)
max scale (red): 84.5 e/Å^3	max scale (red): 83.3 e/Å^3	max scale (red): 2 e/Å^3

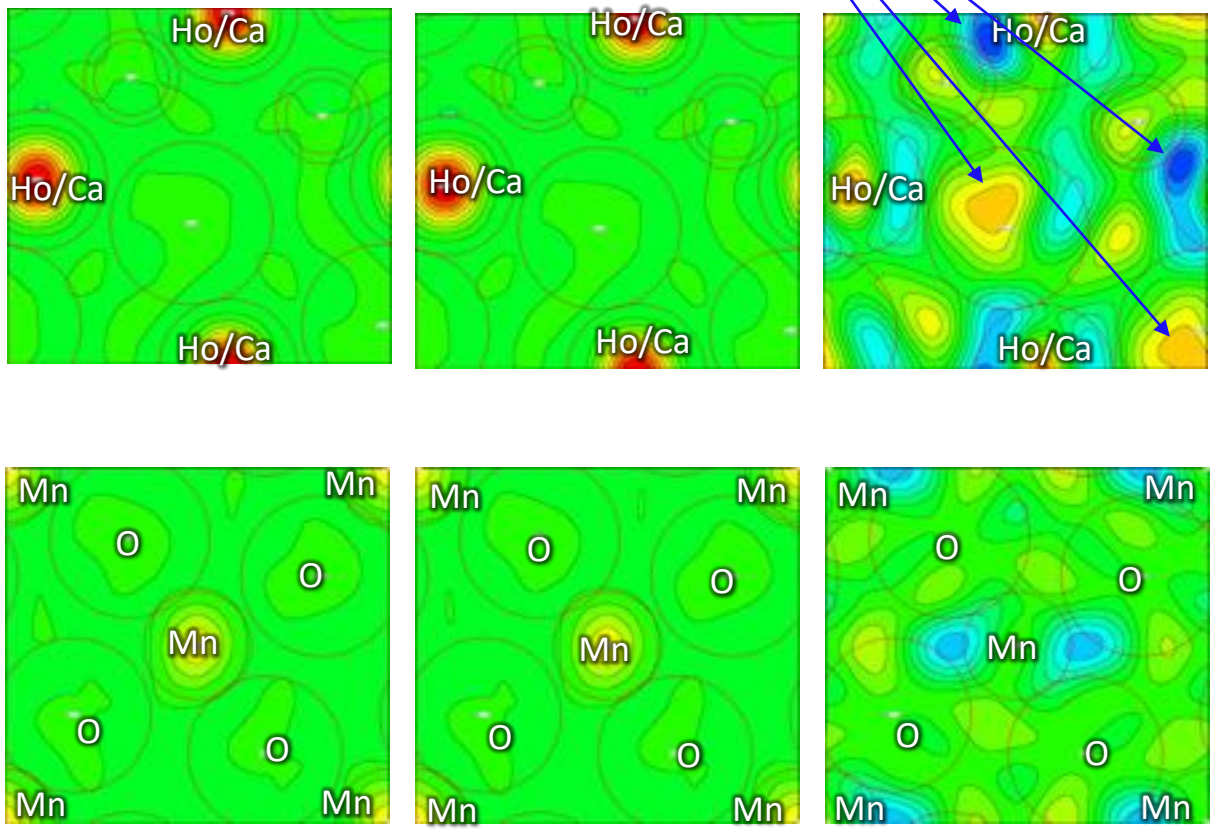

Fobs	:	Fourier electron density map from Observed data
Fcalc	:	Fourier electron density map from Calculated structure
Fobs-Fcalc	:	Fourier electron density difference (indicate if calculated structure are match with observed data)

What are the Differences?

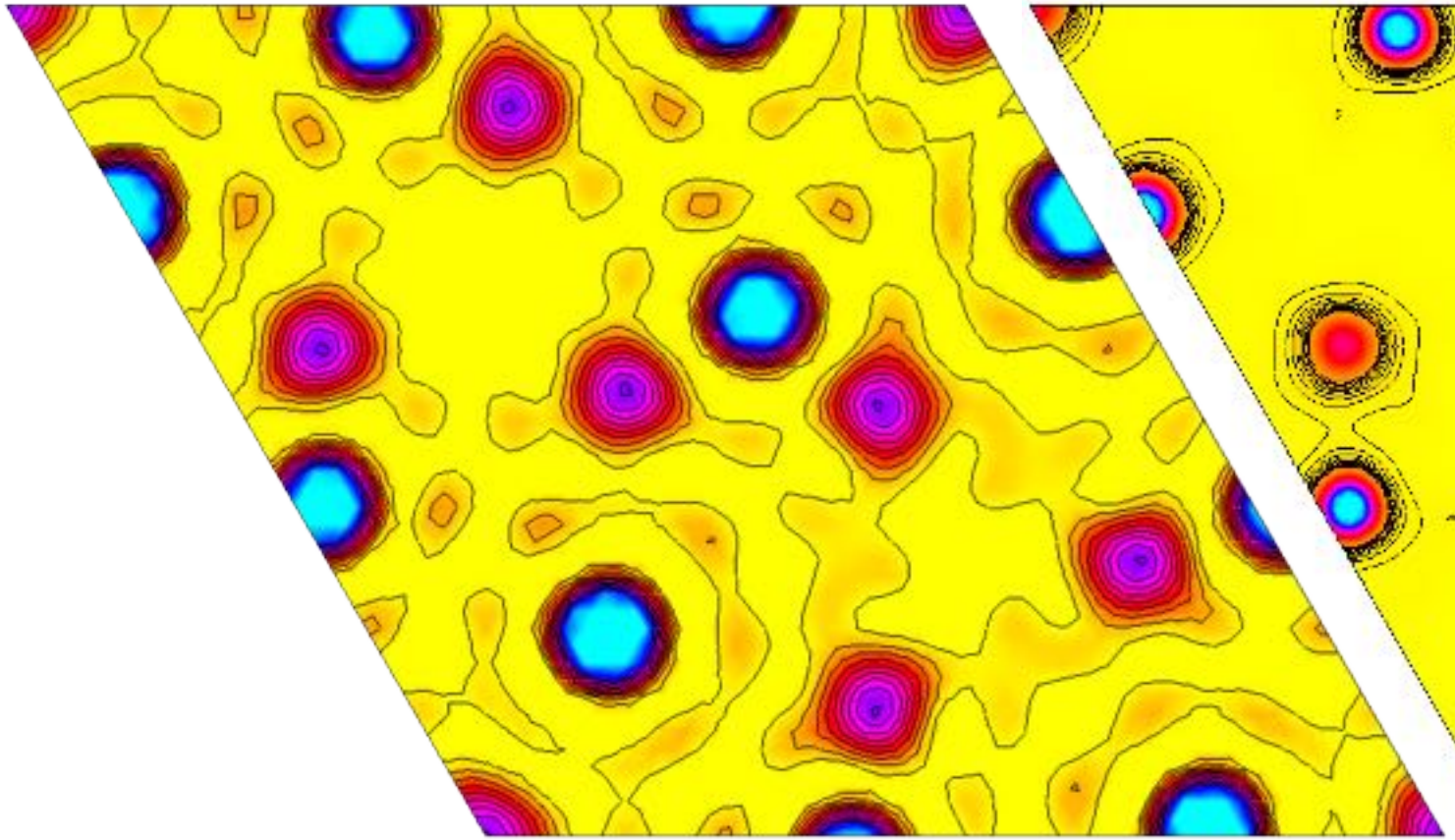

Fourier Synthesis

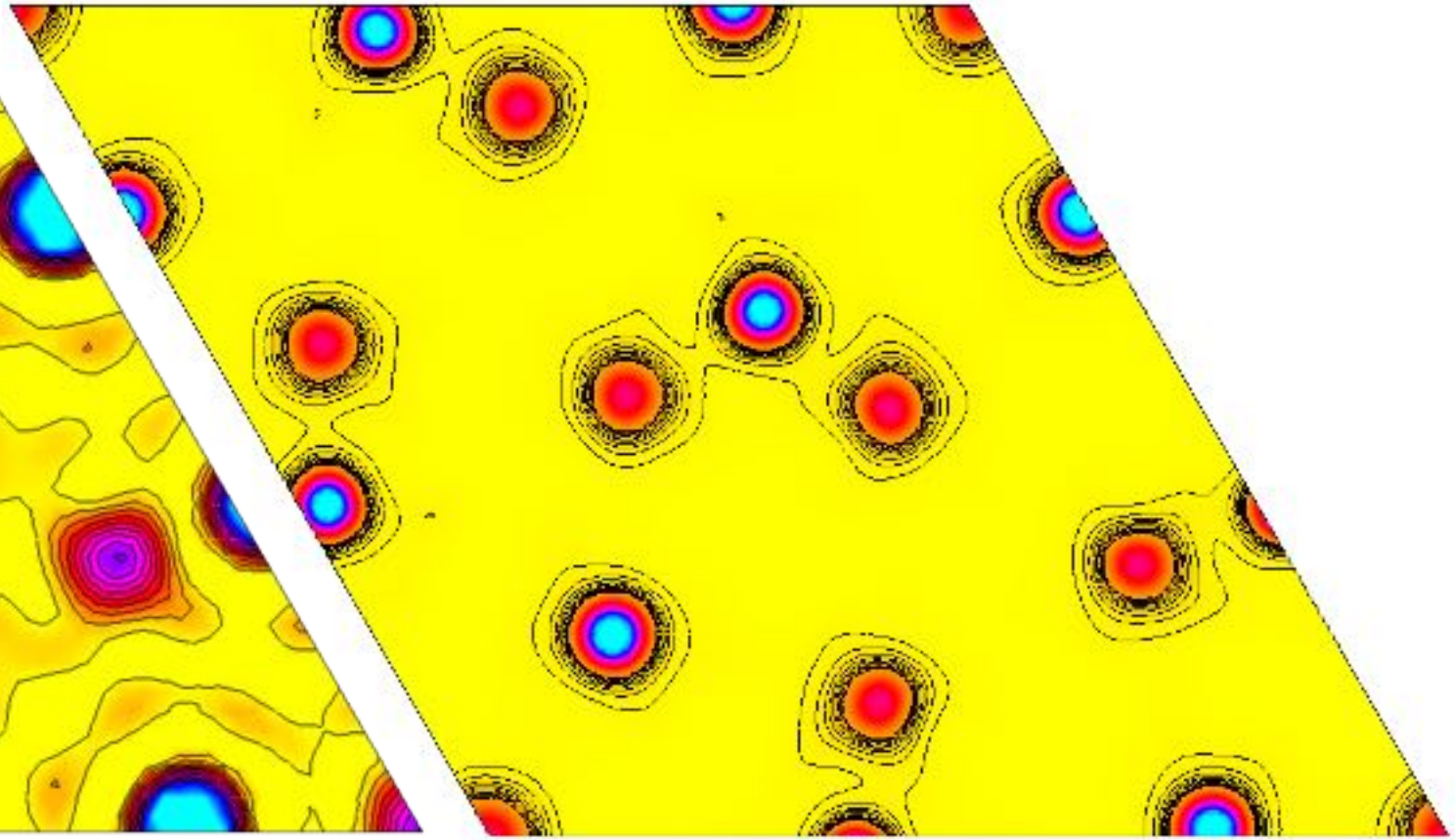

Maximum Entropy Method

Fourier Synthesis

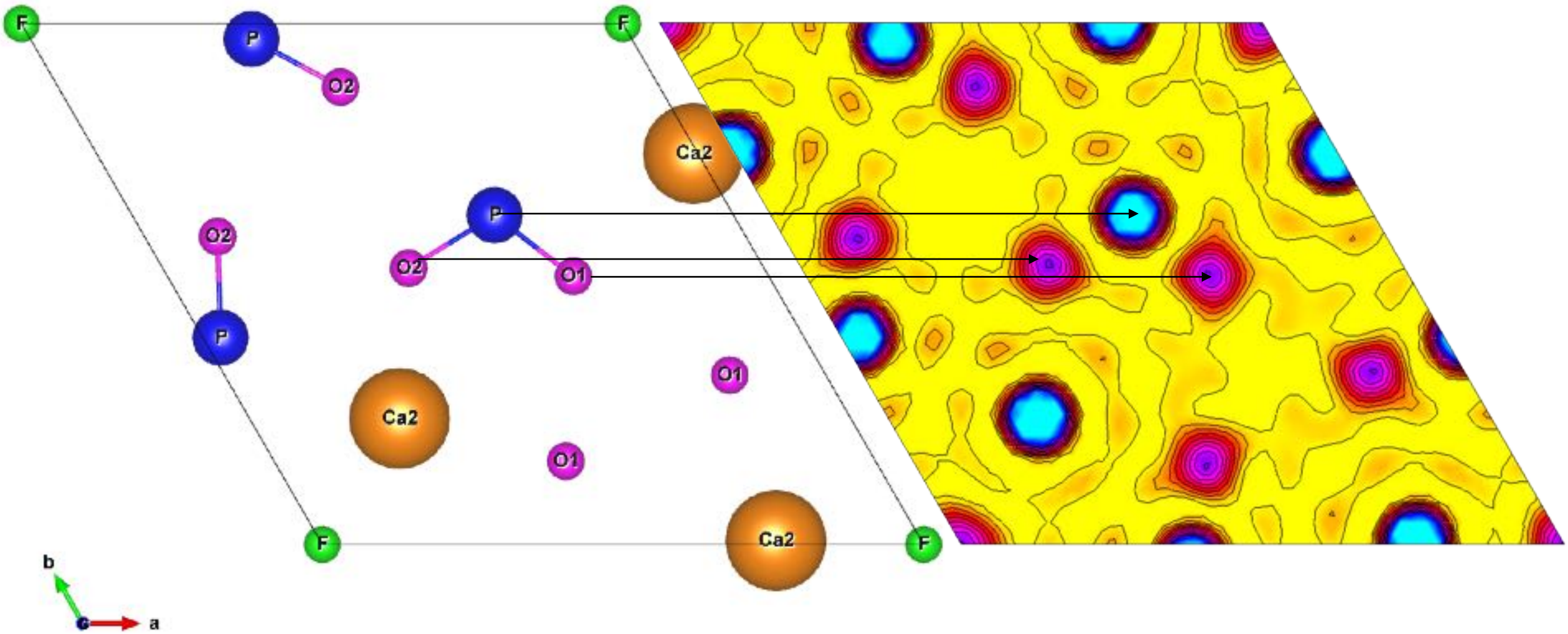

Maximum Entropy Method

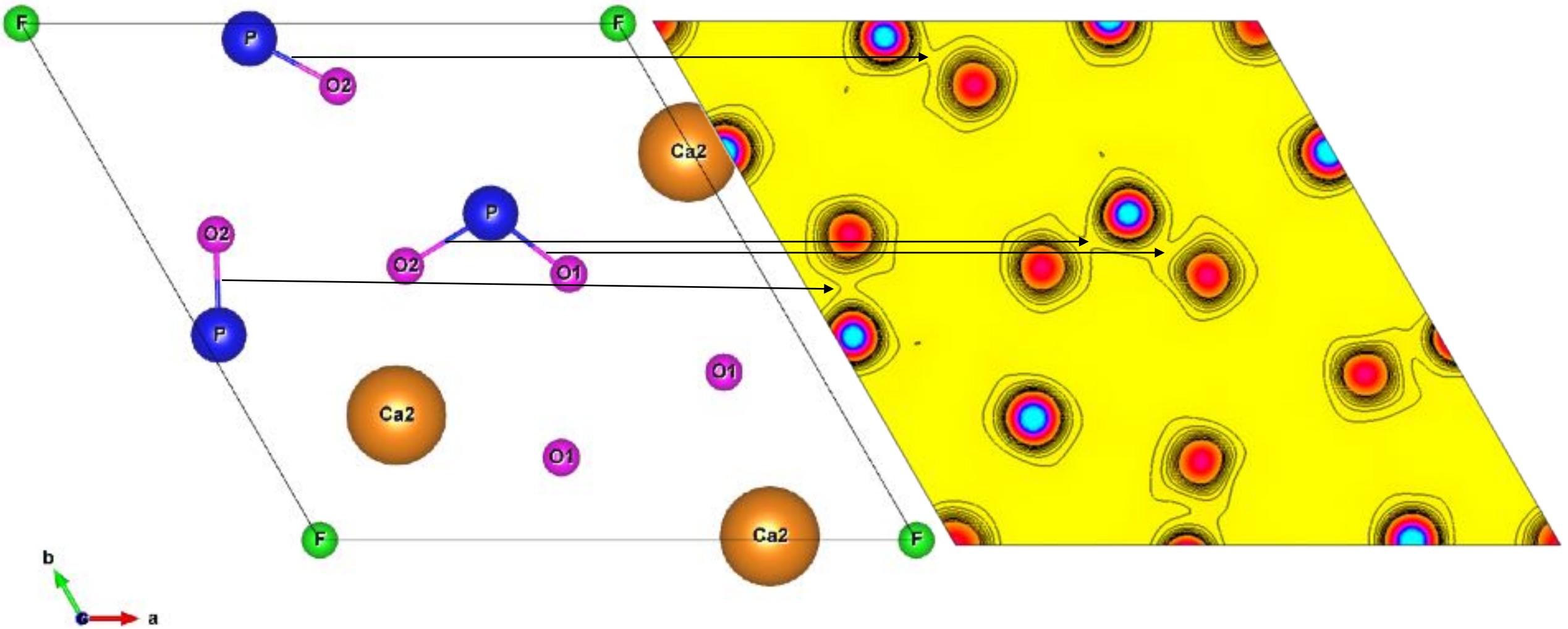

Electron Density profile of P-O bonds

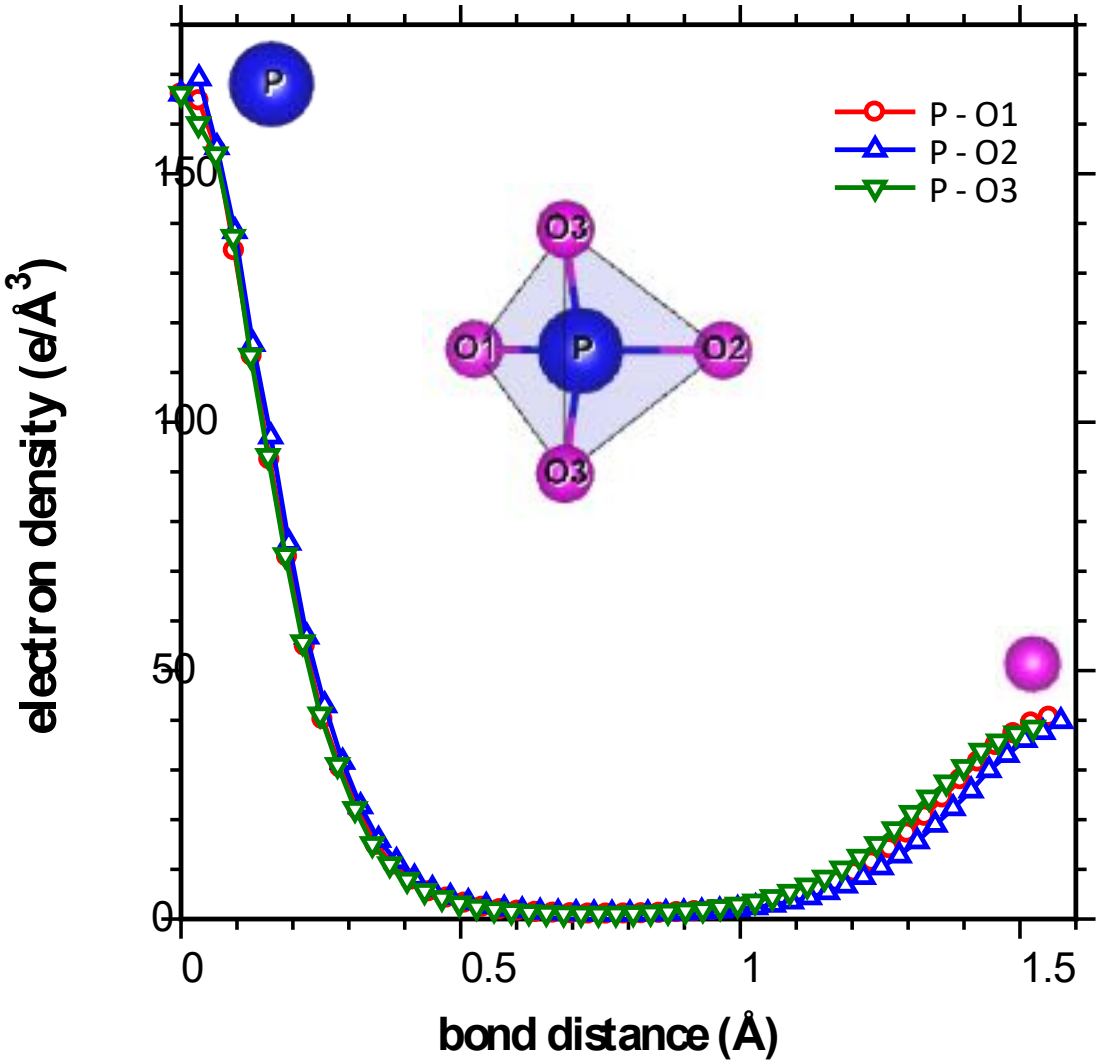

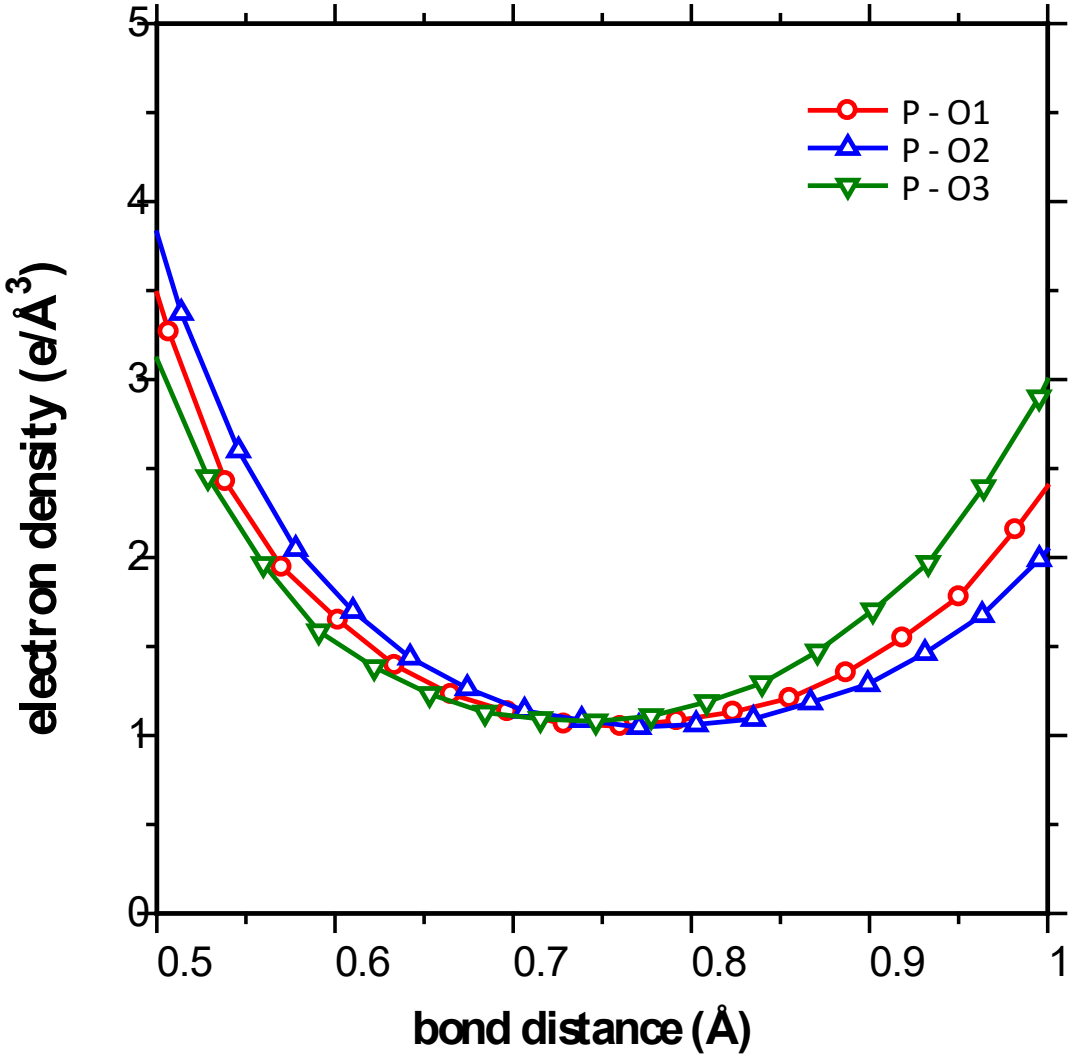

Electron Density profile of P-O bonds

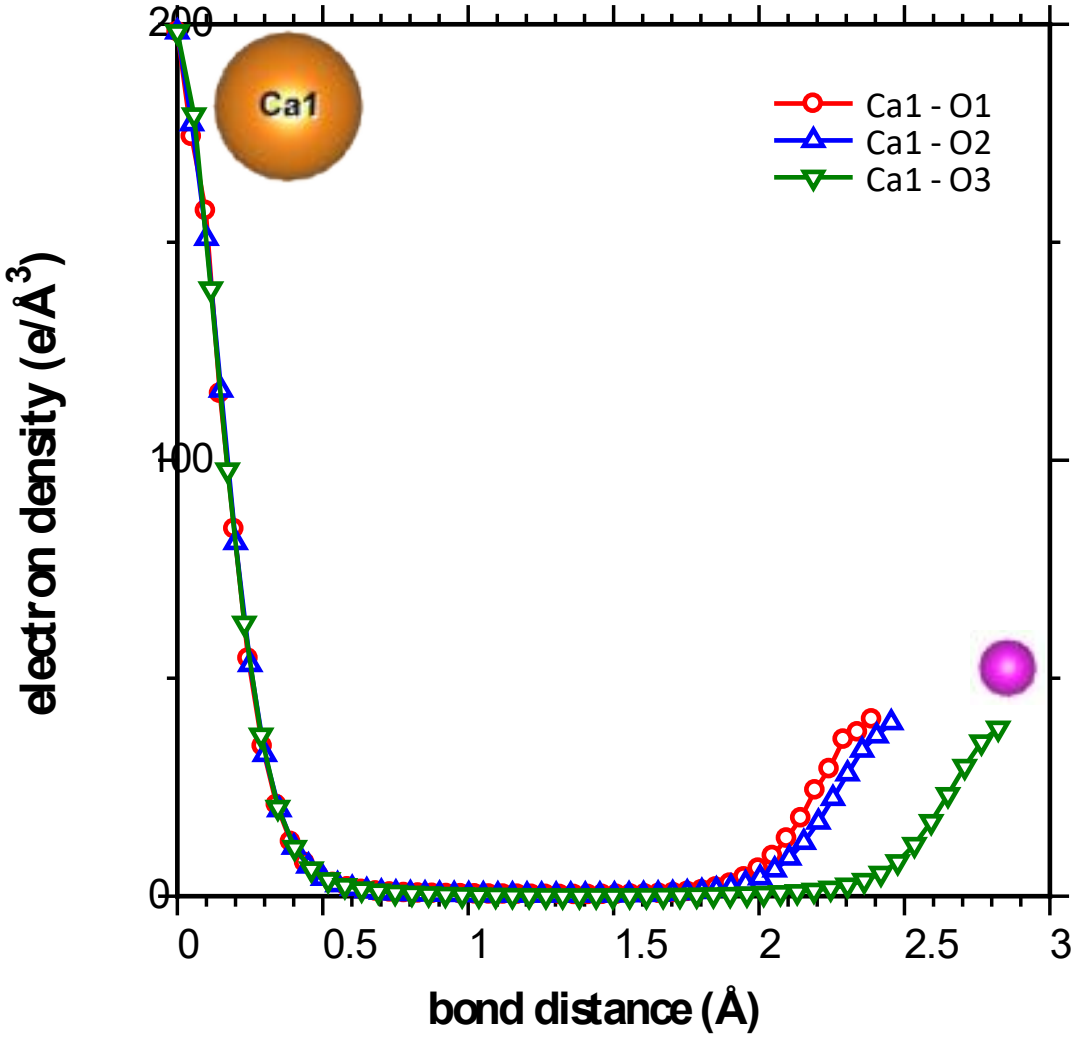

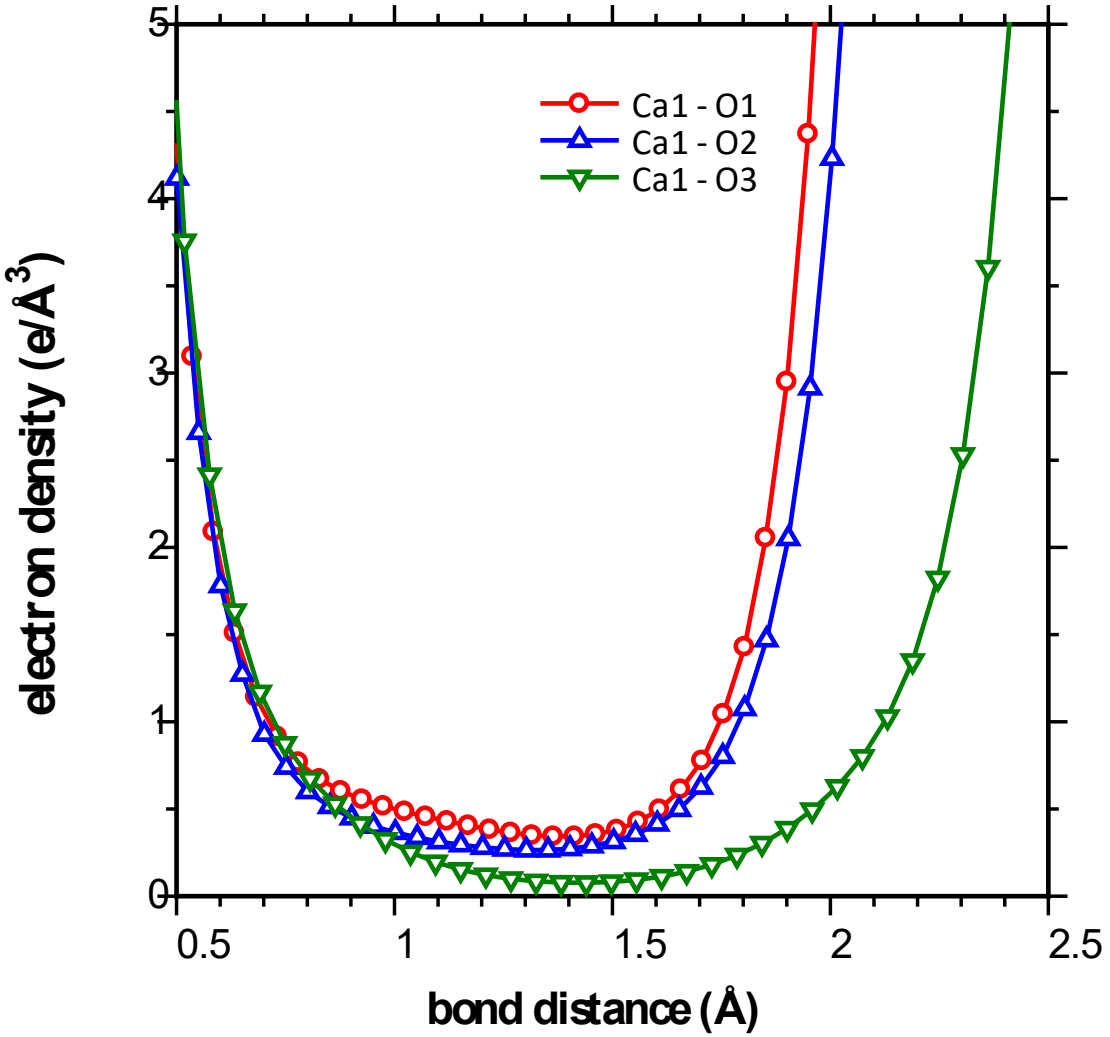

Electron Density profile of P-O bonds

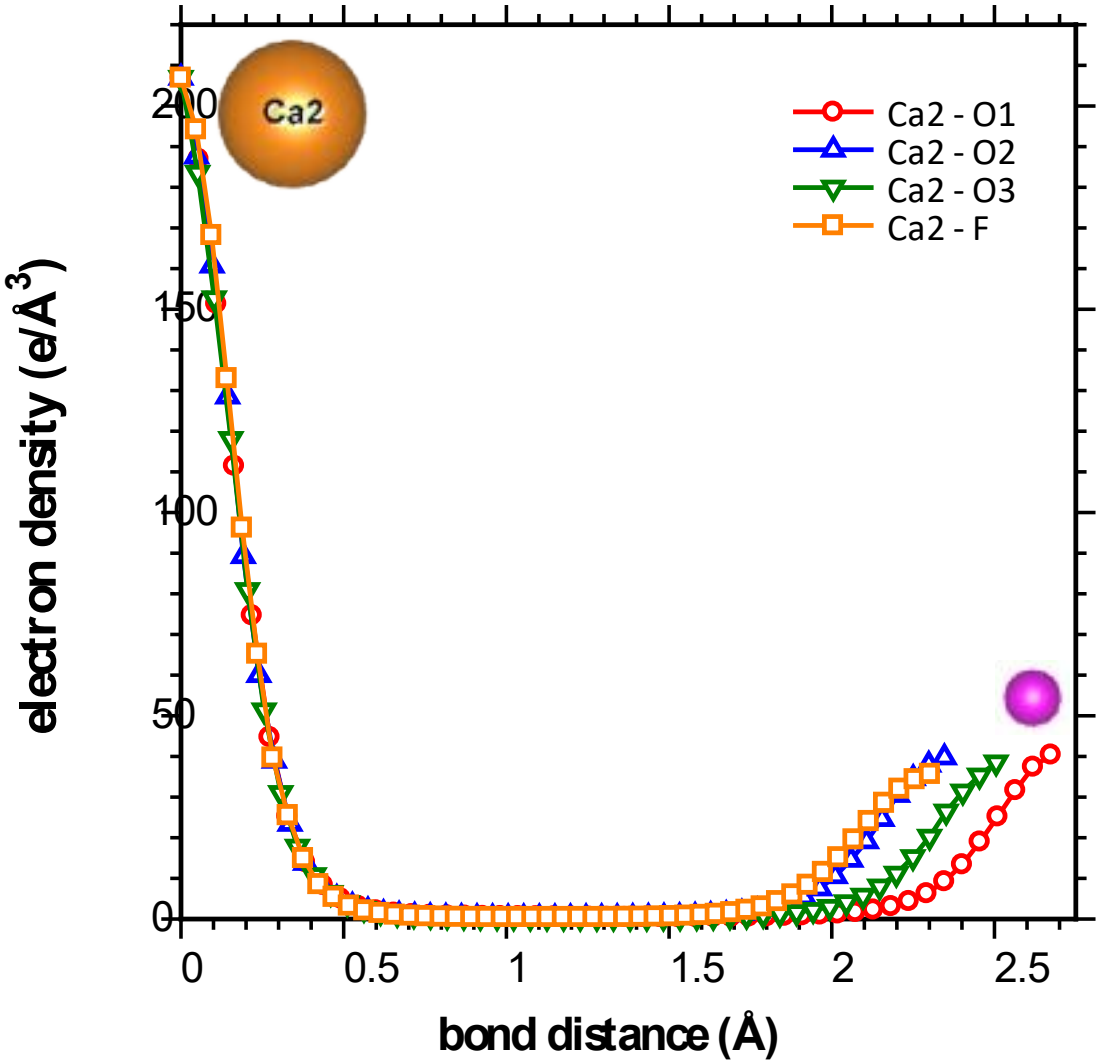

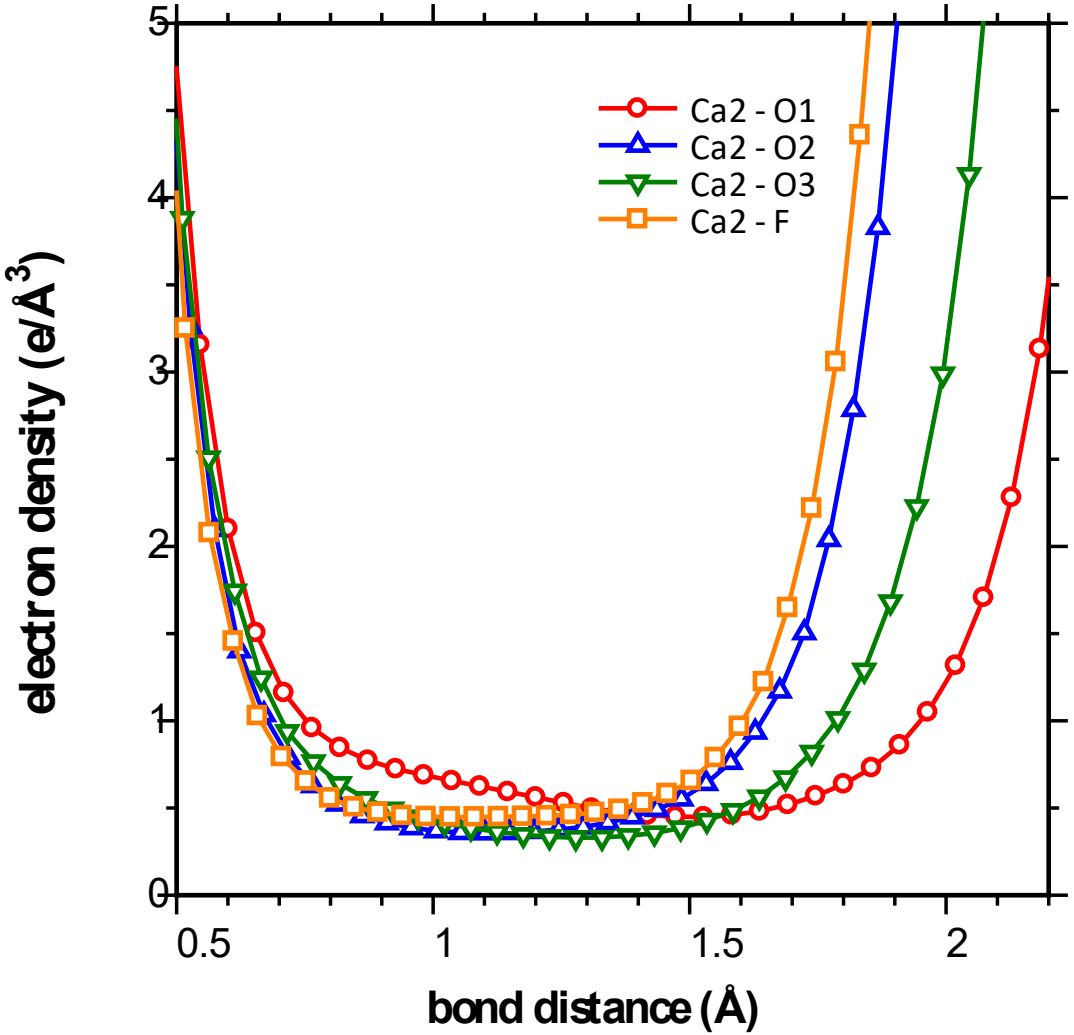

- Published Articles
- under
- ==========
- Crystallography
- X-Ray &
- Neutron diffraction
- ==========
- Diffraction Lab. Result

ELSEVIER CellPress

Visualizing crystal structure evolution of electrode materials upon doping and during charge/discharge cycles in lithium-ion batteries

Dongwei Ma [1,*], Jing Yang [4,5], Mayke Manawan [5,6], Chenglu Yang [1], Jichuli Li [1], Yongzi Liang [4], Tina Feng [3], Yong Wei Zhang [2], Jia Hong Pan [1,7,8,9,*]

https://doi.org/10.1016/j.xpro.2021.101099

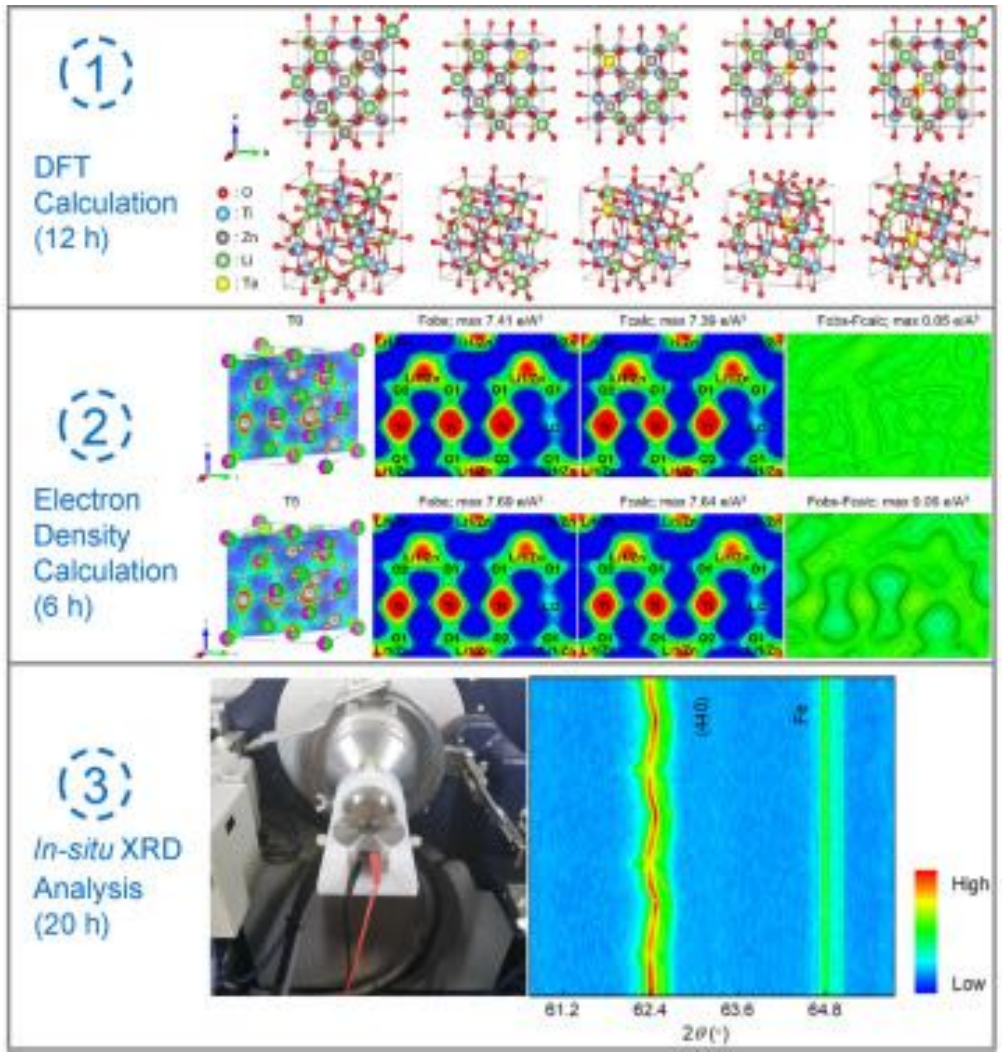

Highlights

- Monodisperse Ta^{5+}-doped $Li_2ZnTi_3O_8$ spheres from TiO_2 spheres as self-template
- DFT and electron density calculations for crystal structure parameters
- *In-situ* XRD analysis to visualize crystal structure evolution of electrodes

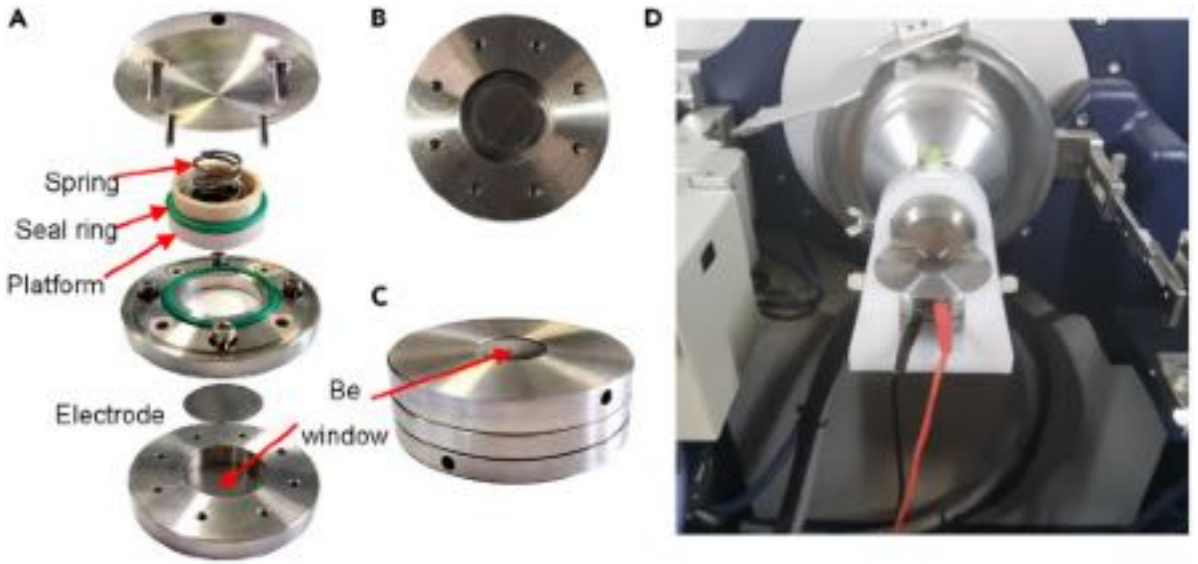

ELSEVIER

Structural, magnetic and magnetocaloric properties of double perovskite Ho_2MMnO_6 (M = Fe, Co, and Ni)

K.P. Shinde [a,b], M. Manawan [c], S.Y. Park [d], Y. Jo [e], V.M. Tien [a], Y. Pham [a], S.C. Yu [a], N. Kaianda [f], M. Yarmolich [f], A. Petrov [f], D.H. Kim [a,b,*]

https://doi.org/10.1016/j.jmmm.2021.168666

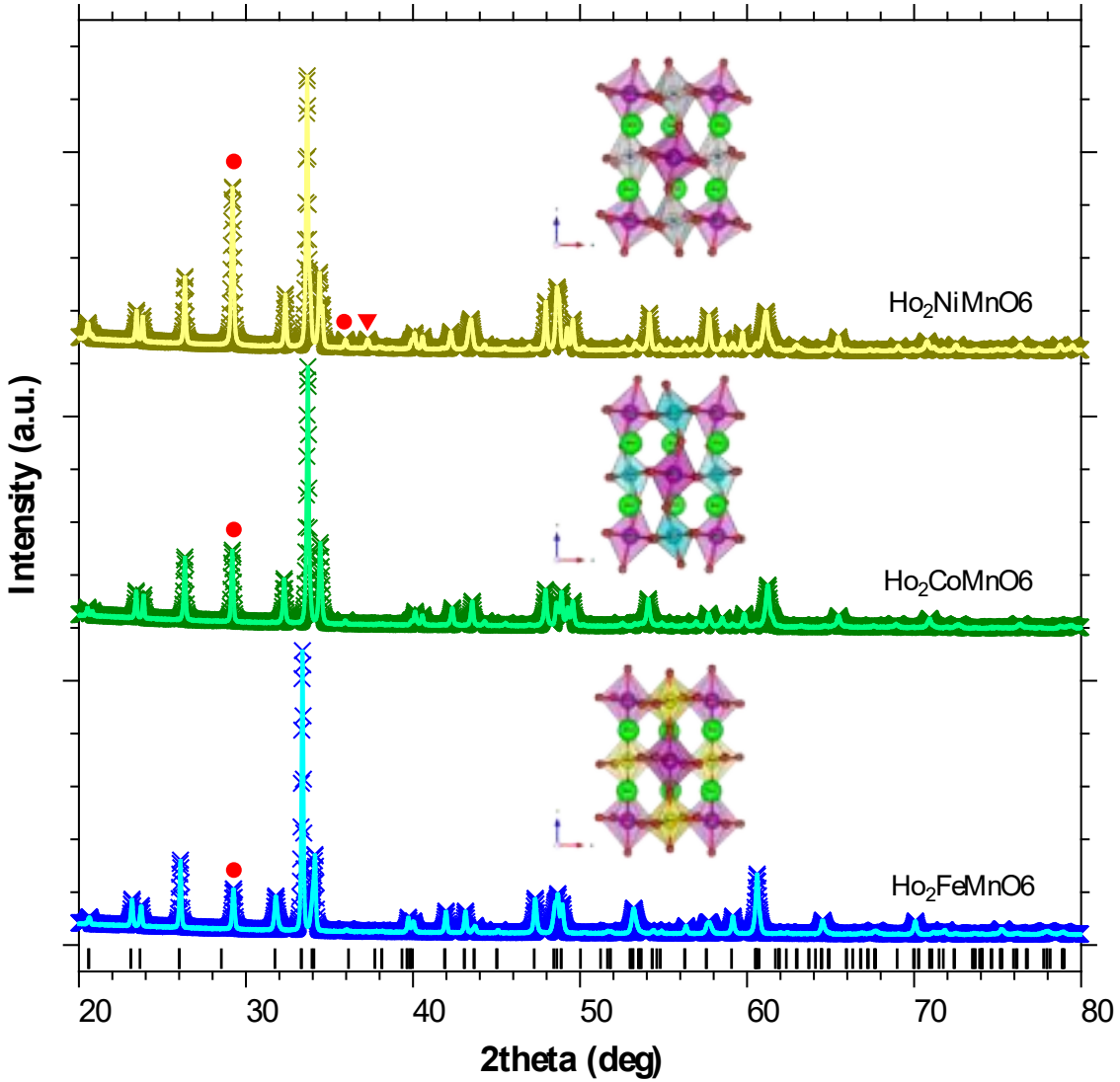

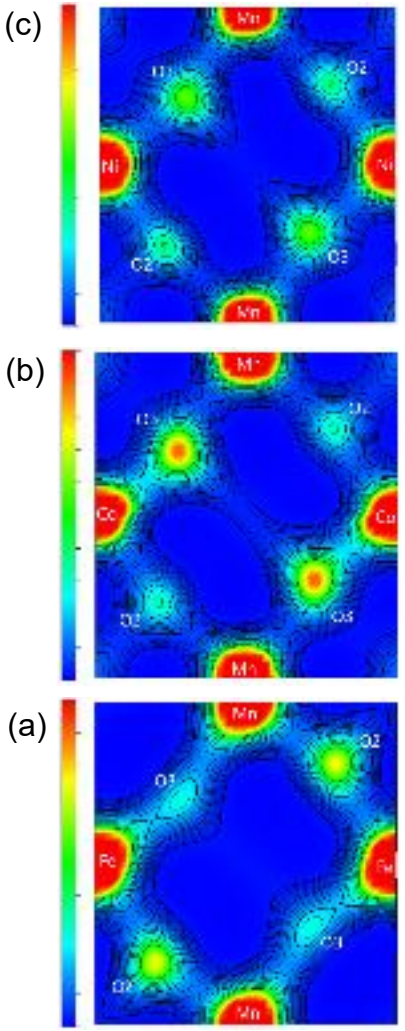

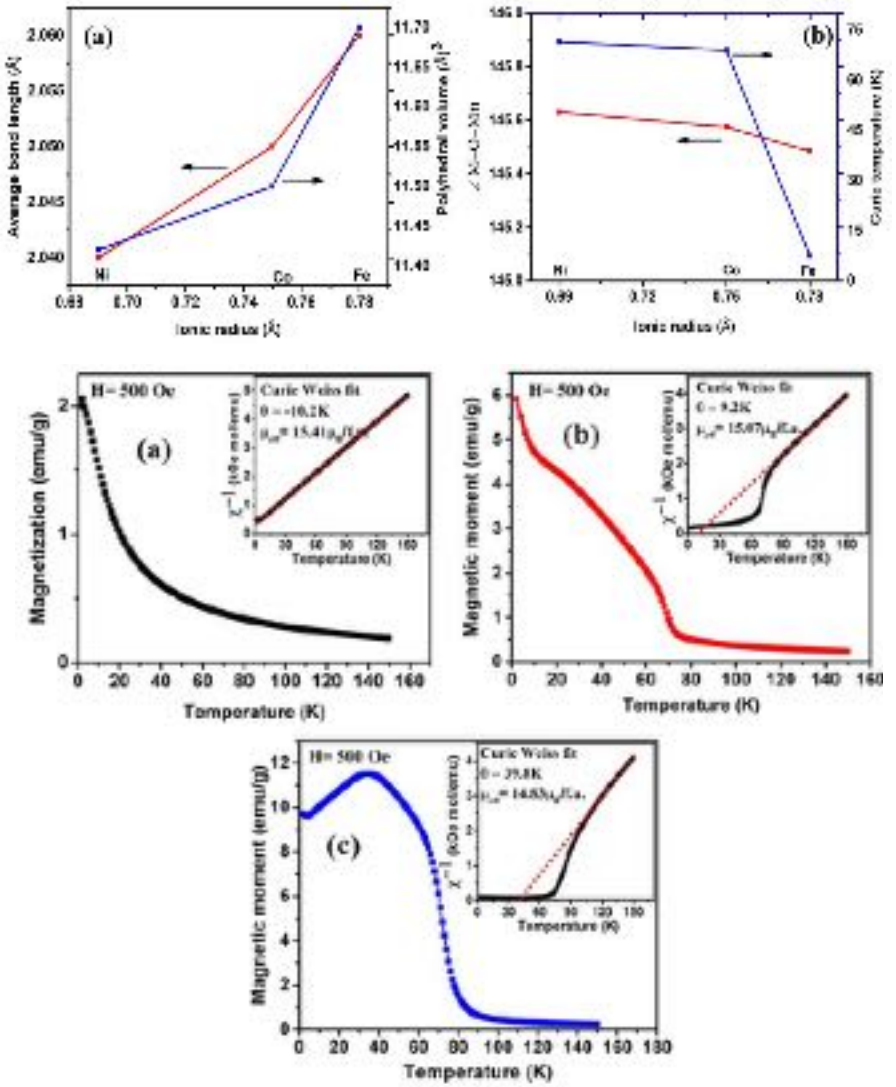

Study of structural, magnetic, and magnetocaloric properties of $Ho_{1-x}Ca_xMnO_3$

K. P. Shinde, E. J. Lee, M. Manawan, A. H. Lee, S.-Y. Park, Y. Jo, B. K. Koo & J. S. Park

https://doi.org/10.1007/s00339-021-04991-y

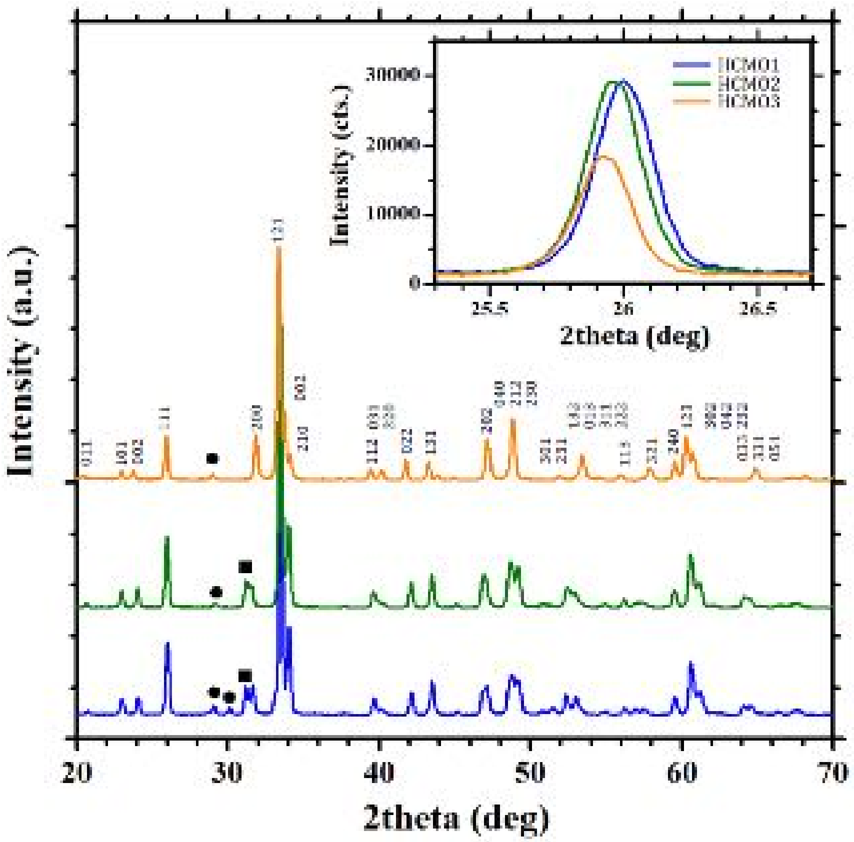

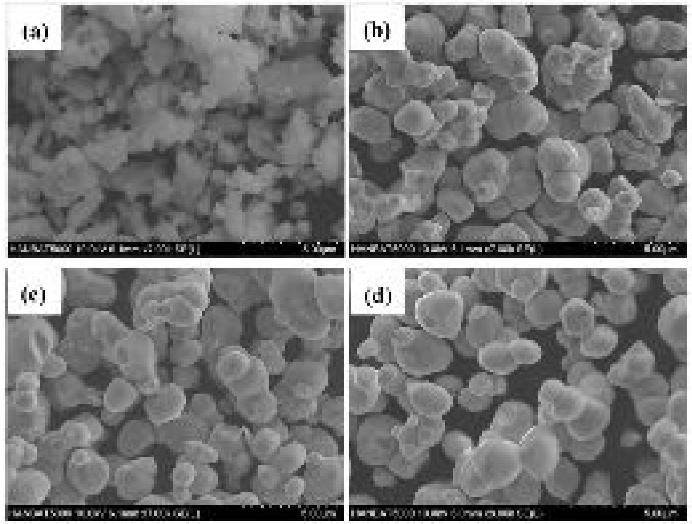

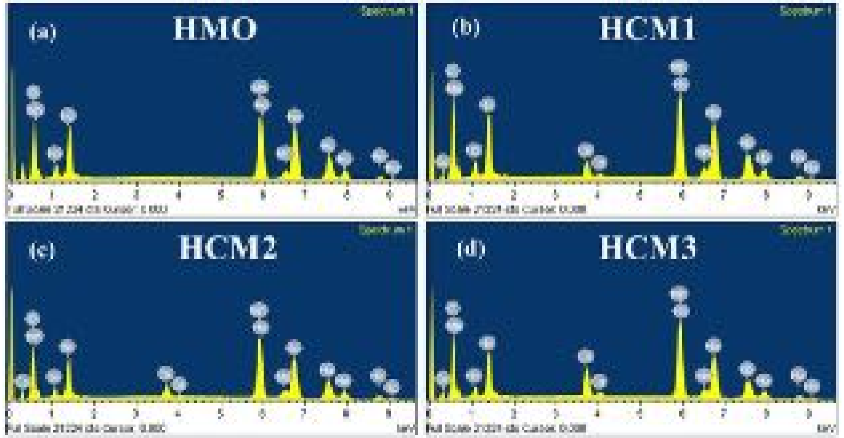

		HMO	HCM1	HCM2	HCM3
Space Group		P63cm	Pnma	Pnma	Pnma
Cell Mass (g/mol)		1650.20(1)	[illegible]	971.14(2)	921.64(1)
Cell Volume (Å^3)		[illegible]	[illegible]	[illegible]	[illegible]
Crystal Density (g/cm^3)		7.140(0)	[illegible]	[illegible]	[illegible]
Crystal Size (nm)		105(7)	[illegible]	[illegible]	[illegible]
Lattice Parameters	a (Å)	6.1451(2)	[illegible]	[illegible]	5.7102(2)
	b (Å)	6.1451(2)	[illegible]	[illegible]	[illegible]
	c (Å)	11.4057(4)	[illegible]	[illegible]	[illegible]
Ho	X		0.42212	0.43161	0.43512
	Y	–	0.25000	0.25	0.25
	Z		0.01370	0.01744	0.01565
	Occupancy	–	[illegible]	0.7591	[illegible]
Ca	X		0.43403	[illegible]	0.43140
	Y	–	0.25000	0.25	0.25
	Z	–	[illegible]	[illegible]	[illegible]
	Occupancy		[illegible]	[illegible]	[illegible]
Rexp		2.06	[illegible]	1.54	[illegible]
Rwp		7.23	4.45	4.57	[illegible]
GoF		3.51	[illegible]	[illegible]	[illegible]

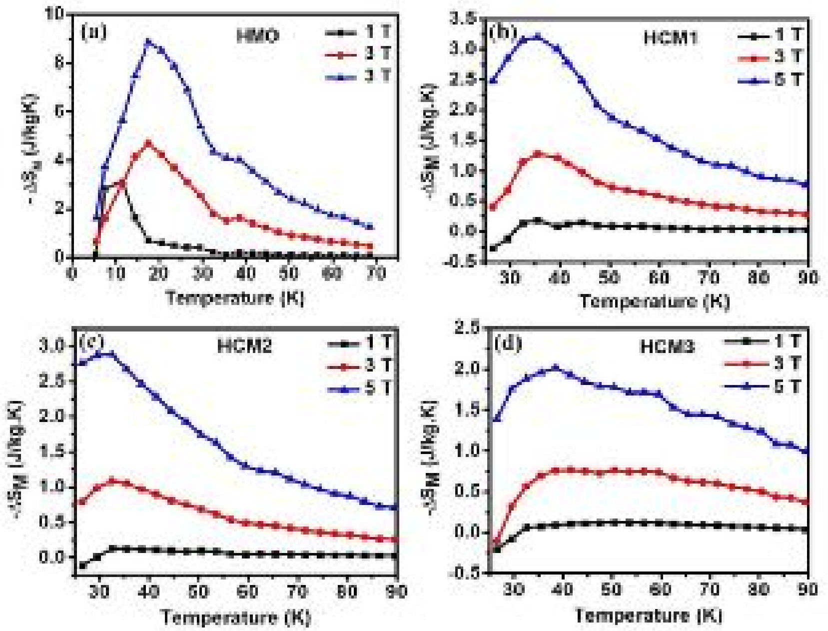

nature SCIENTIFIC REPORTS

Structural, magnetic, and magnetocaloric properties of R_2NiMnO_6 (R = Eu, Gd, Tb)

K. P. Shinde, E. J. Lee, M. Manawan, A. Lee, S.-Y. Park, Y. Jo, K. Ku, J. M. Kim & J. S. Park

https://doi.org/10.1038/s41598-021-99755-2

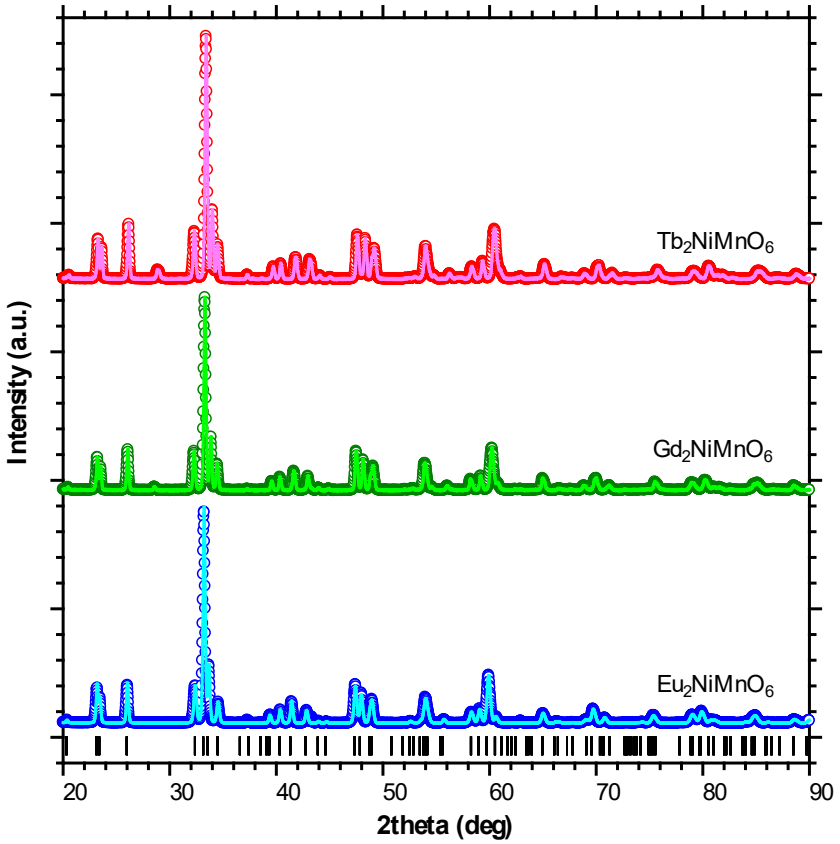

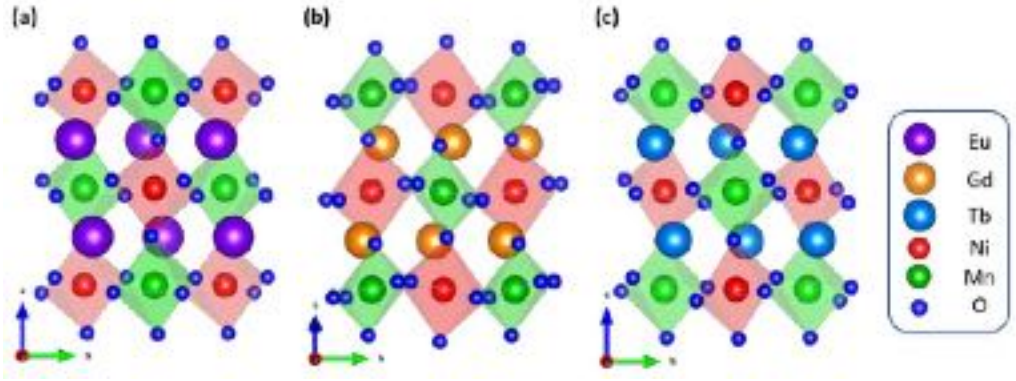

	Bond length (Å)		
	Eu_2NiMnO_6	Gd_2NiMnO_6	Tb_2NiMnO_6
Ni - O1	1.9961(1)	2.0781(2)	1.8256(1)
Ni - O2	2.0051(2)	1.6247(1)	1.7962(0)
Ni - O3	1.9391(0)	2.0505(2)	1.9416(4)
Mn - O1	1.9481(2)	1.9120(1)	2.0444(2)
Mn - O2	1.9611(2)	2.2756(3)	2.0468(0)
Mn - O3	1.9731(0)	1.8169(1)	1.9057(2)
	Bond Angle (°)		
	Eu_2NiMnO_6	Gd_2NiMnO_6	Tb_2NiMnO_6
Ni - O1 - Mn	153.07(2)	147.30(4)	161.84(2)
Ni - O2 - Mn	150.99(1)	157.80(1)	141.65(4)
Ni - O3 - Mn	151.47(1)	155.12(3)	155.95(1)

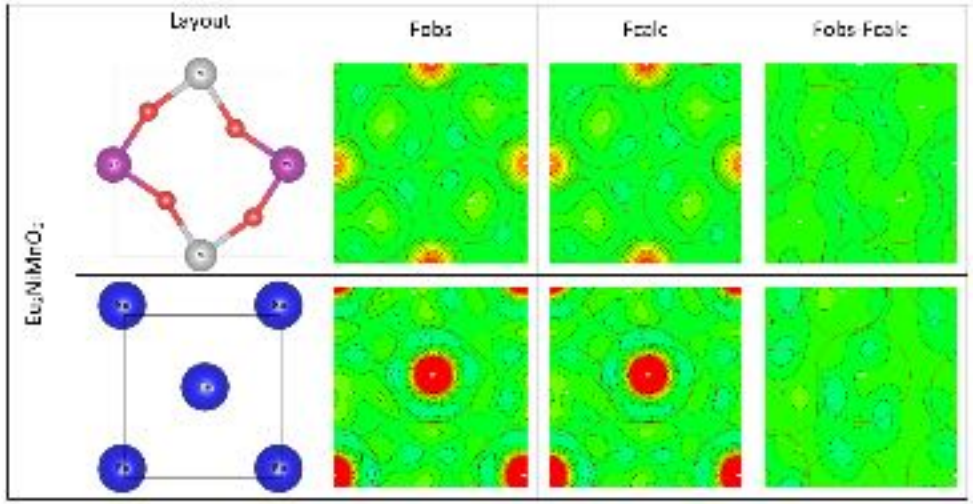

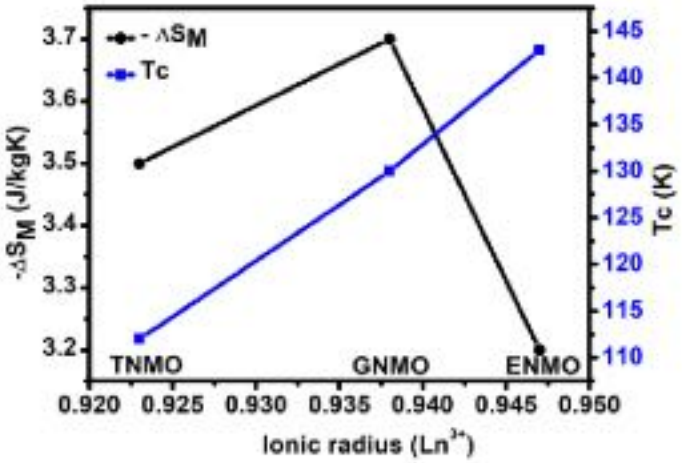

Visualizing lithium ions in the crystal structure of Li_3PO_4 by *in situ* neutron diffraction

M. Manawan, E. Kartini and M. Avdeev

https://doi.org/10.1107/S1600576721008700

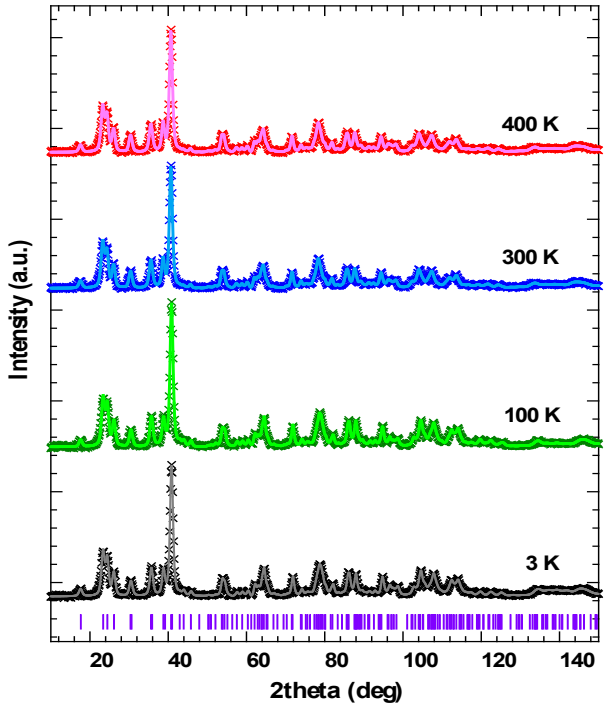

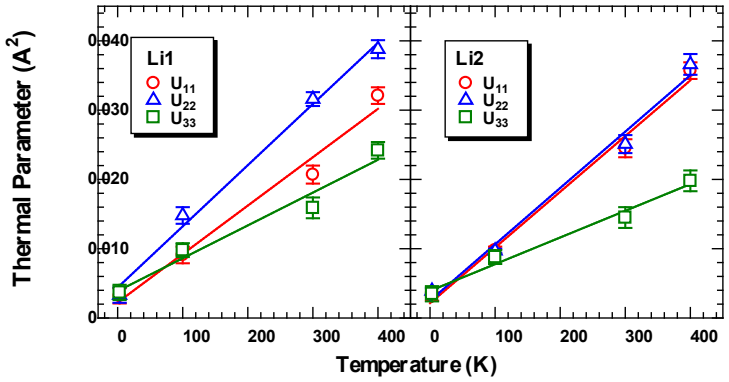

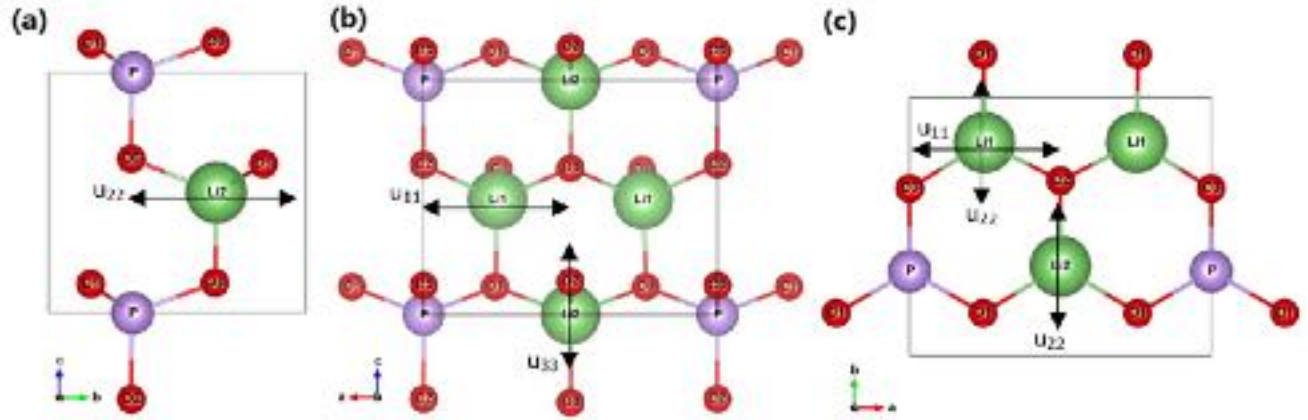

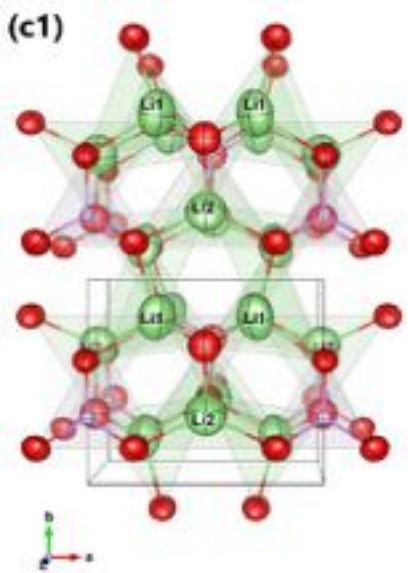

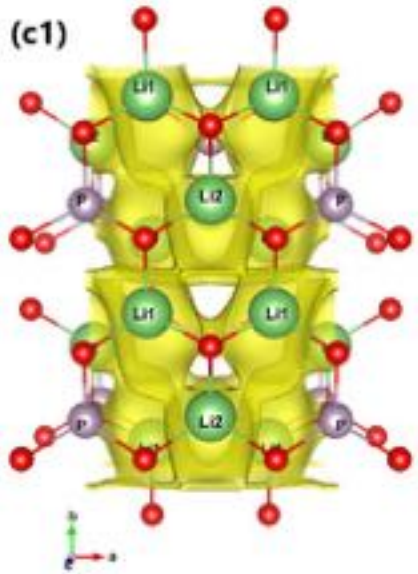

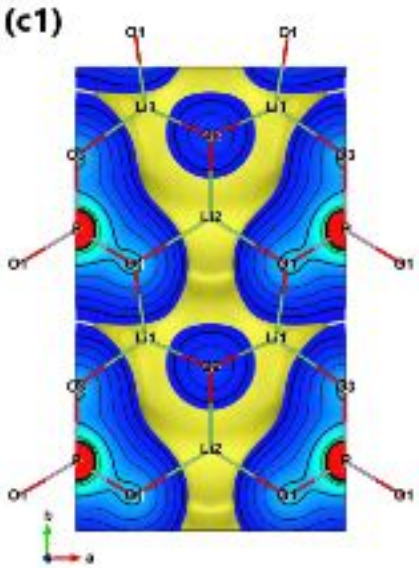

Unveiling the Formation Mechanism and Phase Purity Control of Nanostructured $Li_4Ti_5O_{12}$ via a Hydrothermal Process

Kaiming Li, Xundong Dai, Maykel Manawan, Qing Wang*, and Jia Hong Pan*

https://doi.org/10.1021/acs.cgd.1c00727

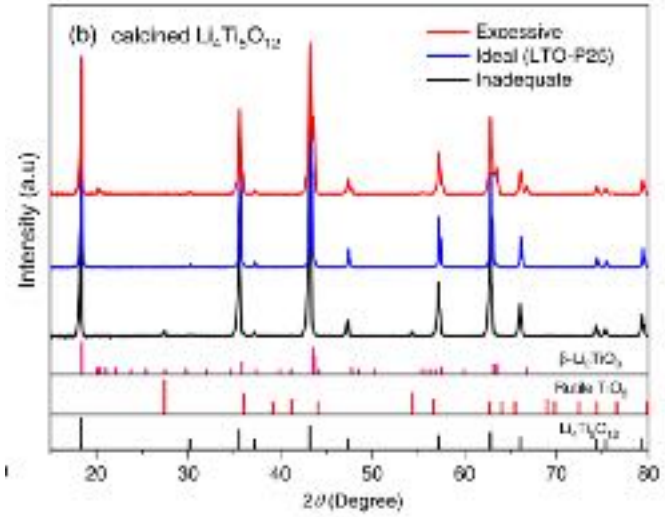

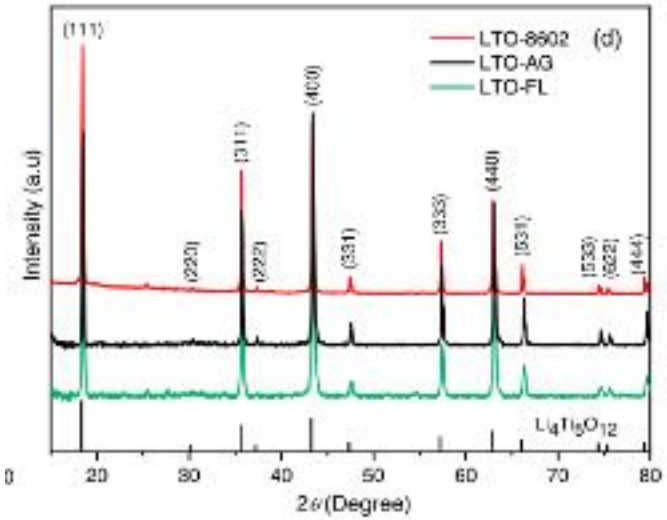

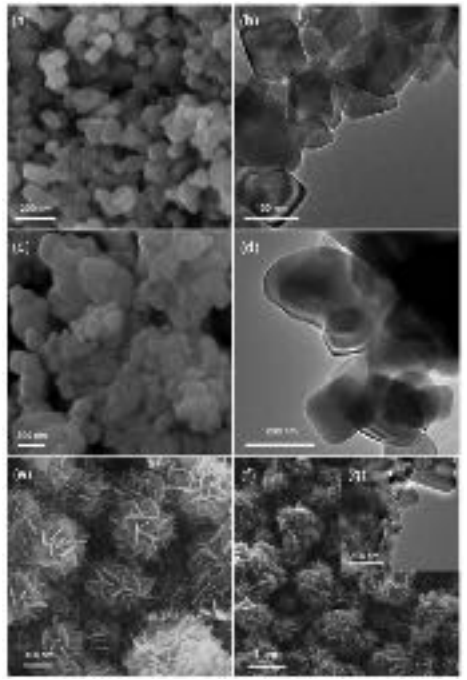

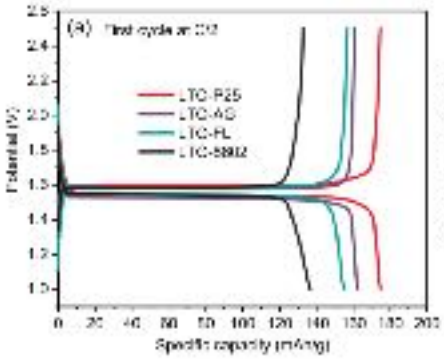

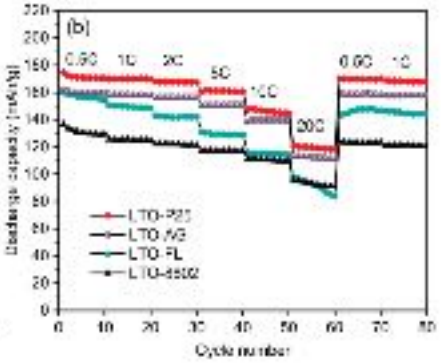

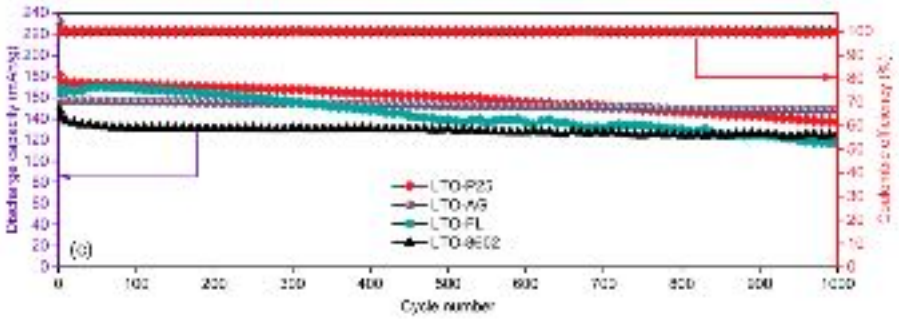

CellPress
Science that Inspires

iScience
A Cell Press journal

Solid-state self-template synthesis of Ta-doped $Li_2ZnTi_3O_8$ spheres for efficient and durable lithium storage

Dongwei Ma,[*] Jiahui Li,[1] Jing Yang,[2] Chengfu Yang,[1] Maykel Manawan,[3] Yongri Liang,[4] Ting Feng,[5] Yong-Wei Zhang,[2] and Jia Hong Pan[1,6,*]

https://doi.org/10.1016/j.isci.2021.102991

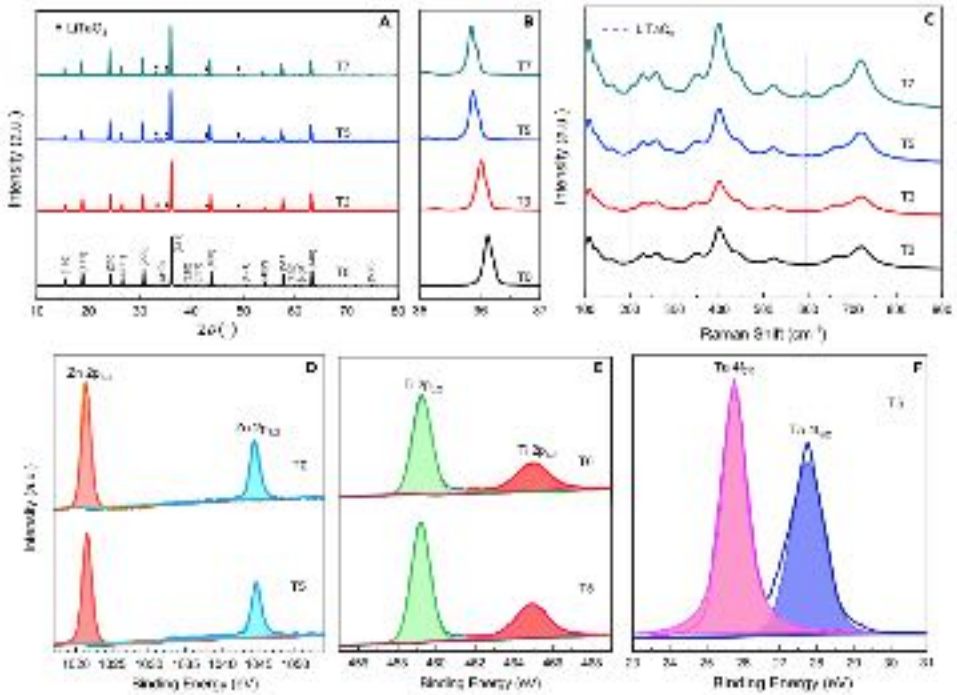

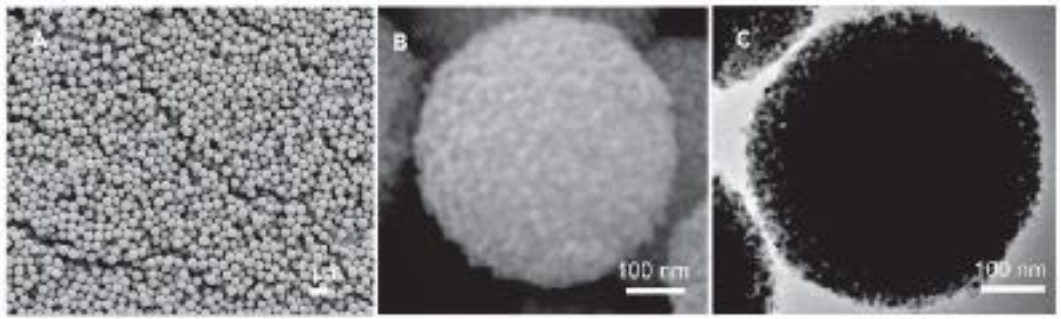

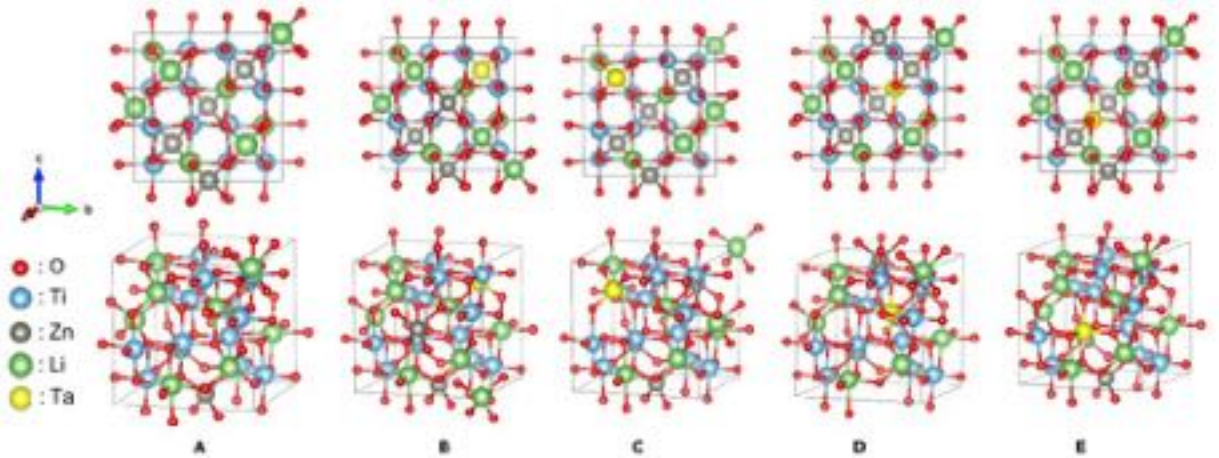

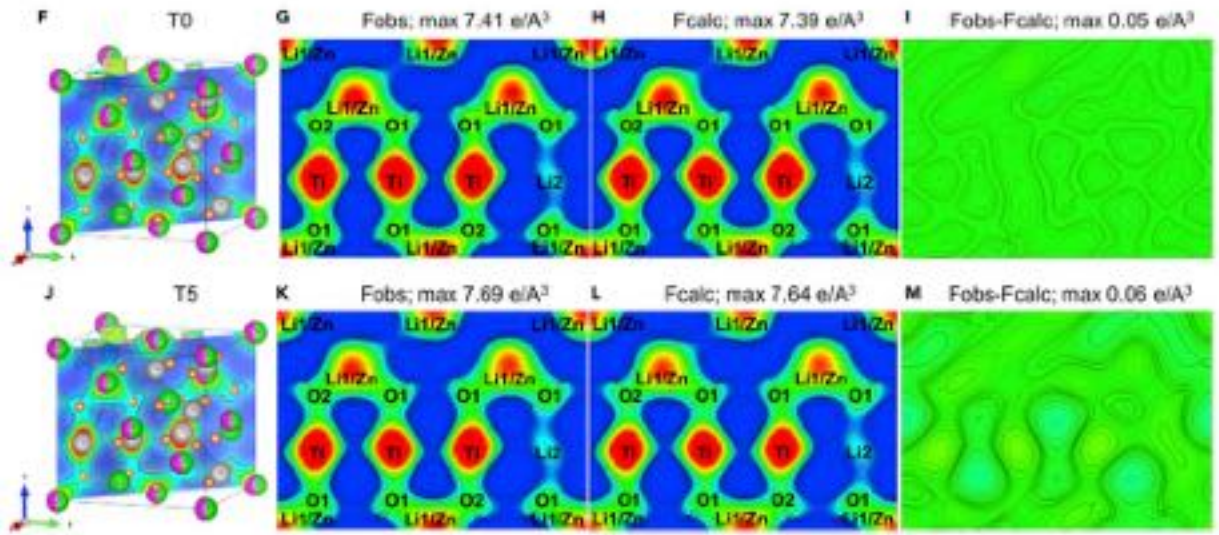

XRD Residual Stress and Texture Analysis on 6082T Aluminum Alloy

Maykel Manawan[1,a*], Sovian Aritonang[1,b], Masayu Elita[1,c], Antonius Suban Hali[2,d], Nono Darsono[3,e], Toto Sudiro[4,f], Permono Adi Putro[5,g], Risdiana[6,h]

https://doi.org/10.4028/www.scientific.net/MSF.1028.409

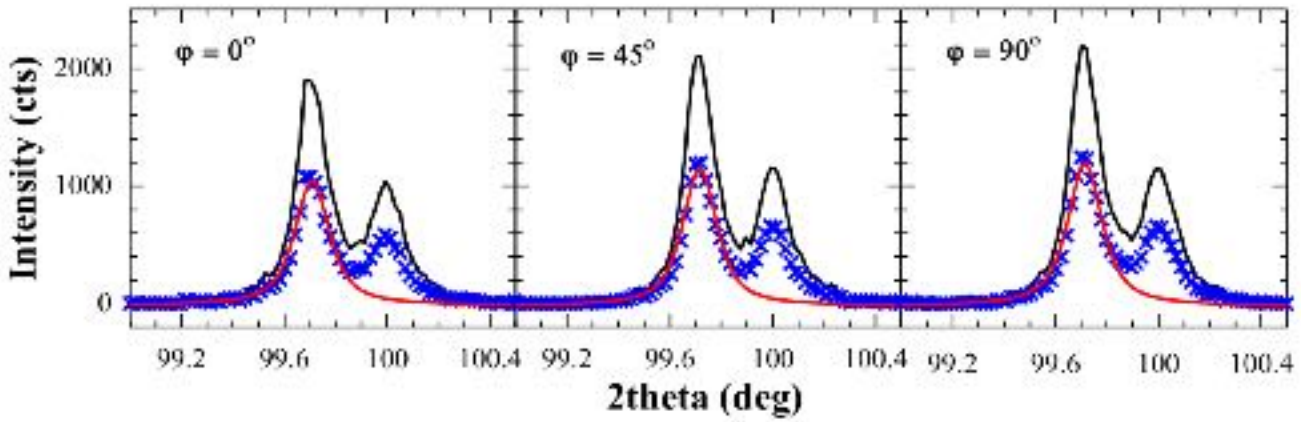

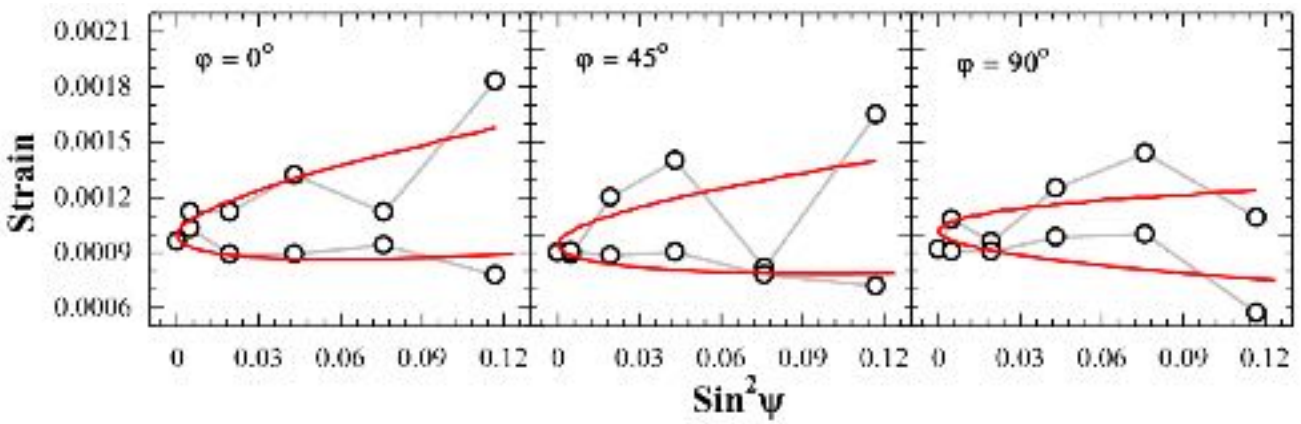

φ (°)	Normal Stress (MPa)	Shear Stress (MPa)
0	109.3 ± 21.2	-28.7 ± 6.1
45	68.9 ± 19.4	-25.6 ± 8.5
90	-9.9 ± 9.4	-20 ± 8.5

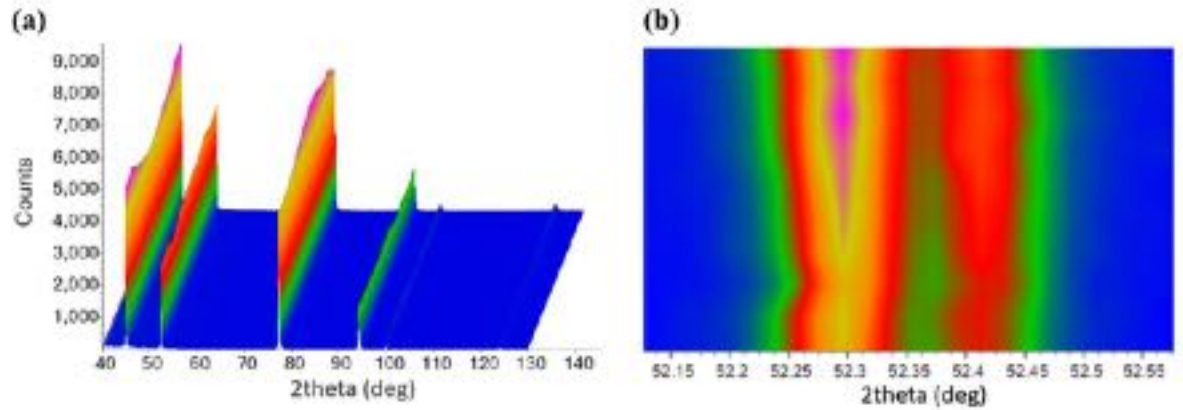

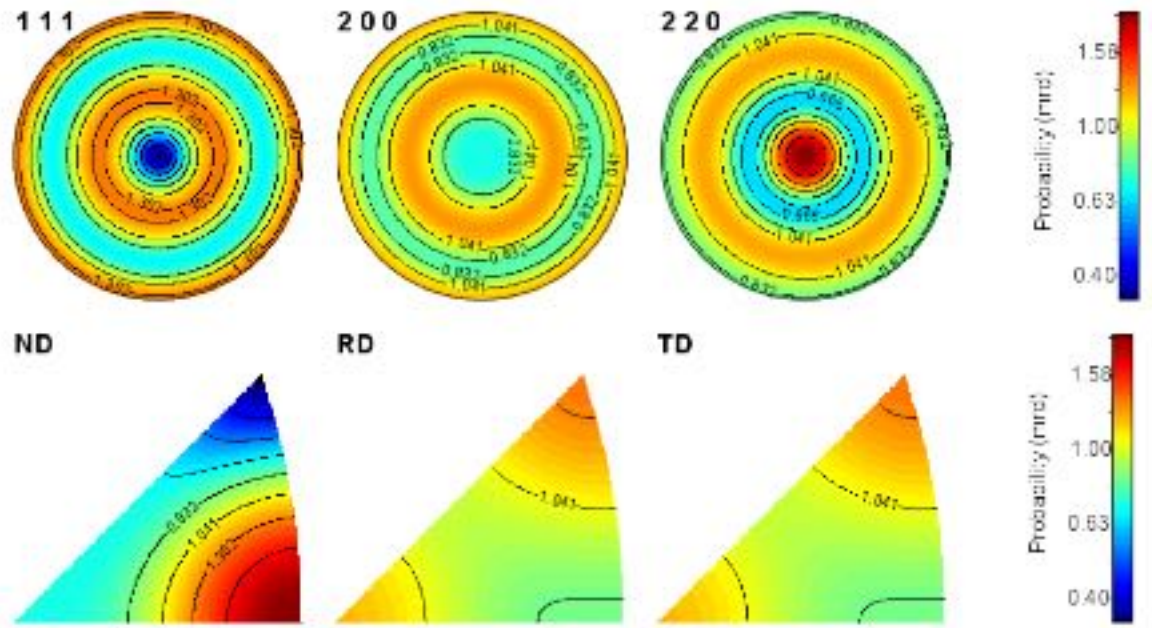

Crystal Characterization of Anionic Salt Compounds as Composite of Solid Propellant Oxidizing Agent

Sovian Aritonang[1,a], Maykel Manawan[1,b*], Mas Ayu E. H[1,c], Timbul Siahaan[1], Shofi Muktiana S.[1], Hanung Bayu Setiawan[1], Sih Wuri Andayani[2], Gaos Abdul Karim[2], Alfiz Muhammad Qizwini[2], Otong Nurhilal[3], Togar Saragi[3], Risdiana[3]

https://doi.org/10.4028/www.scientific.net/MSF.1028.269

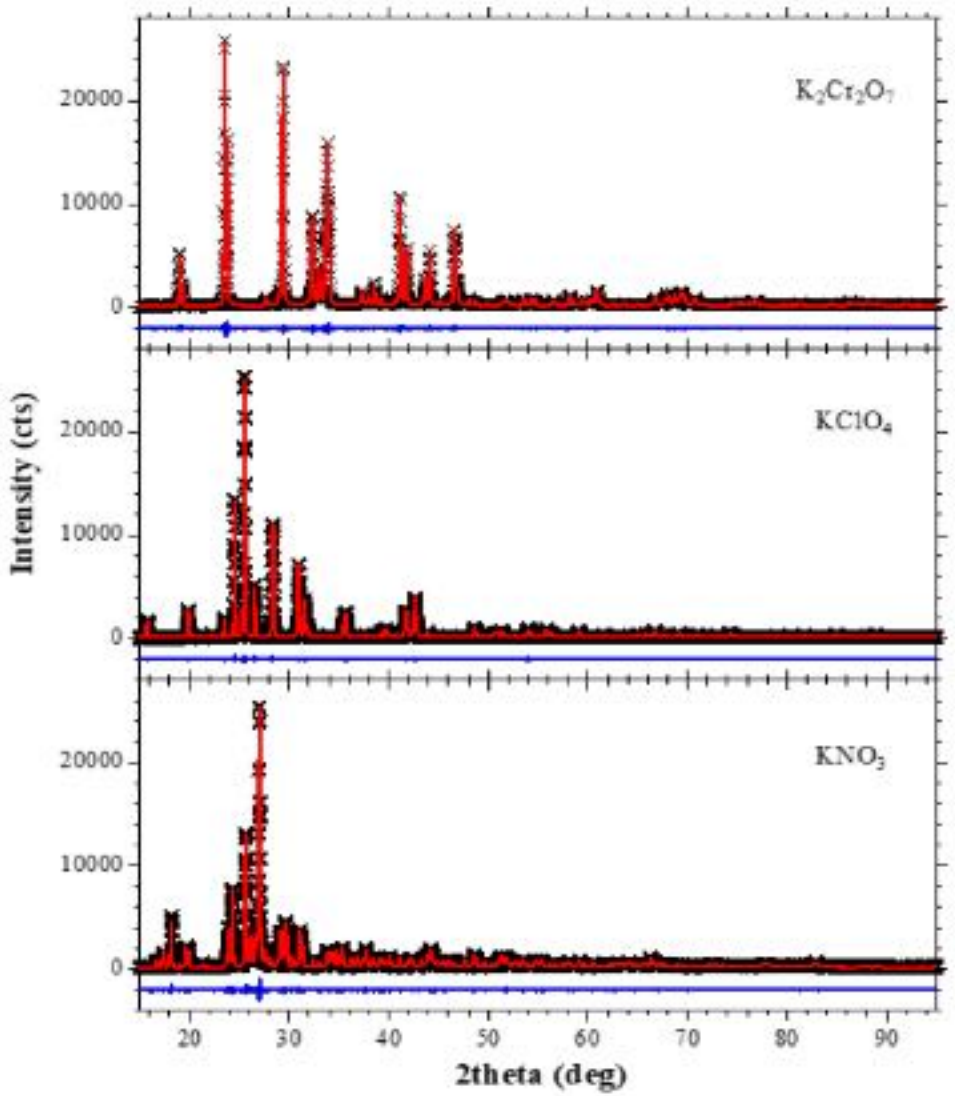

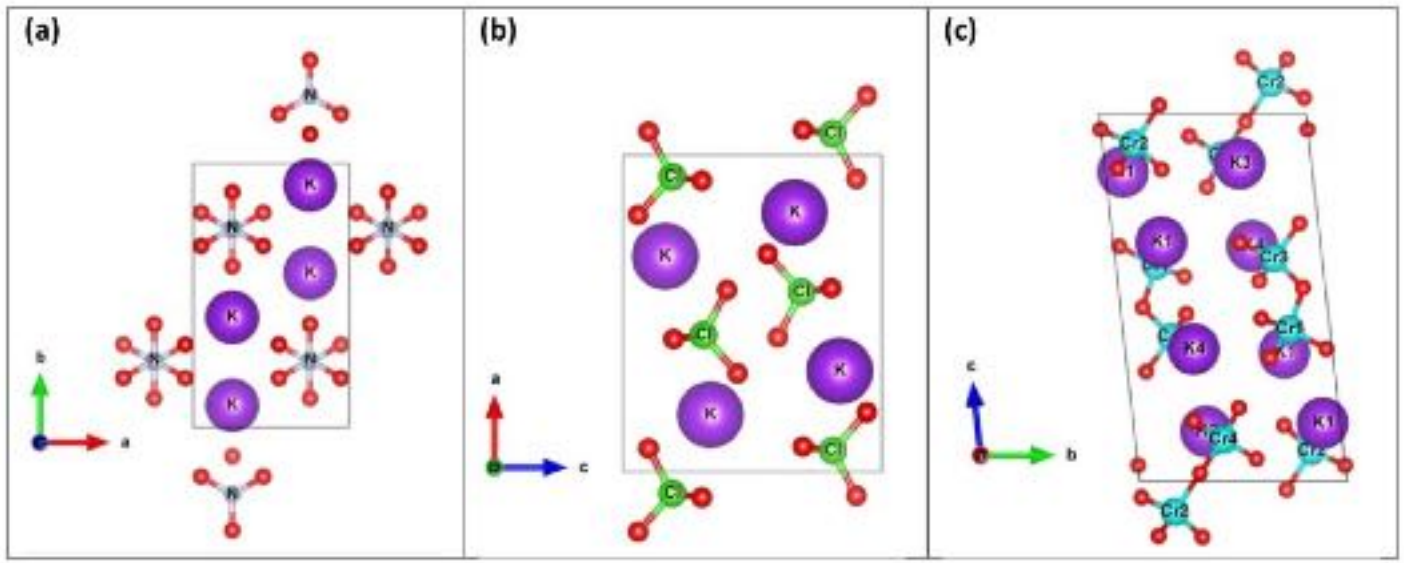

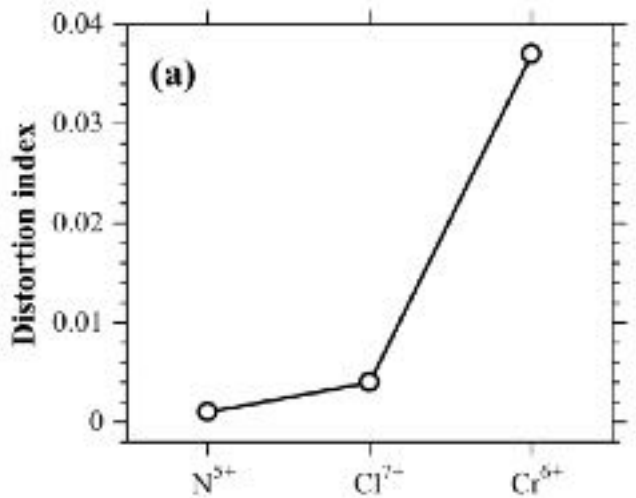

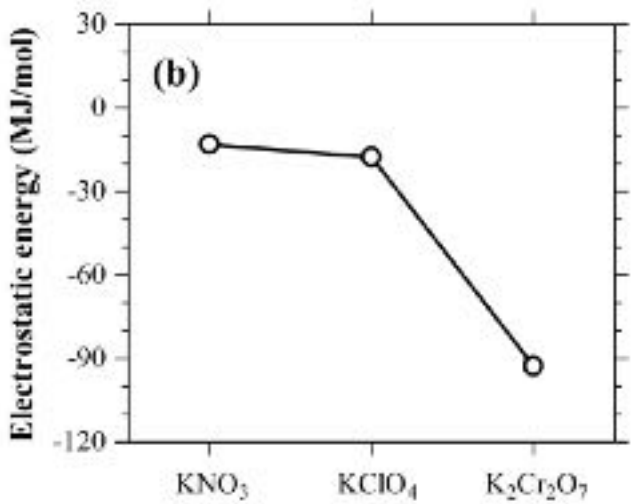

Progress in Natural Science: Materials International 30 (2020) 168–173

Contents lists available at ScienceDirect

Progress in Natural Science: Materials International

journal homepage: www.elsevier.com/locate/pnsmi

Original research

Solid electrolyte composite $Li_4P_2O_7$–Li_3PO_4 for lithium ion battery

Evvy Kartini[a,*], Valentina Yapriadi[b], Heri Jodi[a], Maykel Manawan[c], Cipta Panghegar[d], Wahyudianingsih[a]

[a] Center for Science and Technology of Advanced Materials, National Nuclear Energy Agency, South Tangerang, 15314, Indonesia
[b] Faculty of Engineering, Leeds University, UK
[c] Energy Engineering, Jakarta State Polytechnic, Depok, Indonesia
[d] Polytechnique Institute of Nuclear Technology, Yogyakarta, Indonesia

Table 2
Bond distance calculation of quenched samples at 600 °C, 800 °C and 900 °C.

600 °C						800 °C						900 °C					
$Li_4P_2O_7$			$LiPO_3$			$Li_4P_2O_7$			Li_3PO_4			$Li_4P_2O_7$			Li_3PO_4		
Bond		Distance	Bond		Distance	Bond		Distance	Bond		Distance	Bond		Distance	Bond		Distance
Li1	- O6	1.87	Li1	- O2	1.912	Li1	- O6	1.869	Li1	- O1	1.947	Li1	- O6	1.869	Li1	- O1	1.946
	- O1	1.95		- O14	1.967		- O1	1.95		- O3	1.994		- O1	1.949		- O3	1.994
	- O4	1.976		- O1	1.978		- O4	1.974		- O3	1.994		- O4	1.975		- O3	1.994
	- O4	1.976		- O7	1.989		- O4	1.974		- O2	2.047		- O4	1.975		- O2	2.047
Li2	- O6	1.913	Li2	- O3	1.965	Li2	- O6	1.913	Li2	- O1	1.93	Li2	- O6	1.913	Li2	- O1	1.93
	- O2	1.94		- O8	1.967		- O2	1.94		- O2	1.944		- O2	1.94		- O2	1.944
	- O5	2.009		- O11	1.996		- O5	2.008		- O3	1.95		- O5	2.009		- O3	1.949
	- O1	2.01		- O13	1.987		- O1	2.008		- O3	1.992		- O1	2.01		- O3	1.992
Li3	- O3	1.865	Li3	- O14	1.877	Li3	- O3	1.864				Li3	- O3	1.865			
	- O2	1.874		- O10	1.898		- O2	1.872					- O2	1.873			
	- O7	2.085		- O10	1.997		- O7	2.084					- O7	2.085			
	- O5	2.105		- O1	1.997		- O5	2.105					- O5	2.104			
Li4	- O5	1.926	Li4	- O6	1.907	Li4	- O5	1.926				Li4	- O3	1.926			
	- O3	1.926		- O3	1.934		- O3	1.926					- O5	1.926			
	- O4	2.008		- O6	1.935		- O4	2.008					- O4	2.008			
	- O1	2.011		- O8	1.996		- O1	2.01					- O1	2.011			
			Li5	- O7	1.914												
				- O7	1.914												
				- O2	1.973												
				- O2	1.973												

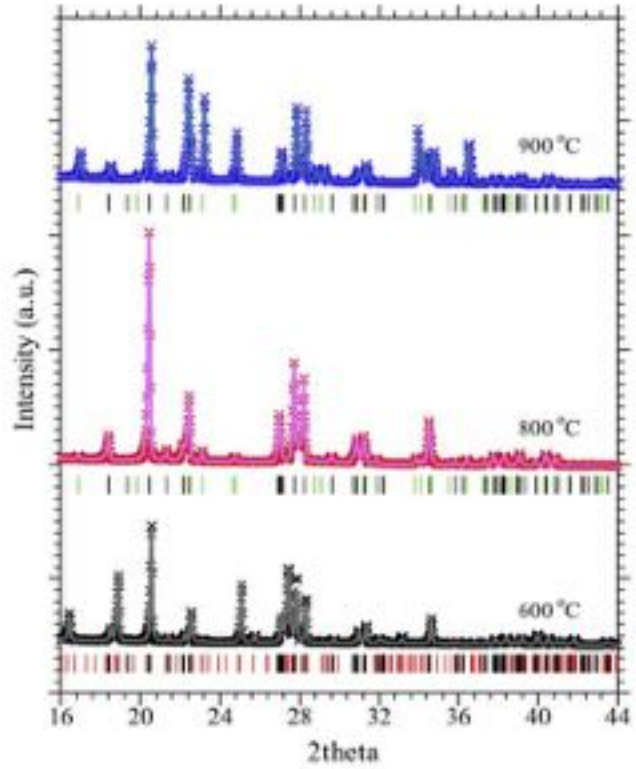

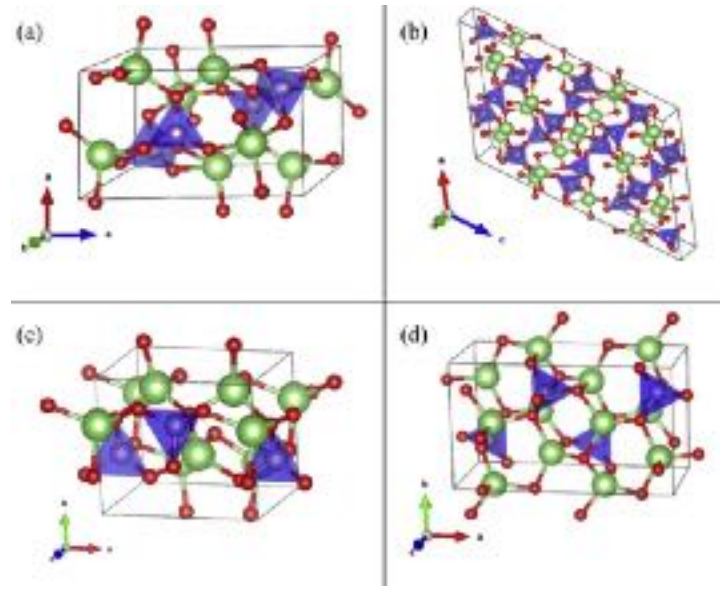

Contents lists available at ScienceDirect

Powder Technology

journal homepage: www.elsevier.com/locate/powtec

In-situ synthesis and characterization of nano-structured NiAl-Al_2O_3 composite during high energy ball milling

Maryam Beyhaghi [a,*], Jalil Vahdati Khaki [b], Maykel Manawan [c,d], Alireza Kiani-Rashid [b], Mehrdad Kashefi [b], Stefan Jonsson [e]

[a] Department of Metallurgy and Ceramics, Faculty of Engineering, Mashhad Branch, Islamic Azad University, Mashhad, Iran
[b] Department of Metallurgical and Materials Engineering, Ferdowsi University of Mashhad, 91775-1111 Mashhad, Iran
[c] Department of Physics, Universitas Indonesia, Depok 16424, Indonesia
[d] Energy Engineering, Politeknik Negeri Jakarta, Depok 1624, Indonesia
[e] Department of Materials Science and Engineering, Royal Institute of Technology, SE-10044 Stockholm, Sweden

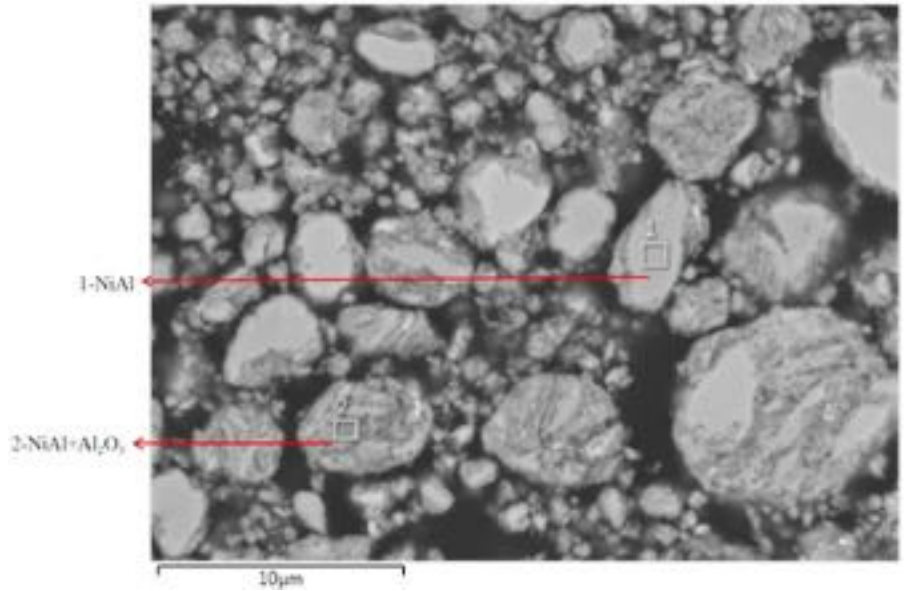

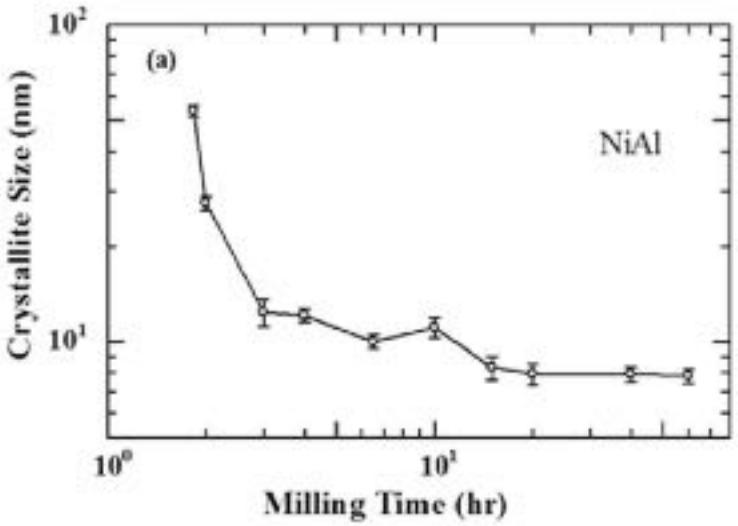

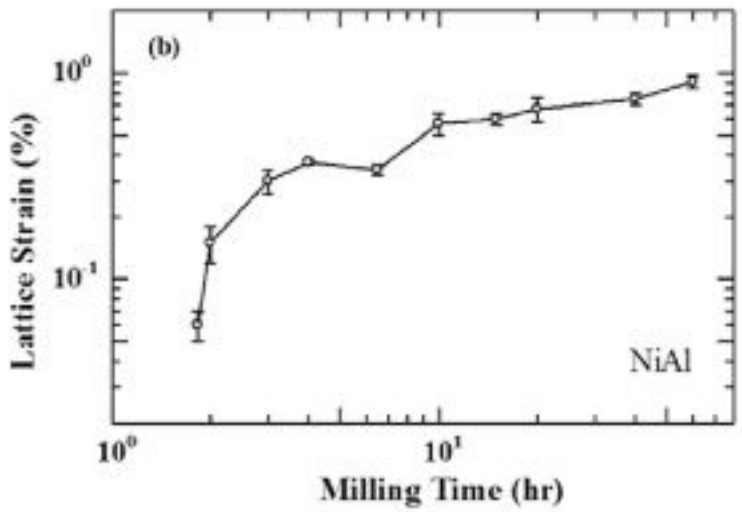

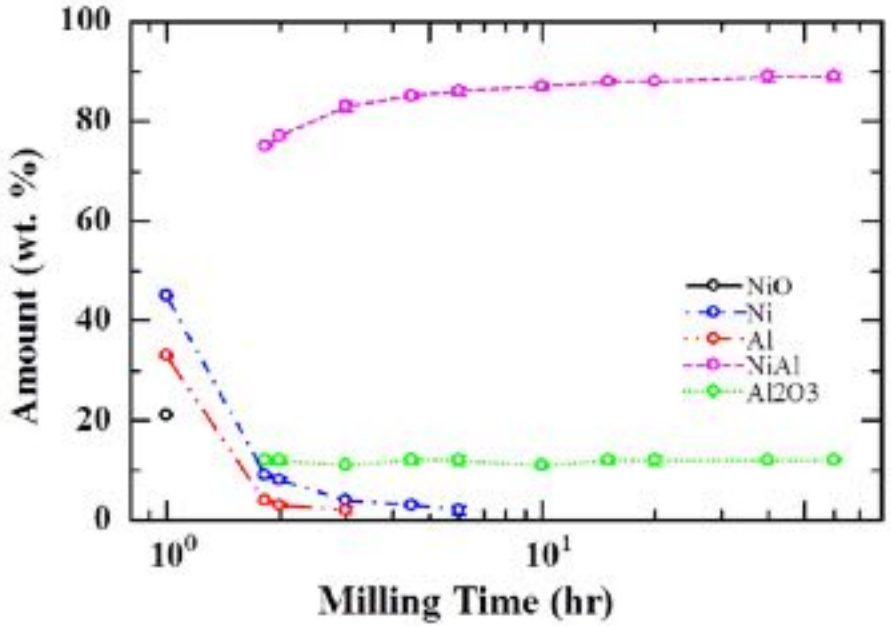

Contents lists available at ScienceDirect

Catalysis Today

journal homepage: www.elsevier.com/locate/cattod

Anatase and rutile in evonik aeroxide P25: Heterojunctioned or individual nanoparticles?

Xiongzhen Jiang[a,1], Maykel Manawan[b,1], Ting Feng[c], Ruifeng Qian[a], Ting Zhao[a], Guanda Zhou[a], Fantai Kong[d,*], Qing Wang[e,*], Songyuan Dai[a], Jia Hong Pan[a,*]

[a] Beijing Key Laboratory of Energy Safety and Clean Utilization, School of Renewable Energy, North China Electric Power University, Beijing 102206, China
[b] Crystallography and Diffraction Lab, Material Science, Department of Physics, Faculty of Mathematics and Natural Sciences, Universitas Indonesia, Depok 16424, Indonesia
[c] School of Metallurgical and Ecological Engineering, University of Science & Technology Beijing, Beijing 100083, China
[d] Key Laboratory of Novel Thin Film Solar Cells, Institute of Applied Technology, Chinese Academy of Sciences, Hefei 230031, China
[e] Department of Materials Science and Engineering, Faculty of Engineering, National University of Singapore, Singapore 117576, Singapore

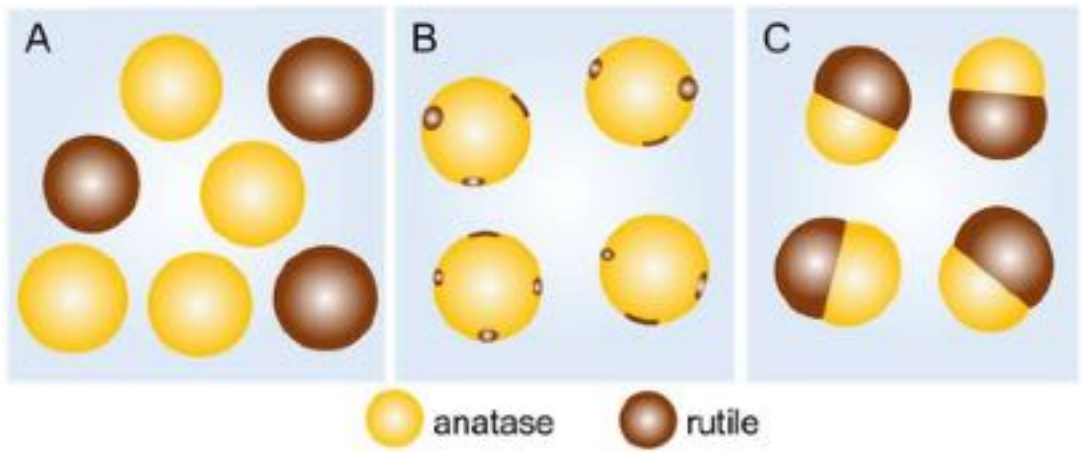

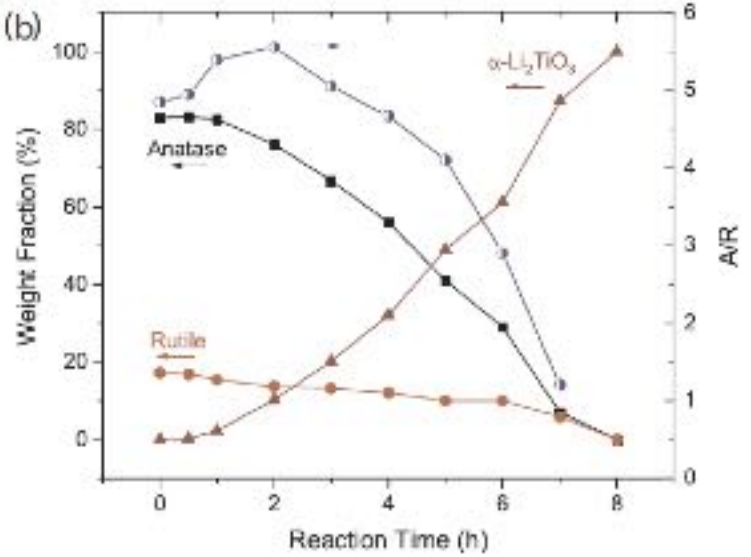

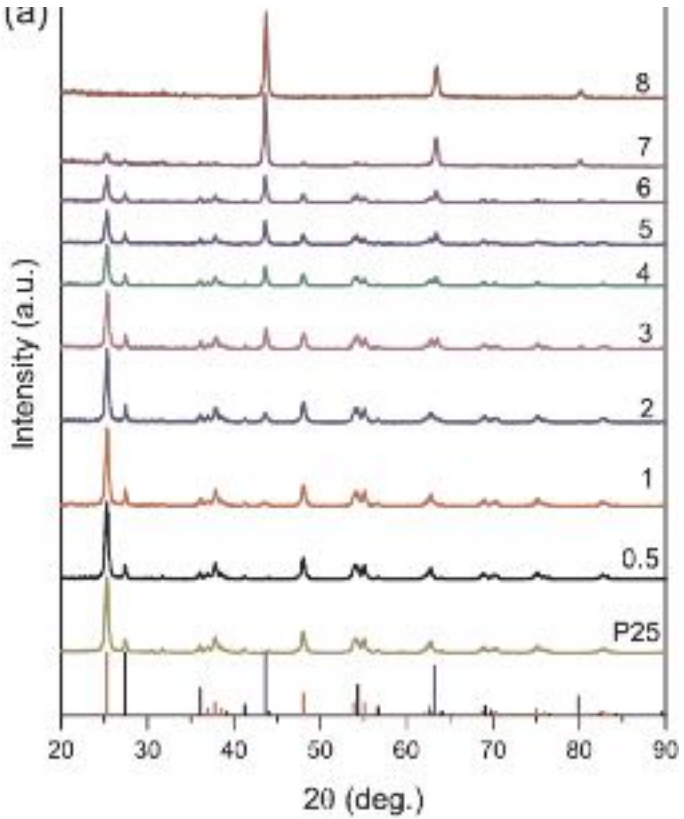

Physica B: Condensed Matter 551 (2018) 320–326

Contents lists available at ScienceDirect

Physica B: Condensed Matter

journal homepage: www.elsevier.com/locate/physb

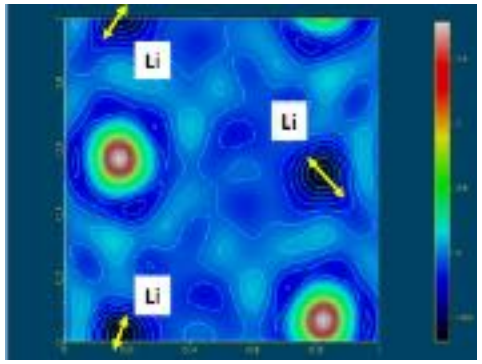

Neutron diffraction study on Li_3PO_4 solid electrolyte for lithium ion battery

Evvy Kartini [a,*], Maykel Manawan [b,c], Malcolm F. Collins [d], Maxim Avdeev [e]

[a] Science and Technology Center for Advanced Materials, National Nuclear Energy Agency (BATAN), Indonesia, Puspiptek Area, Serpong, South Tangerang 15314, Indonesia
[b] Materials Science, Faculty of Mathematic and Natural Science, University of Indonesia, Jl. Margonda Raya, Depok, 16424, Indonesia
[c] Energy Engineering, Polytechnic Negeri Jakarta, Depok, 16424, Indonesia
[d] Department of Physics and Astronomy, McMaster University, 1280 MainStreet West, Hamilton, ON L8S4L8, Canada
[e] Australian Centre for Neutron Scattering (ACNS), Australian Nuclear Science and Technology (ANSTO), Locked Bag 200, Kirrawee DC, NSW, 223, Australia

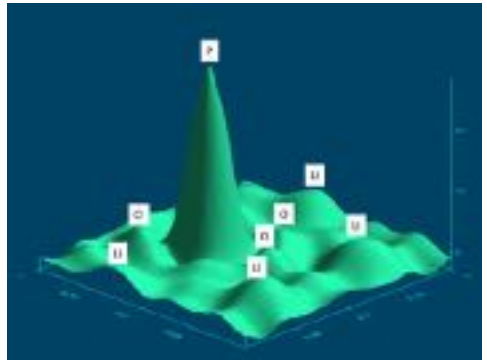

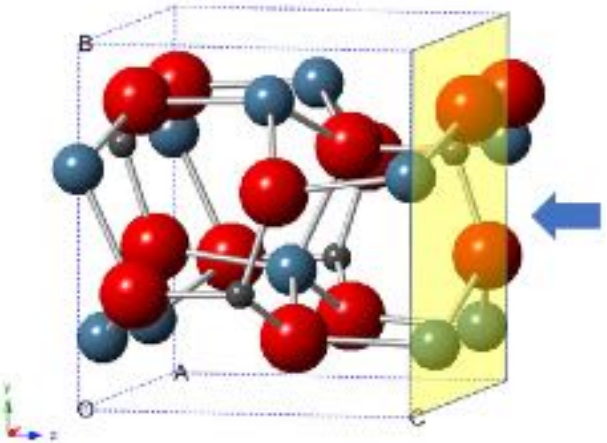

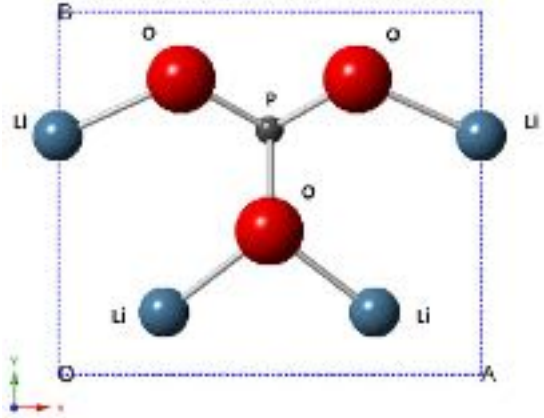

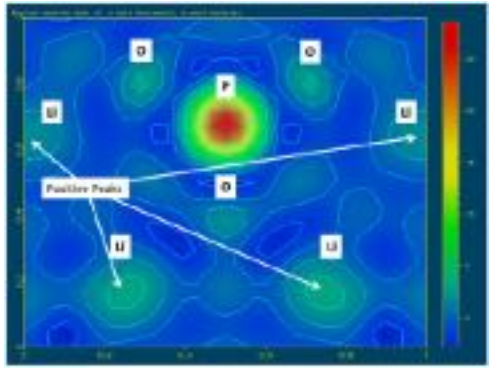

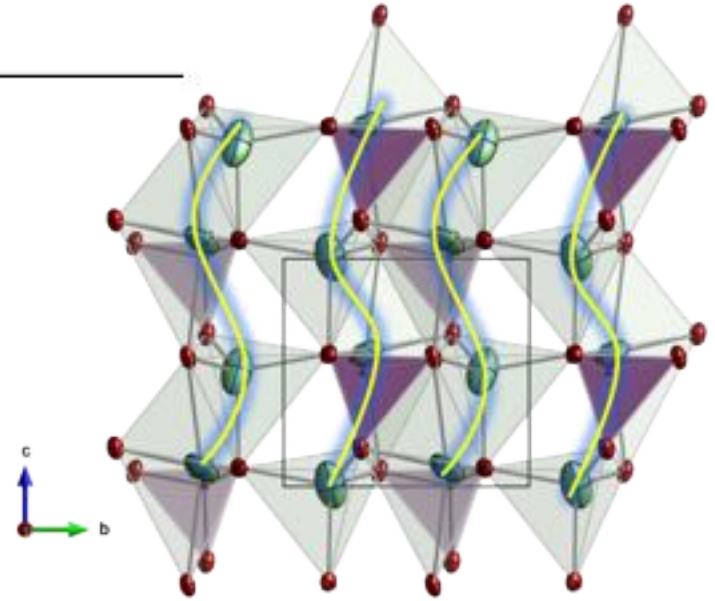

3rd Padjadjaran International Physics Symposium IOP Publishing
IOP Conf. Series: Journal of Physics: Conf. Series **1080** (2018) 012008 doi:10.1088/1742-6596/1080/1/012008

Crystallite size determination of barium hexaferrite nanoparticles using WH-plot and WPPM

M Manawan[1,2,4*], T Saragi[1], A Sukandi[2], Fachrudin[2], B Kurniawan[3], A Manaf[3], E P Boedijono[4] and Risdiana[1]

[1]Department of Physics, Universitas Padjadjaran, Sumedang 45363, Indonesia
[2]Energy Engineering, Politeknik Negeri Jakarta, Depok 16424, Indonesia
[3]Department of Physics, Universitas Indonesia, Depok 16424, Indonesia
[4]Integrated Laboratory, Esa Unggul University, Jakarta 11510, Indonesia

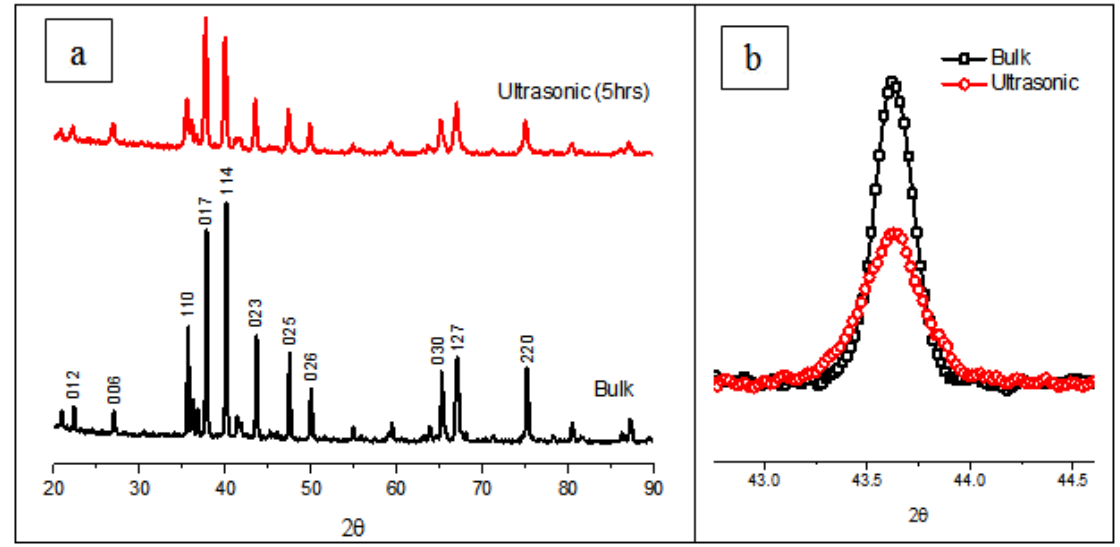

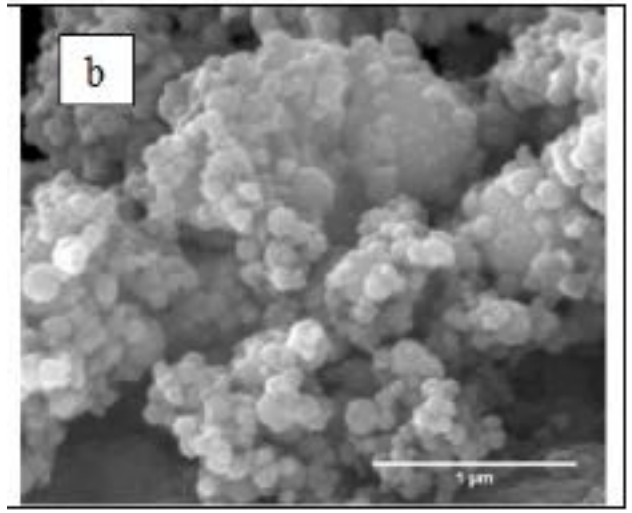

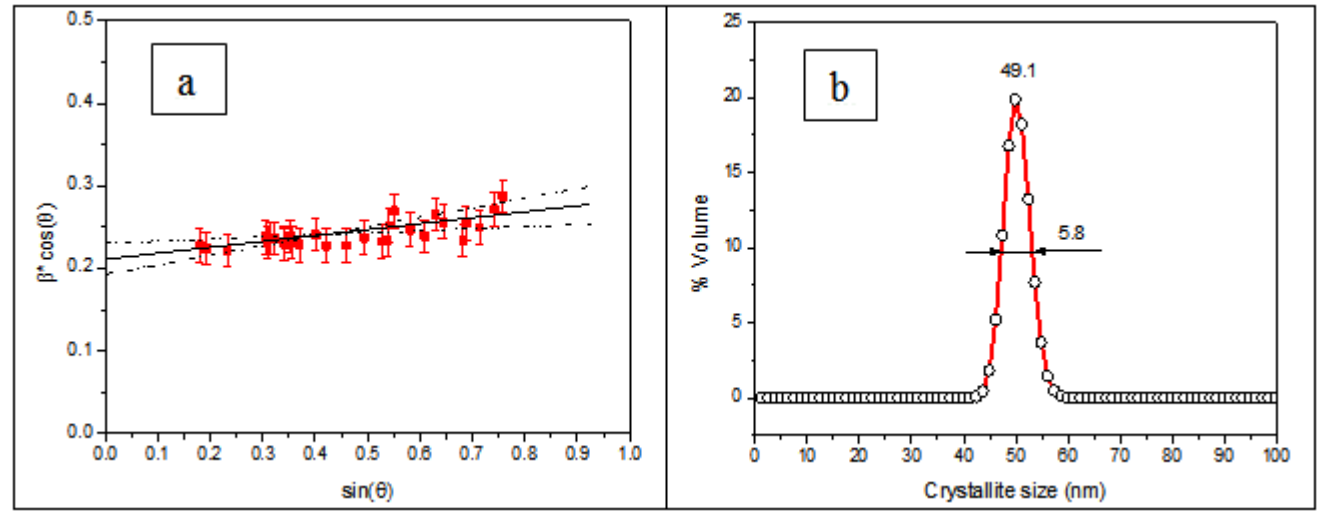

Future Project - MEM, BVS, BVEL, PDF

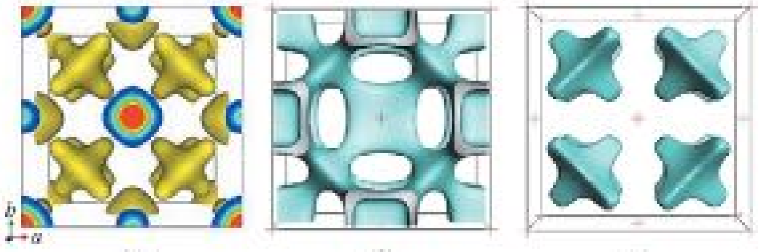

Figure 6
CuI at 773 K. (a) Experimental Cu-ion distribution determined by maximum entropy analysis of neutron diffraction data [adapted with permission from Adipranoto et al. (2009)]. (b) and (c) BVS map (isovalue ±0.1 v.u.) and BVEL (isovalue −1.4 eV, E_{min} −1.5 eV) data calculated for ICSD 163859 (Adipranoto et al., 2009).

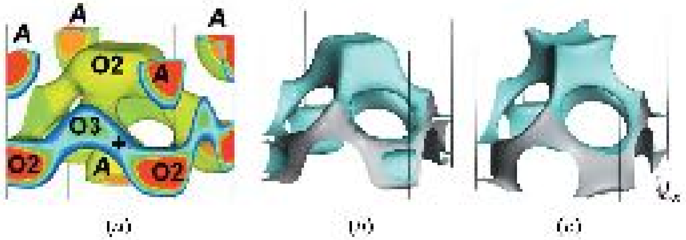

Figure 2
$(Pr_{0.9}La_{0.1})_2(Ni_{0.74}Cu_{0.21}Ga_{0.05})O_{4+\delta}$ (PLNCG) at 1298.7 K. (a) Experimental oxygen-ion distribution determined by maximum entropy analysis of neutron diffraction data [adapted with permission from Yashima et al. (2010)]. A, O2-O3 and the plus symbol denote (Pr,La) atoms, O2-O3 oxygen sites and the diffusion [illegible], respectively. (b) and (c) BVS map [isovalue ±0.2 valence units (v.u.)] and BVEL (isovalue [illegible] eV, E_{min} [illegible] eV) data calculated for ICSD 248042

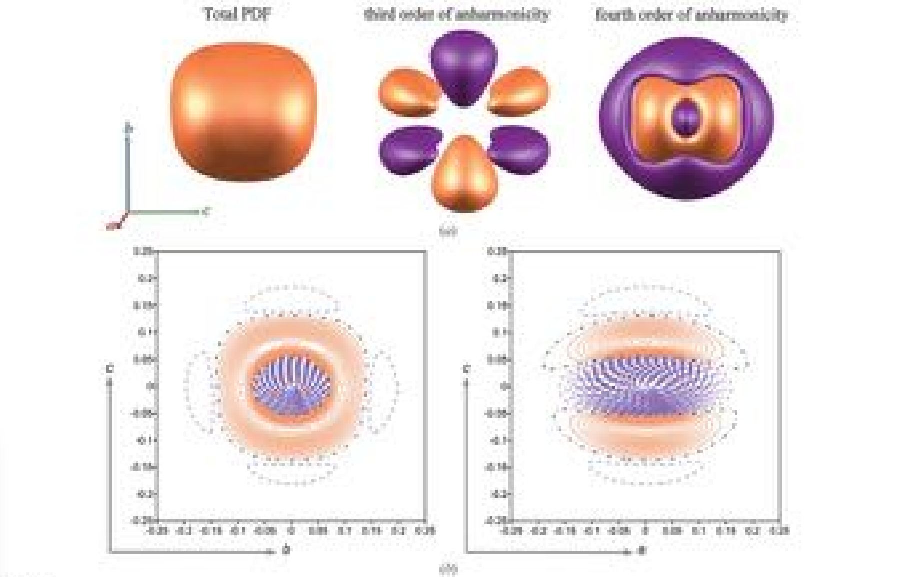

Figure 2
The orthorhombic $KNbO_3$ crystal: probability density distribution function for displacements of Nb from the equilibrium position. (a) 3D image of PDF and its components; isosurfaces are ±300 $Å^{-3}$; (b) 2D image of the anharmonic part of PDF; the step of isolines is 1000 $Å^{-3}$. All PDFs are depicted within a volume of 0.3 × 0.3 × 0.3 Å. Positive PDF values are marked in orange and negative ones are marked in violet. The directions of the unit cell axes are also indicated.

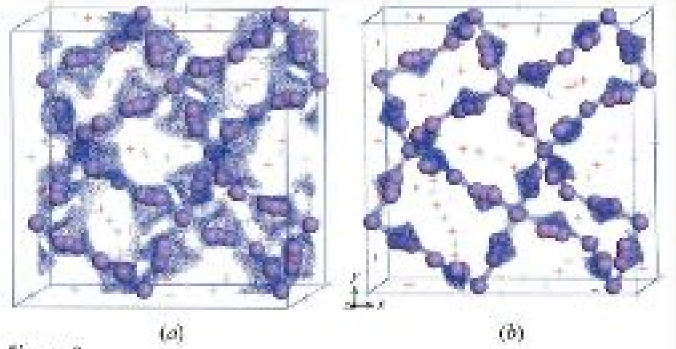

Figure 3
$La_3Li_5O_{12}Ta_2$. Lithium-ion distribution modelled in the diffraction data analysis by a large number of underoccupied atomic sites (spheres) overlaid with (a) a BVS map (isovalue ±0.1 v.u.) and (b) BVEL (isovalue −3.2 eV, E_{min} −4.0 eV) data calculated for ICSD 154400 (Cussen, 2006). The shaded areas represent regions of low BV mismatch and BVEL values.

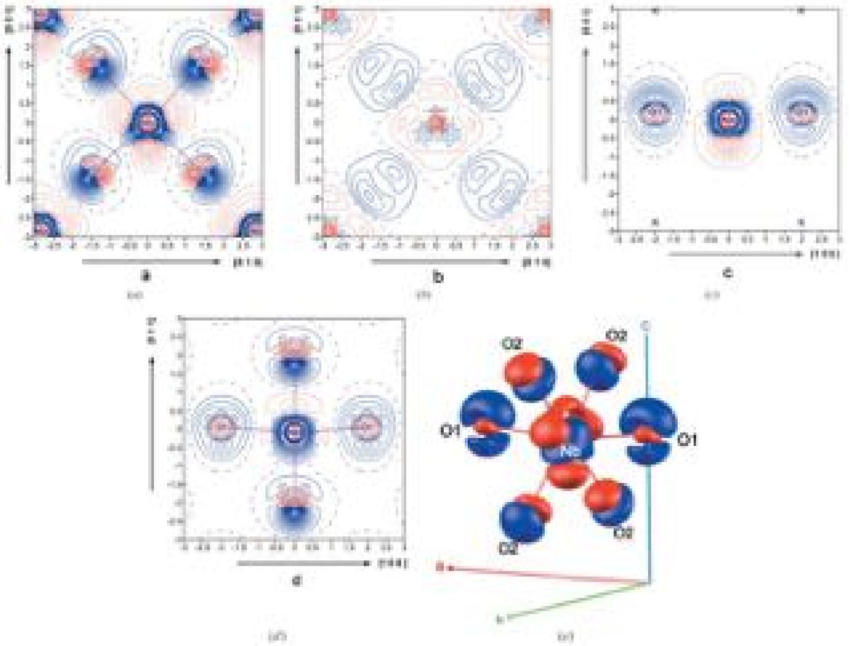

Figure 3
Deformation electron density in the NbO_6 octahedron along the Nb—O1 and Nb—O2 lines: (a)(b)(c)(d) are experimental maps and (b) is a theoretical map. Areas of 2D electron-density accumulation relative to a procrystal are shown in blue. The step of the isolines is 0.1 e $Å^{-3}$. (e) The 3D image of the experimental deformation density consists of two surfaces: red (−0.3) and blue (0.3 e $Å^{-3}$).

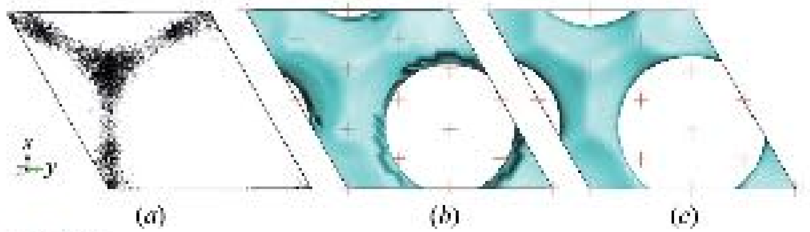

Figure 5
Na^+ β alumina. (a) $Na_{1+x}Al_{11}O_{17+x/2}$ for x = 0.22. *Molecular Dynamics* simulation of Na^+ ion distribution at 700 K [adapted with permission from Thomas (1992)]. (b) and (c) BVS map (isovalue ±0.15 v.u.) and BVEL (isovalue −1.0 eV, E_{min} −2.3 eV) data calculated for ICSD 60635 (Yamaguchi & Suzuki, 1968).

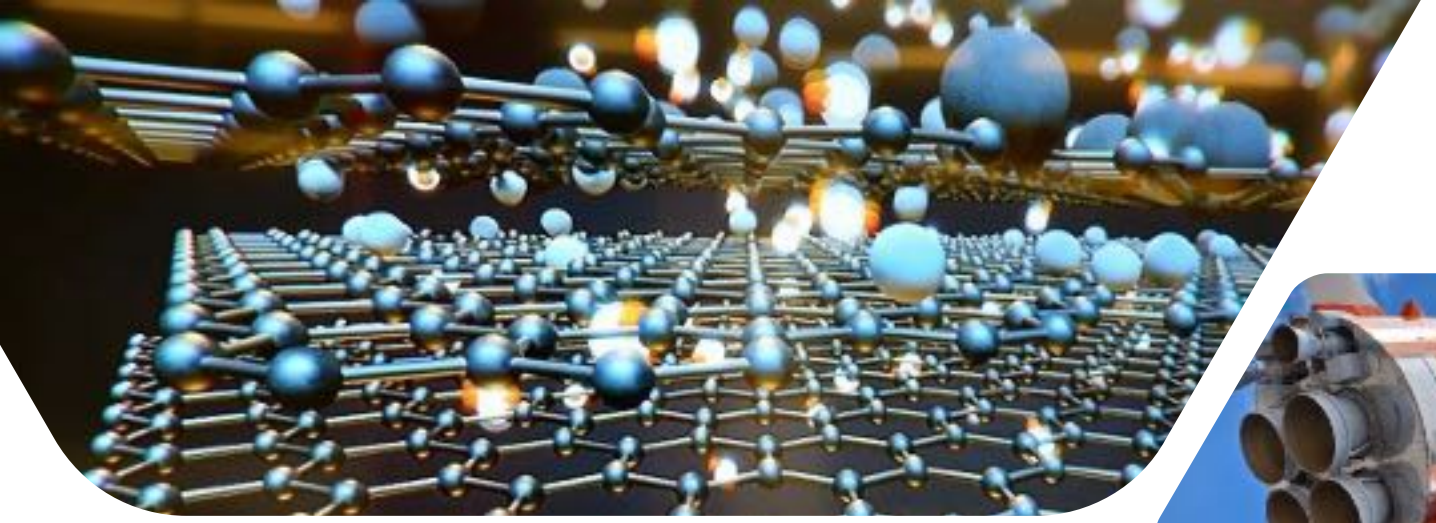

Thank You

Professional Community & Collaborators

https://www.researchgate.net/profile/Maykel_Manawan

Maykel Manawan

78.69 · Dr · Edit your information

Crystallography, X-ray/Neutron Diffraction

ICDD® International Centre for Diffraction Data

Education Subcommittee

Introduction

Maykel Manawan currently works as a lecturer and researcher at Indonesia Defense University. An active member of the International Center for Diffraction Data, ICDD (Education sub-committee). Principal Investigator of the National Li-ion Battery Program (Battery Research Institute-Consortium). Member of Material Research Society Indonesia, MRS-INA. Member of Indonesian Magnetic Society. Member of Indonesia Neutron Scattering Society.

Skills and Expertise

Crystallography | Powder Diffraction | Neutron Diffraction | Protein X-ray Crystallography | Lithium Ion Batteries | Superconductivity and Superconduct... | Magnetic Materials and Magnetism | Density Functional Theory | Material Characterization | Ancient History

https://growkudos.com/projects/crystallography-and-diffraction

SCOPUS ID	:	57202359553
Web of Science ID	:	O-8852-2018
ORCHID ID	:	0000-0003-3782-1307
Google Scholar	:	R6tOeqMAAAAJ&hl
SINTA ID	:	6193883

ANSTO · j-PARC · Siam Photon · DESY. · NEUTRONS FOR SCIENCE

IUCr · Appl Cryst JAC · iScience · A C S · SCIENTIFIC REPORTS nature research · MDPI

ORCID · DOAJ DIRECTORY OF OPEN ACCESS JOURNALS · Google Scholar · Academia.edu · WORLD HISTORY ENCYCLOPEDIA · ELSEVIER · SciVerse Scopus · Scopus WEB OF SCIENCE · MENDELEY · p · RG

batan · LIPI · SEMEN INDONESIA · MTS · GS BATTERY · NUS · QUT

TERIMA KASIH